NOTICE

The quality of this microform is heavily dependent upon the quality of the original thesis submitted for microfilming. Every effort has been made to ensure the highest quality of reproduction possible.

If pages are missing, contact the university which granted the degree.

Some pages may have indistinct print especially if the original pages were typed with a poor typewriter ribbon or if the university sent us an inferior photocopy.

Reproduction in full or in part of this microform is governed by the Canadian Copyright Act, R.S.C. 1970, c. C-30, and subsequent amendments.

AVIS

La qualité de cette microforme dépend grandement de la qualité de la thèse soumise au microfilmage. Nous avons tout fait pour assurer une qualité supérieure de reproduction.

S'il manque des pages, veuillez communiquer avec l'université qui a conféré le grade.

La qualité d'impression de certaines pages peut laisser à désirer, surtout si les pages originales ont été dactylographiées à l'aide d'un ruban usé ou si l'université nous a fait parvenir une photocopie de qualité inférieure.

La reproduction, même partielle, de cette microforme est soumise à la Loi canadienne sur le droit d'auteur, SRC 1970, c. C-30, et ses amendements subséquents.

Three Dimensional Composite Finite Element for Stress Analysis of Anisotropic Laminate Structures

Qian Huang

A Thesis

in

The Department

of

Mechanical Engineering

Presented in Partial Fulfillment of the Requirements
for the Degree of Doctor of Philosophy at
Concordia University
Montreal, Quebec, Canada

February 1989

ISBN 0-315-51325-X

Canada

ABSTRACT

Three Dimensional Composite Finite Element for Stress Analysis of Anisotropic Laminate Structures

Qian Huang, Ph.D.
Concordia University, 1989

This thesis covers three aspects. These are the formulation of the "combined energy" and its variational principle, development of a technique to remove spurious kinematic modes in hybrid finite elements and formulation of a three dimensional composite finite element that can be used to calculate stresses in laminated structures.

In the formulation of the "combined energy", the conjunction condition is utilized. The conjunction condition specifies that at the interlaminar surfaces in composite structures, the in-plane strains, ε_x, ε_y, γ_{xy}, and the transverse stresses, σ_z, τ_{xz}, τ_{yz}, must be continuous, while the transverse strains, ε_z, γ_{xz}, γ_{yz}, and in-plane stresses, σ_x, σ_y, τ_{xy}, are allowed to be discontinuous. The in-plane strains and transverse stresses constitute the basic variables of the combined energy which is different from the traditional potential energy or complementary energy. A variational principle was developed and tested based on this combined energy.

Finite elements involving assumed stress fields have to be free from the spurious kinematic modes. And to achieve this, the concept of modal analysis is introduced for deformable bodies with finite degrees of deformation freedom. A two dimensional 4-node hybrid element and a three dimensional 8-node hybrid element are proposed. In these elements, the stress modes are orthogonal and uncoupled. The zero energy kinetic modes are definitely removed from these hybrid finite elements.

A three dimensional 8-node composite finite element is successfully formulated based on the variational principle of combined energy with incorporation of the modal analysis technique to determine stress modes.

The three dimensional 8-node composite finite element was used to solve problems of a three dimensional isotropic body subjected to hydrostatic pressure, uniaxial extension, pure shear, pure bending, pure torsion, as well as simply supported beam and cantilever beam problems. Comparison with displacement finite element and hybrid finite element shows that for cases where stresses are constant, perfect agreement with elasticity solution was obtained by the the three methods. For bending cases, the composite finite element method shows closer agreement with the hybrid finite element method than the displacement finite element

method.

By means of the composite finite element, stresses in a symmetric angle-ply laminate subjected to uniaxial extension are calculated. The result is quite different from the so-called classical laminate theory. In classical laminate theory it is assumed that strains remain the same throughout the thickness. Also the in-plane shear coupling strains are zero for symmetric angle-ply laminates subjected to a uniaxial tension. Numerical results show that the shear coupling strain caused by anisotropy appears in most parts of the lamina, whereas only within 1/5 ply-thickness near the interlaminar surfaces the shear deformation vanishes abruptly. This creates a strong concentration of the in-plane stresses near the interlayer surfaces. The average tensile stiffness of the laminate calculated with the composite finite element method is higher than that of the free extension case, but much lower than the results obtained from classical laminate theory.

ACKNOWLEDGEMENTS

The author is sincerely grateful to the thesis supervisor Dr. Suong Van Hoa for his financial support and enthusiastic guidance during the course of this work. The continuous encouragement and help provided by the thesis co-supervisor Dr. T. S. Sankar is also acknowledged with gratitude.

The help provided by friends and colleagues Gregor Rohrauer, Hong Su, Weiliang Dai is gratefully acknowledged. Thanks are also due to the professionals in the computer centre of Concordia University for their patient services.

Further, the author is grateful to his mother Yun-hua Guan, his wife Shao-hua Zhou and his son Feng Huang for their moral support and understanding.

The author also wishes to express his appreciation to Dr. Wei-chang Qian, the supervisor of author's first Ph.D. degree in China, for his helpful lecture in the field of generalized variational principles.

Table of Contents

List of Figures

List of Symbols

A	potential energy density
a_1, a_2, a_3	Lamé coefficients of transformation from natural coordinates into Cartesian system coordinates
a	characteristic length for nondimensionalization
B	complementary energy density
B	transformation matrix of strain – nodal displacements relations
C	combined energy density
D_L	transformation matrix of compatibility relation in terms of nodal displacements
E	Young's modulus
$\overline{F}$	prescribed body force
f	equivalent nodal force
G	mapping matrix for stiffness in stress parameter space to nodal displacement space
g	subscript for globally continuous variables
H	compliance matrix in stress parameter space
J	Jacobian matrix
$\|J\|$	Jacobian determinant
K	stiffness matrix in nodal displacement space
L	subscript for locally continuous variables or for laminate
m	total number of assumed stress field modes

n	total number of generalized displacements
$\mathbf{N}$	shape function for displacement interpolation
$\mathbf{P}$	assumed stress modes, where each column is one of the assumed stress field modes
$\mathbf{p}$	local vector, $\mathbf{p} = \{\sigma_x, \sigma_y, \tau_{xy}, -\varepsilon_z, -\gamma_{xz}, -\gamma_{yz}\}^T$
$\mathbf{Q}$	stiffness matrix in strain space
$\mathbf{q}$	global vector, $\mathbf{q} = \{ \varepsilon_x, \varepsilon_y, \gamma_{xy}, \sigma_z, \gamma_{xz}, \gamma_{yz} \}^T$
$\mathbf{R}$	combined constitutive relation between the local vector p and global vector q
$\mathbf{R}_i$	row vector of $\mathbf{R}$
$\mathbf{r}$	basic vector, $\mathbf{r} = \{ u, v, w, \sigma_z, \tau_{xz}, \tau_{yz} \}^T$
$\mathbf{S}$	compliance matrix in stress space
$\bar{\mathbf{T}}$	prescribed boundary force density
$\mathbf{u}$	displacement vector
u, v, w	components of displacement
x, y, z	Cartesian coordinates
$\boldsymbol{\beta}$	stress parameter vector
$\boldsymbol{\Phi}$	strain matrix in terms of the nodal displacements
$\boldsymbol{\Gamma}$	stress matrix in terms of the nodal displacements
γ	shear strain
$\boldsymbol{\delta}$	nodal displacement
$\boldsymbol{\varepsilon}$	strain, i.e. $\boldsymbol{\varepsilon} = \{ \varepsilon_x, \varepsilon_y, \gamma_{xy}, \varepsilon_z, \gamma_{xz}, \gamma_{yz} \}^T$ in Chapter 3, $\boldsymbol{\varepsilon} = \{ \varepsilon_x, \varepsilon_y, \varepsilon_z, \gamma_{xy}, \gamma_{yz}, \gamma_{zx} \}^T$
ξ, η, ζ	natural coordinates of finite element
λ	eigenvalue of stiffness matrix K
ν	Poisson's ratio

σ	stress, i.e. $\sigma = \{\sigma_x, \sigma_y, \tau_{xy}, \sigma_z, \tau_{xz}, \tau_{yz}\}^T$
	in Chapter 3, $\sigma = \{\sigma_x, \sigma_y, \sigma_z, \tau_{xy}, \tau_{yz}, \tau_{zx}\}^T$
τ	shear stress
~	hat, represents nondimensional quantities
-	hat, represents prescribed quantities
2-D	two dimensional
3-D	three dimensional
4-node	indicate a finite element with four nodes
8-node	indicate a finite element with eight nodes
FEM	finite element method
LTH	classical laminate theory

Chapter 1. Introduction

Composite materials are different from the conventional materials because they possess anisotropic relations between stress and strain and, in practice, they appear as laminations in structures. The anisotropy causes coupling strains. On the other hand lamination may restrict the coupling strains and result in coupling stresses.

In the 1950s-1970s, the 3-D anisotropic elasticity theory was developed [1]. It is applicable to each lamina of the composite, and does not cause great difficulty for computation. However, lamination introduces discontinuities in composithe structures. Thus, for te 3D elasticity, the interlayer surfaces constitute boundary conditions if a conventional approach is followed. One of the objectives of this thesis is to provide a differential formulation and a corresponding variational principle based on 3-D anisotropic elasticity that considers discontinuities at the interfaces.

In the 1970s, the so-called classical lamination theory was presented in graduate text books across North America and Europe [25,26,27] and has been widely used to estimate the stress and strain in the central region (far from traction boundaries and free edges) of laminated composite plates. This practical theory is based on an assumption that the strains are uniform across the thickness of the laminate for uniaxial extension and linear for pure bending. However, numerical results

presented in this thesis show that in an angle-ply laminate subjected to uni-axial tension the shear coupling strain vanishes only within a very thin layer close to the interface. The influence of this constraint only spreads over a thickness about 1/5 of the ply-thickness. The shear coupling strain appears in most regions of the lamina with a value almost the same as under free extension without bonding between layers. This causes a large error in results obtained by classical theory. For a symmetric angle-ply laminate with ply angle at $\pm 42^{o}$, the maximum axial stress (along loading direction) calculated by the finite element method is 86% larger than the one calculated by laminate theory. For ply angle at $\pm 57^{o}$, the maximum in-plane shear coupling stress calculated by finite element is 255% larger than the one calculated by laminate theory. The numerical results also show the existence of a second coupling stress, the in-plane transverse stress, due to the non-uniform Poisson's effects, whose maximum value is up to 1.26 times the average applied tensile stress. This is not accounted for in classical laminate theory. From the numerical results, it can be seen that there is a strong concentration for in-plane stresses near bonding interface. On one hand, the average tensile stress of symmetric laminates under uni-axial extension obtained numerically is close to that in the laminate without bonding between layers. On the other hand, the maximum axial tensile stress near bonding interfaces obtained numerically

is up to 3.3 times than average applied stress when $\theta=30^{o}$. Obviously, it is necessary to improve the practical theory for engineering design.

Since the 1960s, determination of the interlaminar stresses in composite materials, especially near the traction-free edges, has been a topic attracting a lot of attention. Most of these works involve local stresses. Some authors discovered that the effects of shear deformation in the interlaminar regions are of importance with respect to strength and other properties of the composites. The failure of composites has often been attributed to delamination due to interlaminar stresses near the traction free edge regions. These previous studies can be classified as follows:

a) Finite Difference Method: Pipes and Pagano (1970, 1972, 1974) [2,56,57], Altus et al (1980) [3], (displacement formulation).

b) Finite Element Method: Displacement Formulation with a high order plate element, Heppler et al (1980) [5], Engblom et al (1985) [4], Pandya et al (1988) [74]. With a 3-D element, Yeh et al (1986) [6], Natarajan, Lucking and Hoa (1984,1986) [7,8], Chaudhuri et al (1987) [65]. Stress Formulation, Rybicki (1971) [9]. Hybrid Formulation, Mau , Tong and Pian (1972) [54], Nishioka and Atluri (1980) [73], Wang et al (1983,1984) [13,72], Khalil et al (1986) [10], Spilker (1986) [12], Sun and Liou (1987) [60,63], Mixed

formulation Moriya (1986) [50], Kwon and Akin (1987) [61], Hwang and Sun (1988) [59] (iterative procedure).

c) Perturbation Method: Hsu et al (1977) [14], (displacement formulation). Boundary-layer Matching Method, Tang and Levy (1976) [15], (stress formulation). Boundary Layer Theory, Ye and Yang (1988) [79]. Matched Asymptotic Expansion Method, Bar-Yoseph and Pian et al (1981, 1983, 1986) [16,17,70], (stress formulation).

d) Variational Method: Rayleigh-Ritz Method, Pagano (1978) [18], (mixed formulation), Garlerkin Method, Wang and Dickson (1978) [19], (mixed formulation), Mixed Variational Principle, Vong (1986) [71], Chatterjee and Ramnath (1988) [58], Force Balance Method, Kassapoglou and Lagace (1987) [82,83] (complementary energy principle), Energy Method, Zhang (1988) [75].

e) Transfer Matrix Method, Oery et al (1984) [20].

f) Experimental Method, Whitney et al (1972) [21], Berhaus et al (1975) [22], Herakovich et al (1985) [86].

For theoretical and numerical methods, a simpler way to classify the above works is as follows: 'Displacement Formulation', 'Stress Formulation', 'Mixed Formulation' and 'Hybrid Formulation'. In displacement formulation, the displacement field is assumed. In stress formulation, the stress field is assumed. 'Mixed formulation' means that both stress and displacement fields are assumed. 'Hybrid formulation' means that at the boundary surface the assumed

field is different from that in the interior.

Some authors gave attention to the conjunction conditions at the interlayer surfaces, such as Spilker (1980) [23], Bar-Yoseph and Pian (1981) [16], who emphasize the continuity of stresses σ_z, τ_{xz}, τ_{yz} and prefer the stress formulations. Reissner's work, (1984) [48], based on potential energy principle, presents a mixed variational theorem, which requires a semi-potential energy density through partial Legendre transformation. Later he (1986) [49] based his work on a generalized potential energy principle, which requires a semi-complementary energy density through partial Legendre transformation. Reissner gave some examples, however he did not give the general form of the semi energy densities. Moriya (1986) [50] developed an 8-node mixed plate finite element based on the modified Hu-Washizu principle. Both Reissner and Moriya took in-plane strains, ε_x, ε_y, γ_{xy}, and transverse stresses, σ_z, τ_{xz}, τ_{yz}, as independent quantities for analysis of laminated structures. The author (1987) [55] presented a new type of elastic energy, in the quadratic form, in terms of in-plane strains, ε_x, ε_y, γ_{xy}, and transverse stresses σ_z, τ_{xz}, τ_{yz}. On this basis, the author developed a laminate functional and established a corresponding variational principle.

Considering the shear deformation, some authors

modified the laminated plate theory to include various high-order terms. Those include Pagano (1969) [93], Whitney (1972) [62], Lo , Christensen and Wu (1977) [91], Reddy (1984) [92], Whitcomb et al (983,1985) [84,90], Rehfield et al (1985) [89], Valisetty et al (1985) [88], Ueng and Zhang (1985) [87], Conti et al (1985) [85], Murakami (1986) [94], Krishna (1987) [77,80], Toledano , Murakami et al (1986,1987) [66 - 68] whose works were based upon Reissner's mixed variational theorem [48].

Suppression of the free-edge delamination also received attention in works by Kim et al (1985) [95], Hong (1987) [81], Garg (1988) [78], Moriya et al (1988) [76]. Moriya controlled the order of the singularity by varing geometrical shape of the free edge.

In summary, stress analysis in laminated composites encounters two difficulties.

The first difficulty is the discontinuity in laminated structures. At the interlayer surfaces, the in-plane strains and the transverse stresses must be continuous, while the other strains and stresses may be described by a finite discontinuity which is caused by the abrupt change of material property or orientation. For the stratified discontinuous medium neither stress nor strain tensors are continuous. Some components of stress or strain are

continuous, but others are not. Therefore the conventional displacement formulation and stress formulation are not capable of handling the stratified discontinuous medium as a whole. With traditional approaches, the interlaminar surfaces must be treated as boundaries with six continuity conditions between every two adjacent layers (three stresses and three strains). The other three stresses and three strains must be permitted a finite discontinuity. If the six globally continuous components of stress and strain are taken as basic variables, then the six continuity conditions at the interfaces should be satisfied automatically. Also if restrictions on other components of stress and strain are imposed properly, the possible discontinuities will occur naturally. Reissner's mixed variational theorems (1984,1986) [48,49], Moriya's mixed plate finite element (1986) [50] along with the author's third type of elastic energy and its variational principle (1987) [55] are all formulated based on the globally continuous components of stress and strain.

If the transverse stresses are taken as independent unknown variables, a second difficulty arises. This difficulty is the spurious kinematic modes. Finite elements involving an assumed stress field are cursed with zero-energy mode. These have plagued the hybrid stress method since the beginning. Some experienced authors added higher order stress field terms to suppress the zero

energy deformation modes. However, the additional terms may cause stiffening of the elements. A few authors give necessary or sufficient conditions to avoid zero energy modes for hybrid element (see Chapter 3). Spilker (1982) [34] suggested using a complete set of each order of the polynomials for the stress field. Rubinstein , Punch and Atluri (1983, 1984) [35,36], using symmetric group theory, gave some choices for a least-order stress field. Using the polynomial terms they constructed the stress modes. However, most of these choices of stress modes result in weakened stiffness matrices for some high order stress modes. Pian et al (1983) [51] provided a systematic procedure to determine the irreducible polynomial terms of the stress field.

To assume a partial stress field for the analysis of laminated structures, it is necessary to reconstruct those irreducible polynomial terms into natural stress modes. This thesis introduces a modal analysis concept for deformable body with finite degrees of freedom and tries to find out the natural stress modes for the complete and partial stress field in 3-D, 8-node hybrid and composite finite elements respectively. Then the 3-D, 8-node composite finite element is formulated hereby for analysis of composite laminates, whose stiffness matrix is formed by combining a semi-displacement stiffness matrix in terms of in-plane strains and a semi-hybrid stiffness matrix in

terms of transverse stress. Moriya (1986) [50], based on a modified Hu-Washizu principle, formulated an 8-node plate element, in which the stiffness matrix also consists of two parts. It can be shown that these two parts are equivalent to the two semi-stiffness matrices presented in this thesis.

Chapter 2 of this thesis discusses the continuity and discontinuity in laminated structures. It introduces a concept of combined energy based on particular stresses mixed with specific strains. It also presents a corresponding variational principle for the stratified discontinuous medium as a whole.

Chapter 3 introduces a concept of modal analysis for a deformable body with finite degrees of freedom. It also presents the natural stress modes for 2-D, 4-node and 3-D, 8-node hybrid finite elements.

In Chapter 4 a 3-D, 8-node composite finite element for laminated composites is developed. Its formulation is based on the variational principle of combined energy with incorporation of modal analysis technique to determine the stress modes.

Chapter 5 shows a numerical example. A symmetric angle-ply laminate subjected to a uniaxial extensional

loading is analysed using the composite finite element method. The numerical results are in agreement with the results obtained by displacement FEM and hybrid FEM, but are quite different from results obtained by the classical laminate theory. The results are discussed in detail.

Chapter 2. Variational Principle of Combined Energy

The conventional approaches for stress analysis of composite laminates have encountered discontinuity problems. In this Chapter, the C^1 continuity of displacements in the in-plane directions and C^0 continuity of displacement along thickness direction are discussed. Also , the global continuity of transverse stresses and local continuity of in-plane stresses are examined. Then, the formulations of stress analysis in both differential equation form and variational functional form are presented.

2.1 Continuity in laminated structures

In the composite laminates there are discontinuities due to variation in material property or the orientation of fibers. On the other hand, for perfectly bonded laminates, the displacements are continuous and so are the reaction forces at interlaminar surfaces.

The lamina plane is denoted by cartesian coordinates x, y , and in the thru thickness direction by z.

Within each lamina, all components of displacement, strain and stress are continuous.

At interlaminar surfaces in perfect bonding, the displacements are continuous. Their in-plane derivatives, ε_x, ε_y, γ_{xy} are therefore continuous. The reaction forces give rise to transverse stresses σ_z, τ_{xz}, τ_{yz} and these are also continuous.

This means the in-plane strains and transverse stresses are globally continuous, and other components of strain and stress are at least locally continuous within each layer. The partial stress or strain can be defined as

$$\varepsilon_g = \{ \varepsilon_x, \varepsilon_y, \gamma_{xy} \}^T, \quad \varepsilon_L = \{ \varepsilon_z, \gamma_{xz}, \gamma_{yz} \}^T,$$
$$\sigma_g = \{ \sigma_z, \tau_{xz}, \tau_{yz} \}^T, \quad \sigma_L = \{ \sigma_x, \sigma_y, \tau_{xy} \}^T.$$

To consider the effects of discontinuities in properties and orientations of anisotropic materials, the in-plane strains and transverse stresses are combined and defined as global field vector $\mathbf{q}$.

$$\mathbf{q} = \begin{Bmatrix} \varepsilon_g \\ \sigma_g \end{Bmatrix} = \{\varepsilon_x, \varepsilon_y, \gamma_{xy}, \sigma_z, \tau_{xz}, \tau_{yz}\}^T. \qquad (2.1.1)$$

and the in-plane stresses and transverse strains are combined and defined as local field vector $\mathbf{p}$.

$$\mathbf{p} = \begin{Bmatrix} \sigma_L \\ -\varepsilon_L \end{Bmatrix} = \{\sigma_x, \sigma_y, \tau_{xy}, -\varepsilon_z, -\gamma_{xz}, -\gamma_{yz}\}^T. \qquad (2.1.2)$$

in which the negative sign is introduced to ensure the symmetry of the combined constitutive relation. The global field vector $\mathbf{q}$ and the local field vector $\mathbf{p}$ are related by,

$$p = R\, q. \tag{2.1.3}$$

where R is called the combined constitutive matrix.

If we denote

$$\sigma = \begin{Bmatrix} \sigma_L \\ \sigma_g \end{Bmatrix} = \{\sigma_x, \sigma_y, \tau_{xy}, \sigma_z, \tau_{xz}, \tau_{yz}\}^T \tag{2.1.4}$$

$$\varepsilon = \begin{Bmatrix} \varepsilon_g \\ \varepsilon_L \end{Bmatrix} = \{\varepsilon_x, \varepsilon_y, \gamma_{xy}, \varepsilon_z, \gamma_{xz}, \gamma_{yz}\}^T \tag{2.1.5}$$

then,

$$\sigma = Q\, \varepsilon = \begin{bmatrix} Q_1 & Q_2 \\ Q_2^T & Q_3 \end{bmatrix} \begin{Bmatrix} \varepsilon_g \\ \varepsilon_L \end{Bmatrix} \tag{2.1.6}$$

$$\varepsilon = S\, \sigma = \begin{bmatrix} S_1 & S_2 \\ S_2^T & S_3 \end{bmatrix} \begin{Bmatrix} \sigma_L \\ \sigma_g \end{Bmatrix} . \tag{2.1.7}$$

where Q is the stiffness matrix and S is the compliance matrix of the lamina.

Using equation (2.1.6), σ_L and ε_L can be expressed in terms of σ_g and ε_g, then, the matrix R in eq. (2.1.3) is given by,

$$R = \begin{bmatrix} Q_1 - Q_2 Q_3^{-1} Q_2^T & Q_2 Q_3^{-1} \\ Q_3^{-1} Q_2^T & -Q_3^{-1} \end{bmatrix} . \tag{2.1.8}$$

Similarly, using eq.(2.1.7), R can be alternately written as

$$R = \begin{bmatrix} S_1^{-1} & -S_1^{-1} S_2 \\ -S_2^T S_1^{-1} & S_2^T S_1^{-1} S_2 - S_3 \end{bmatrix} . \tag{2.1.9}$$

Because S and Q are symmetric matrices, it can be shown that,

$$R^T = R. \tag{2.1.10}$$

At the interlaminar surface, the global field vector q

is the same for two layers, but the constitutive matrices **R** are different (caused by variation in material or fiber orientation). Generally, the local field vector **p** is described by a finite discontinuity.

$$\begin{aligned} \mathbf{p}^{(i)} &= \mathbf{R}^{(i)}\mathbf{q}|_{\text{interface}} \\ \mathbf{p}^{(i+1)} &= \mathbf{R}^{(i+1)}\mathbf{q}|_{\text{interface}} \end{aligned} \tag{2.1.11}$$

where i refers to layer i.

This is a clear approach for satisfying the continuity conditions automatically and for calculating the discontinuity naturally. The basic equations of 3-D laminate theory are developed in next section.

2.2 Basic Equations

The following six globally continuous variables are taken as the basic variables.

$$\mathbf{r} = \{u, v, w, \sigma_z, \tau_{xz}, \tau_{yz}\}^T \tag{2.2.1}$$

Using these variables, the governing equations and boundary conditions are shown as follows.

1. The global field vector $\mathbf{q}$ is related to the basic variables by,

$$\mathbf{q} = \mathbf{B}\,\mathbf{r} \tag{2.2.2}$$

where

$$\mathbf{B} = \begin{bmatrix} \frac{\partial}{\partial x} & 0 & 0 & 0 & 0 & 0 \\ 0 & \frac{\partial}{\partial y} & 0 & 0 & 0 & 0 \\ \frac{\partial}{\partial y} & \frac{\partial}{\partial x} & 0 & 0 & 0 & 0 \\ 0 & 0 & 0 & 1 & 0 & 0 \\ 0 & 0 & 0 & 0 & 1 & 0 \\ 0 & 0 & 0 & 0 & 0 & 1 \end{bmatrix}$$

2. The combined constitutive relation is :

$$\mathbf{p} = \mathbf{R}\,\mathbf{q}\ . \tag{2.2.3}$$

The matrix $\mathbf{R}$ can be denoted as,

$$\mathbf{R} = [\mathbf{R}_1^T, \mathbf{R}_2^T, \ldots, \mathbf{R}_6^T]^T$$

where $\mathbf{R}_i$ is the row vector of $\mathbf{R}$. Thus, the component of local vector can be expressed as

$$p_i = \mathbf{R}_i\mathbf{q} = \mathbf{R}_i\mathbf{B}\mathbf{r} \tag{2.2.4}$$

3. The equilibrium equations are :

$$\begin{aligned} &\frac{\partial}{\partial x}(\mathbf{R}_1\mathbf{B}\mathbf{r}) + \frac{\partial}{\partial y}(\mathbf{R}_3\mathbf{B}\mathbf{r}) + \frac{\partial}{\partial z}(\tau_{xz}) + \overline{F}_x = 0 \\ &\frac{\partial}{\partial x}(\mathbf{R}_3\mathbf{B}\mathbf{r}) + \frac{\partial}{\partial y}(\mathbf{R}_2\mathbf{B}\mathbf{r}) + \frac{\partial}{\partial z}(\tau_{yz}) + \overline{F}_y = 0 \\ &\frac{\partial}{\partial x}(\tau_{xz}) + \frac{\partial}{\partial y}(\tau_{yz}) + \frac{\partial}{\partial z}(\sigma_z) + \overline{F}_z = 0. \end{aligned} \tag{2.2.5}$$

4. The compatibility equations are :

$$R_4Br = -\frac{\partial w}{\partial z}$$

$$R_5Br = -\frac{\partial u}{\partial z} - \frac{\partial w}{\partial x} \qquad (2.2.6)$$

$$R_6Br = -\frac{\partial v}{\partial z} - \frac{\partial w}{\partial x}$$

The physical meaning of left hand terms in the three equations are the locally continuous strains ε_z, γ_{xz}, γ_{yz}. These three equations are similar to the strain - displacement relation. However, the locally continuous strains are functions of the globally continuous stresses and strains, i.e. the global field vector **q**. The left hand terms of above equations involve the transverse stresses and first derivatives of displacements with respect to x,y. They become the compatibility equations. This is a rigorous form to relieve the requirement of C^1 continuity of displacements along z-direction and to allow a finite discontinuity for first derivatives of displacements with respect to z at interlaminar surfaces.

5. The boundary conditions are :

at prescribed displacement boundaries,

$$u = \bar{u}$$

$$v = \bar{v} \qquad (2.2.7)$$

$$w = \bar{w}$$

and at prescribed force boundaries,

$$R_1 Brn_x + R_3 Brn_y + \tau_{xz} n_z = \overline{T}_x$$
$$R_3 Brn_x + R_2 Brn_y + \tau_{yz} n_z = \overline{T}_y \qquad (2.2.8)$$
$$\tau_{xz} n_x + \tau_{yz} n_y + \sigma_z n_z = \overline{T}_z .$$

6. Conjunction conditions at interlayer surfaces are :

$$u^{(i)} = u^{(i+1)},$$
$$v^{(i)} = v^{(i+1)},$$
$$w^{(i)} = w^{(i+1)}, \qquad (2.2.9)$$
$$\sigma_z^{(i)} = \sigma_z^{(i+1)},$$
$$\tau_{xz}^{(i)} = \tau_{xz}^{(i+1)},$$
$$\tau_{yz}^{(i)} = \tau_{yz}^{(i+1)}.$$

2.3 Variational Principle of Combined Energy

In the previous section, it is mentioned that the combined constitutive matrix R is symmetrical (eq. 2.1.10). Thus,

$$R_{ij} = R_{ji} \qquad (2.3.1)$$

If we define C as a quadratic form of the global vector,

$$\begin{aligned} 2C = {} & (R_{11}q_1 + R_{12}q_2 + R_{13}q_3 + R_{14}q_4 + R_{15}q_5 + R_{16}q_6)q_1 \\ & + (R_{21}q_1 + R_{22}q_2 + \ldots + R_{26}q_6)q_2 \\ & + \ldots \\ & + (R_{61}q_1 + R_{62}q_2 + \ldots + R_{66}q_6)q_6 \end{aligned} \qquad (2.3.2)$$

or

$$C = \frac{1}{2} \sum_{i,j} R_{ij} q_i q_j . \qquad (2.3.3)$$

Then,

$$\partial C/\partial q_i = R_{i1}q_1 + R_{i2}q_2 + \ldots + R_{i6}q_6 = p_i . \qquad (2.3.4)$$

Obviously, C is a new type of energy and it can be called the combined energy (in the first presentation [55], the author called it the hybrid energy). Similarly the potential energy can be expressed as a quadratic form of strain,

$$A = \frac{1}{2} \sum_{i,j} Q_{ij} \varepsilon_i \varepsilon_j . \qquad (2.3.5)$$

Also the complementary energy can be expressed as a quadratic form of stress,

$$B = \frac{1}{2} \sum_{i,j} S_{ij} \sigma_i \sigma_j . \qquad (2.3.6)$$

A variational principle could be established by means of the weighted residual method corresponding to the basic equations stated above.

If the basic equations stated in the previous section are expressed in terms of the globally continuous basic variables in the functional form, the conjunction

conditions at the interlaminar surfaces will be satisfied, and the necessity of involving conjunction conditions is therefore eliminated. This means the continuity conditions are satisfied as forced constraints in advance. Also if the relation between the global vector and basic variable in eq.(2.2.2), which contains a part of the strain-displacement relation, is also chosen as forced constraint in the functional form, the number of variables in the functional can be minimized. The prescribed displacement boundary conditions are easy to satisfy and and they are handled during the numerical procedure in in order to reduce the integral calculations.

Thus, the following relations will be satisfied as forced constraints in advance.

a) Partial strain-displacement relation (2.2.2).

b) Prescribed displacement boundary conditions (2.2.7).

c) Continuity conditions at the interlayer surfaces (2.2.9).

The following other relations are Euler equations or natural boundary conditions of the functional, which will be satisfied by the stationary conditions of the functional a posteriori.

a) Equilibrium equations (2.2.5).

b) Combined constitutive relations (2.1.3).

c) Compatibility conditions (2.2.6).

d) Prescribed force boundary conditions (2.2.8).

Introducing these relations into the weighted residual integral and denoting it by I, we have,

$$
\begin{aligned}
I = \sum_i \iiint_{V_i} [& \left(\frac{\partial \sigma_x}{\partial x}+\frac{\partial \tau_{xy}}{\partial y}+\frac{\partial \tau_{xz}}{\partial z}+\bar{F}_x\right)A^* + \left(\frac{\partial \tau_{xy}}{\partial x}+\frac{\partial \sigma_y}{\partial y}+\frac{\partial \tau_{yz}}{\partial z}+\bar{F}_y\right)B^* + \\
& + \left(\frac{\partial \tau_{xz}}{\partial x}+\frac{\partial \tau_{yz}}{\partial y}+\frac{\partial \sigma_z}{\partial z}+\bar{F}_z\right)C^* + \\
& + \left(\frac{\partial C}{\partial \varepsilon_x}-\sigma_x\right)D^* + \left(\frac{\partial C}{\partial \varepsilon_y}-\sigma_y\right)E^* + \left(\frac{\partial C}{\partial \gamma_{xy}}-\tau_{xy}\right)F^* + \\
& + \left(\frac{\partial C}{\partial \sigma_z}+\varepsilon_z\right)G^* + \left(\frac{\partial C}{\partial \tau_{xz}}+\gamma_{xz}\right)H^* + \left(\frac{\partial C}{\partial \tau_{yz}}+\gamma_{yz}\right)I^* + \\
& + \left(\varepsilon_z - \frac{\partial w}{\partial z}\right)J^* + \left(\gamma_{xz} - \frac{\partial u}{\partial z} - \frac{\partial w}{\partial x}\right)K^* + \left(\gamma_{yz} - \frac{\partial v}{\partial z} - \frac{\partial w}{\partial y}\right)L^*] dv + \\
+ \iint_{S_{\sigma i}} [& (\sigma_x n_x+\tau_{xy}n_y+\tau_{xz}n_z-\bar{T}_x)M^* \\
& + (\tau_{xy}n_x+\sigma_y n_y+\tau_{yz}n_z-\bar{T}_y)N^* + \\
& + (\tau_{xz}n_x+\tau_{yz}n_y+\sigma_z n_z-\bar{T}_z)Q^*] ds = 0, \qquad (2.3.7)
\end{aligned}
$$

where $A^*, B^*, \ldots, L^*$ are arbitrary functions within each layer in the interior of an anisotropic elastic body V_i, M^*, N^*, Q^* are arbitrary functions at the force boundaries $S_{\sigma i}$, and i refers to the layer number.

Without loss of generality, these arbitrary functions can be defined as,

$$A^*= -\delta u, \quad B^*= -\delta v, \quad C^*= -\delta w,$$

$$D^*= \delta(\frac{\partial u}{\partial x}), \quad E^*= \delta(\frac{\partial v}{\partial y}),$$

$$F^*= \delta(\frac{\partial u}{\partial y} + \frac{\partial v}{\partial x}) \tag{2.3.8}$$

$$G^*= \delta\sigma_z, \quad H^*= \delta\tau_{xz}, \quad I^*= \delta\tau_{yz},$$

$$J^*=-\delta\sigma_z, \quad K^*=-\delta\tau_{xz}, \quad L^*=-\delta\tau_{yz}$$

in the V_i of each layer,and

$$M^*= \delta u, \quad N^*= \delta v, \quad Q^*= \delta w \tag{2.3.9}$$

at the force boundaries.

For each layer, the normal direction of the upper interface is,

$$(n_x,n_y,n_z) = (0,0,1), \tag{2.3.10}$$

and the normal of lower interface is,

$$(n_x,n_y,n_z) = (0,0,-1). \tag{2.3.11}$$

Integrating by parts and using boundary conditions (2.2.7), we have,

$$\begin{aligned}
&\sum_i \iiint_{V_i} (\frac{\partial\sigma_x}{\partial x} + \frac{\partial\tau_{xy}}{\partial y} + \frac{\partial\tau_{yz}}{\partial z})\delta u \, dv \\
&= \sum_i \{-\iiint_{V_i} (\sigma_x\delta\frac{\partial u}{\partial x} + \tau_{xy}\delta\frac{\partial u}{\partial y} + \tau_{xz}\delta\frac{\partial u}{\partial z}) \, dv \\
&\qquad +\iint_{S_{\sigma i}} (\sigma_x n_x+\tau_{xy}n_y+\tau_{xz}n_z)\delta u \, ds \\
&\qquad +\iint_{S_{up}} \tau_{xz}\delta u \, ds - \iint_{S_{low}} \tau_{xz}\delta u \, ds \} \\
&= -\sum_i \{\iiint_{V_i} (\sigma_x\delta\frac{\partial u}{\partial x} + \tau_{xy}\delta\frac{\partial u}{\partial y} + \tau_{xz}\delta\frac{\partial u}{\partial z}) \, dv\}
\end{aligned}$$

$$+\iint_{S_{\sigma i}} (\sigma_x n_x+\tau_{xy} n_y+\tau_{xz} n_z)\delta u \, ds, \qquad (2.3.12)$$

in which the τ_{xz} are continuous at the interface and S_{up}, S_{low} refer to the upper and lower interface. At the interface the normals of the two adjacent layers have opposite signs and the same magnitude.

Performing the same operations for the other directions, the integral I can be written as

$$\begin{aligned} I=\sum_i \iiint_{V_i} \{ & (\sigma_x \delta\frac{\partial u}{\partial x}+\tau_{xy}\delta\frac{\partial u}{\partial y}+\tau_{xz}\delta\frac{\partial u}{\partial z})+(\tau_{xy}\delta\frac{\partial v}{\partial x}+\sigma_y\delta\frac{\partial v}{\partial y}+\tau_{yz}\delta\frac{\partial v}{\partial z})+ \\ & +(\tau_{xz}\delta\frac{\partial w}{\partial x}+\tau_{yz}\delta\frac{\partial w}{\partial y}+\sigma_z\delta\frac{\partial w}{\partial z})-(\bar{F}_x\delta u+\bar{F}_y\delta v+\bar{F}_z\delta w)+ \\ & +\delta\varepsilon_x(\frac{\partial C}{\partial \varepsilon_x}-\sigma_x)+\delta\varepsilon_y(\frac{\partial C}{\partial \varepsilon_y}-\sigma_y)+\delta\gamma_{xy}(\frac{\partial C}{\partial \gamma_{xy}}-\tau_{xy})+ \\ & +\delta\sigma_z(\frac{\partial C}{\partial \sigma_z}+\varepsilon_z)+\delta\tau_{xz}(\frac{\partial C}{\partial \tau_{xz}}+\gamma_{xz})+\delta\tau_{yz}(\frac{\partial C}{\partial \tau_{yz}}+\gamma_{yz})- \\ & -\delta\sigma_z(\varepsilon_z-\frac{\partial w}{\partial z})-\delta\tau_{xz}(\gamma_{xz}-\frac{\partial u}{\partial z}-\frac{\partial w}{\partial x})-\delta\tau_{yz}(\gamma_{yz}-\frac{\partial v}{\partial z}-\frac{\partial w}{\partial y})\}dv- \\ & -\iint_{S_\sigma} (\bar{T}_x\delta u+\bar{T}_y\delta v+\bar{T}_z\delta w)\, ds=0. \end{aligned} \qquad (2.3.13)$$

Simplifying, we have,

$$\begin{aligned} I = \sum_i \iiint_{V_i} \{ & \delta C+\delta[\sigma_z\frac{\partial w}{\partial z}+\tau_{xz}(\frac{\partial u}{\partial z}+\frac{\partial w}{\partial x})+\tau_{yz}(\frac{\partial v}{\partial z}+\frac{\partial w}{\partial y})]- \\ & -\delta(\bar{F}_x u+\bar{F}_y v+\bar{F}_z w)\}dv- \\ & -\iint_{S_{\sigma i}} \delta(\bar{T}_x u+\bar{T}_y v+\bar{T}_z w)ds=0. \end{aligned} \qquad (2.3.14)$$

It can be seen that the weighted residual integration is a complete variation. Thus, the integral can be

rewritten as the variation of a functional:

$$\Pi_L=\sum_i\{\iiint_{V_i}[C+\sigma_z\frac{\partial w}{\partial z}+\tau_{xz}(\frac{\partial u}{\partial z}+\frac{\partial w}{\partial x})+\tau_{yz}(\frac{\partial v}{\partial z}+\frac{\partial w}{\partial y})-\bar{F}_x u-\bar{F}_y v-\bar{F}_z w]dv\}$$

$$-\iint_{S_\sigma}(\bar{T}_x u+\bar{T}_y v+\bar{T}_z w)ds. \qquad (2.3.15)$$

and, $\delta\Pi_L = 0$ under the conditions (2.2.2, 2.2.7 and 2.2.9).

The author give Π_L the name of laminate functional It can be shown that the process of derivation used above can be reversed step by step. The author introduces the following stationary variational principle of combined energy for solving a laminated composite as follows:

Principle

Among all the sets of admissible displacements u,v,w and admissible stresses $\sigma_z,\tau_{xz},\tau_{yz}$, which possess global continuity and satisfy the prescribed displacement boundary conditions, the partial relation of displacements with strains $\varepsilon_x,\varepsilon_y,\gamma_{xy}$ as well as the continuity condition at the interlayer surfaces, the actual set of $\{u,v,w,\sigma_z,\tau_{xz},\tau_{yz}\}$ can be given by the stationary conditions of the functional Π_L defined in eq.(2.3.15).

The above variational principle can be extended to any elastic body and can be stated as:

Principle

Among all the sets of admissible displacements u,v,w

and admissible stresses $\sigma_z, \tau_{xz}, \tau_{yz}$, which possess global continuity and satisfy the prescribed displacement boundary conditions, the partial relation of displacements with strains ε_x, ε_y, γ_{xy}, the actual set of $\{u, v, w, \sigma_z, \tau_{xz}, \tau_{yz}\}$ can be given by the stationary conditions of the functional Π_L defined as:

$$\Pi_L = \iiint_V [C + \sigma_z \frac{\partial w}{\partial z} + \tau_{xz}(\frac{\partial u}{\partial z} + \frac{\partial w}{\partial x}) + \tau_{yz}(\frac{\partial v}{\partial z} + \frac{\partial w}{\partial y}) - \bar{F}_x u - \bar{F}_y v - \bar{F}_z w] dv$$

$$- \iint_{S_\sigma} (\bar{T}_x u + \bar{T}_y v + \bar{T}_z w) ds. \qquad (2.3.16)$$

It came to the author's attention in the later part of this thesis that Reissner has already done some work along the line of what has been presented earlier in this thesis. In the following discussion, comparison between Reissner's theorems and the author's will be presented.

2.4 Comparison with Reissner's mixed variational theorems

2.4.1 Reissner's mixed variational theorem 1 (1984) [48]

The section "Derivation" from [48] can be quoted as follows:

- "We begin with a statement of the classical variational equation for displacements, for simplicity's sake subject to the assumptions of absent body forces and

traction-free boundary portions $z=\pm h/2$, and of displacement boundary conditions over all cylindrical boundary portions $f(x_1,x_2)=0$. With a view towards our ultimate purpose, we write this equation in the form

$$\delta \iiint U(\varepsilon_{ij},\varepsilon,\gamma_i)dzdx_1dx_2 = 0 \qquad (2.4.1.1)$$

where $\varepsilon_{ij}=(u_{i,j}+u_{j,i})/2$, $\varepsilon=u_{z,z}$ and $\gamma_i=u_{i,z}+u_{z,i}$, for $i,j=1,2$.

To obtain the intended result we begin by rewriting (2.4.1.1), with the help of Lagrange multipliers σ and τ_i, as

$$\delta \iiint \{U+(u_{z,z}-\varepsilon)\sigma+(u_{i,z}+u_{z,i}-\gamma_i)\tau_i\}dzdx_1dx_2=0, \qquad (2.4.1.2)$$

and we separate the function U in this into two parts

$$U(\varepsilon_{ij},\varepsilon,\gamma_i)=U_0(\varepsilon_{ij})+U_1(\varepsilon,\gamma_i,\varepsilon_{ij}) \qquad (2.4.1.3)$$

such that $U_0(\varepsilon_{ij})=U(\varepsilon_{ij},0,0)$ and $U_1=U-U_0$.

We next use three of the Euler equations associated with (2.4.1.2),

$$\sigma=\partial U_1/\partial\varepsilon, \quad \tau_i=\partial U_1/\partial\gamma_i \qquad (2.4.1.4a,b)$$

as three simultaneous equations for the determination of ε, γ_1, γ_2 in the form

$$\varepsilon=\varepsilon(\sigma,\tau_i,\varepsilon_{ij}),\ \gamma_j=\gamma_j(\sigma,\tau_i,\varepsilon_{ij}),$$

and we define a complementary function W through a partial Legendre transformation

$$W(\sigma,\tau_i,\varepsilon_{ij})=\sigma\varepsilon(\sigma,\tau_i,\varepsilon_{ij})+\tau_i\gamma_i(\ldots) - U_1[\varepsilon(\ldots),\gamma_j(\ldots),\varepsilon_{ij}] \qquad (2.4.1.5)$$

where then, in the usual way, $\varepsilon=\partial W/\partial\sigma$ and $\gamma_i=\partial W/\partial\tau_i$.

Introduction of (2.4.1.5) and (2.4.1.3) into (2.4.1.2) gives as the wanted mixed variational theorem the equation

$$\delta \iiint \{U_o(\varepsilon_{ij})+u_{z,z}\sigma+(u_{i,z}+u_{z,i})\tau_i- \\ -W(\sigma,\tau_i,\varepsilon_{ij})\}dzdx_1dx_2=0 \qquad (2.4.1.6)$$

with arbitrary δu_i, δu_z, $\delta\tau_i$, $\delta\sigma$, and with $\delta\varepsilon_{ij}=(\delta u_{i,j}+\delta u_{j,i})/2$.

An alternative version of (2.4.1.6), with the variations $\delta\sigma$ and $\delta\tau_i$ restricted so as to be consistent with constraint conditions $(\sigma,\tau_i)_{z=\pm h/2}=0$ and $\tau_{i,i}+\sigma_{,z}=0$, evidently may be deduced from (2.4.1.6) so as to read

$$\delta \iiint \{U_o-u_i\tau_{i,z}-W\}dzdx_1dx_2=0." \qquad (2.4.1.7)$$

2.4.2 Reissner's mixed variational theorem 2 (1986) [49]

The section "Derivation of the mixed theorem" from [49] can be quoted as:

- "We depart from a statement of the known variational theorem for displacements and all stresses, in the form

$$\delta \iiint [W(\sigma_1,\sigma_2,\sigma_3,\tau_1,\tau_2,\tau_3)- \\ -\sigma_i\varepsilon_i-\tau_i\gamma_i]dzdx_1dx_2=0 \qquad \ldots\ldots (2.4.2.1)$$

Here we have written $\sigma_3,\tau_1,\tau_2,\tau_3$ in place of the conventional τ_{12}, τ_{1z}, τ_{2z} and σ_z, with

$$\varepsilon_1=u_{1,1},\quad \varepsilon_2=u_{2,2},\quad \varepsilon_3=u_{1,2}+u_{2,1}, \\ \gamma_1=u_{1,z}+u_{z,1},\quad \gamma_2=u_{2,z}+u_{z,2},\quad \gamma_3=u_{z,z} \qquad (2.4.2.2)$$

with W a given function, and with the variations $\delta\sigma_i$, $\delta\tau_i$, δu_i, δu_z arbitrary. We assume for simplicity the absence of body forces and we omit consideration of the surface integrals which are associated with a complete statement of the theorem. We recall that (2.4.2.1), with the constraint (or defining) relation (2.4.2.2), has the equations of equilibrium and all constitutive equations as Euler differential equations.

With a view towards the result to be established we now consider the three Euler constitutive equations

$$\varepsilon_i=\partial W/\partial\sigma_i \qquad (2.4.2.3)$$

as equations for the determination of σ_i, and we use the solutions

$$\sigma_i=\sigma_i(\varepsilon_j,\tau_j), \qquad (2.4.2.4)$$

of (2.4.2.3) to define a 'semi-complementary energy density' $V(\varepsilon_j,\tau_j)$ through the 'partial' Legendre transformation

$$V=\varepsilon_i\sigma_i(\varepsilon_j,\tau_j)-W[\sigma_i(\varepsilon_j,\tau_j),\tau_j]. \qquad (2.4.2.5)$$

Equation (2.4.2.5) implies as a subsystem of inverted constitutive equations

$$\sigma_i=\partial V/\partial\varepsilon_i, \qquad (2.4.2.6)$$

with these to be considered, in what follows, as constraint equations.

The introduction of W from (2.4.2.5) into (2.4.2.1)

gives as the desired variational equation for displacements and some stresses

$$\delta \iiint [V(\varepsilon_j,\tau_j)+\tau_j\gamma_j]dzdx_1dx_2=0 \qquad (2.4.2.7)$$

To establish the correctness of our statement it is only necessary to verify that (2.4.2.7), with the constraint equation (2.4.2.6) and (2.4.2.2), does in fact have the three equations of equilibrium and three constitutive equations, giving the γ_i as functions of the τ_j and ε_j, as Euler equations. We obtain this result by deducing first from (2.4.2.7) that

$$\iiint[\frac{\partial V}{\partial \varepsilon_j}\delta\varepsilon_j+\frac{\partial V}{\partial \tau_j}\delta\tau_j+\tau_j\delta\gamma_j+\gamma_j\delta\tau_j]dzdx_1dx_2=0 \qquad (2.4.2.8)$$

and then with (2.4.2.6)

$$\iiint[\sigma_j\delta\varepsilon_j+\tau_j\delta\gamma_j+(\frac{\partial V}{\partial \tau_j}+\gamma_j)\delta\tau_j]dzdx_1dx_2=0 \qquad (2.4.2.9)$$

Equation (2.4.2.9) implies the three Euler constitutive equations

$$\gamma_i=-\partial V/\partial \tau_j, \qquad (2.4.2.10)$$

with the equilibrium equations for stress following as Euler equations upon expressing $\delta\varepsilon_j$, and $\delta\gamma_j$ in terms of $\delta u_{i,k}$, $\delta u_{i,z}$, $\delta u_{z,k}$ and $\delta u_{z,z}$, in accordance with equation (2.4.2.2)."

2.4.3 The comparison with Reissner's theorems

The variational principle of combined energy stated in this thesis gives a general form for the variational method

in laminated structures. Reissner's theorem 1 gives a corresponding potential energy form, and Reissner's theorem 2 gives a corresponding complementary energy form.

All of the three principles have the terms

$$\sigma_z\left(\frac{\partial w}{\partial z}\right) + \tau_{xz}\left(\frac{\partial w}{\partial x}+\frac{\partial u}{\partial z}\right) + \tau_{yz}\left(\frac{\partial w}{\partial y}+\frac{\partial v}{\partial z}\right) \qquad (2.4.3.1)$$

to relieve the C^1 continuity requirement of displacement along z-direction and to satisfy the continuity requirement of transverse stresses.

Because the energy functions are different and the constraint conditions used in the derivation are also different, therefore, in these principles, the Euler equations and natural conditions, enforced a posteriori, are different (see and compare sections 2.3, 2.4.2). Strictly speaking, the three principles are not exactly equivalent to each another.

Reissner's theorem 1 is based on the principle of minimum potential energy, taking the potential energy function $A(\varepsilon)$. By using Lagrange multiplier method, a complementary virtual work is introduced. The required final energy form should be a 'semi-potential energy density' through 'partial' Legendre transformation, from $A(\varepsilon)$ to $A(q)$

$$U_o - W = A(q) - \sigma_z \cdot \varepsilon_z(q) - \tau_{xz} \cdot \gamma_{xz}(q) - \tau_{yz} \cdot \gamma_{yz}(q) \qquad (2.4.3.2)$$

where

$$q = \{ \varepsilon_x, \varepsilon_y, \gamma_{xy}, \sigma_z, \tau_{xz}, \tau_{yz} \}^T \qquad (2.4.3.3)$$

Reissner's theorem 2 is based on the generalized potential energy principle, taking complementary energy function $B(\sigma)$

$$W-\sigma_i \varepsilon i-\tau_i \gamma_i = B(\sigma) - \sigma_{ij} \varepsilon_{ij} \qquad (2.4.3.4)$$

Its required final energy form should be a 'semi-complementary energy density' through 'partial' Legendre transformation, from $B(\sigma)$ to $B(q)$

$$V=-B(q)+\varepsilon_x \cdot \sigma_x(q)+\varepsilon_y \cdot \sigma_y(q)+\gamma_{xy} \cdot \tau_{xy}(q) \qquad (2.4.3.5)$$

Before using the two theorems, it is necessary to derive the partial Legendre transformation for the semi-potential energy density $A(q)$ or the semi-complementary energy density $B(q)$.

It can be seen that the combined energy principle stated in this thesis is complete and clear for both physical understanding and numerical calculations. A summary of the similarities and differences between Reissner's theorems and Huang's principle is shown in the Appendix.

Chapter 3. An Approach to Determination Natural Stress Modes in Hybrid Finite Element

Three-dimensional hybrid finite elements have been developed in recent years [13,30,36,38-47,60,63,72,73]. They are based on the assumed interior stress field and boundary displacement field or mixed interior fields. In this Chapter, attempt is made to determine natural stress modes.
modes definitely.

3.1 Assumed Stress Field in Finite Element Method

In the displacement formulation of the finite element method, the nodal displacements are taken as unknown parameters. The displacement field can be described by using the interpolation function for the nodal displacements.

In the stress or hybrid-stress formulation, the stress field can not be described as above, because the total number of nodal stresses is usually more than the degrees of deformation freedom. In principle, there are not enough control equations to govern all the nodal stresses.

Pian (1964) [37] developed a technique to assume this stress field. In his hybrid finite element method, the assumed stress field consists of several stress modes multiplied by a corresponding stress parameter:

$$\begin{aligned}\sigma &= \beta_1\sigma_1+\beta_2\sigma_2+\ldots+\beta_m\sigma_m \\ &= [\,\sigma_1,\sigma_2,\ldots,\sigma_m]\begin{Bmatrix}\beta_1\\ \beta_2\\ \cdot\\ \cdot\\ \beta_m\end{Bmatrix} \\ &= P\,\beta \qquad (3.1.1)\end{aligned}$$

where

$$P = [\,\sigma_1,\sigma_2,\ldots,\sigma_m],$$

σ_i is a vector and is a function of the coordinates. Also, on the boundary of the element, the displacement field is assumed.

$$u = N\,\delta \qquad (3.1.2)$$

where N is the shape function of displacement and δ is nodal displacement. The strain can be expressed as

$$\varepsilon = B\,\delta \qquad (3.1.3)$$

where B is a first derivative matrix of the shape function.

Since the first development of Pian [37], many modifications have been made. Pian and Tong (1972) [96] based on Hellinger-Reissner principle, proposed a mixed model of the hybrid finite element in which both stress and displacement fields are assumed in the interior of the element. If the prescribed displacement boundary

conditions are satisfied in advance, the Hellinger-Reissner principle can be expressed as

$$\delta \Pi_{HR} = 0 \tag{3.1.4}$$

where

$$\Pi_{HR} = \int_V (-\frac{1}{2}\sigma^T S\sigma + \sigma^T \epsilon - \bar{F}^T u)dv - \int_{S_\sigma} \bar{T}^T u ds \tag{3.1.5}$$

Substituting eqs.(3.1.1, 3.1.2, 3.1.3) into eq.(3.1.5)

$$\begin{aligned}\Pi_{HR} = \int_V (&-\frac{1}{2}\beta^T P^T S P \beta \\ &+ \beta^T P^T B \delta - \delta^T N^T \bar{F})dv \\ &- \int_{S_\sigma} \bar{T}^T u ds \\ = &-\frac{1}{2}\beta^T (\int_V P^T S P dv)\beta + \beta^T (\int_V P^T B dv)\delta \\ &- \delta^T (\int_V N^T \bar{F} dv + \int_{S_\sigma} N^T \bar{T} ds)\end{aligned} \tag{3.1.6}$$

If we define

$$H = \int_V P^T S P \, d\Gamma \tag{3.1.7}$$

$$G = \int_V P^T B \, d\Gamma \tag{3.1.8}$$

$$f = \int_V N^T \bar{F} dv + \int_{S_\sigma} N^T \bar{T} ds \tag{3.1.9}$$

then

$$\Pi_{HR} = -\frac{1}{2}\beta^T H \beta + \beta^T G \delta - \delta^T f \tag{3.1.10}$$

Using partial stationary condition

$$\frac{\partial \Pi_{HR}}{\partial \beta} = 0, \tag{3.1.11}$$

we have

$$\beta = H^{-1}G\delta \tag{3.1.12}$$

Substituting eq.(3.1.12) into functional (3.1.10),

$$\Pi_{HR} = \frac{1}{2}\delta^T(G^TH^{-1}G)\delta - \delta^Tf. \tag{3.1.13}$$

If we define

$$K = G^TH^{-1}G \tag{3.1.14}$$

then

$$\Pi_{HR} = \frac{1}{2}\delta^TK\delta - \delta^Tf \tag{3.1.15}$$

From another partial stationary condition

$$\frac{\partial \Pi_{HR}}{\partial \delta} = 0, \tag{3.1.16}$$

the governing equation of nodal displacement is expressed as follows:

$$K\ \delta = f \tag{3.1.17}$$

The meanings of the matrices introduced above are:

- **K** stiffness matrix in nodal displacement space
- **f** equivalent nodal force
- **H** compliance matrix in stress parameter space
- **G** mapping matrix of stiffness matrix from stress parameter space to nodal displacement space

If the stress modes in matrix **P** are assumed improperly or if the matrix P does not include sufficient modes, the rank of stiffness matrix **K** will be

less than the total degrees of deformation freedom. Thus equation (3.1.17) will be singular and it will not be able to govern the nodal displacements. In this case, the matrix P will contain some zero energy stress modes.

The problem then is how to make a proper selection of the stress field modes.

It is possible to suppress zero energy modes by adding stress field terms of higher order. However, more stress terms cause stiffening of the element and, thus, impair the stress analysis.

Fraeijs de Veubeke (1966) [29], Pian and Tong (1969) [28] gave a necessary, but not sufficient condition condition to avoid the zero energy modes.

$$m \geqslant n-r \qquad (3.1.18)$$

in which m is the total number of assumed stress field modes, n is the total number of generalized displacements, of which at least r must be constrained, r being the number of rigid body degrees of freedom of the element.

Brezzi (1974) [32], Babuska, Oden and Lee (1977) [33], presented necessary and sufficient conditions for stability and convergence of a finite element with an assumed stress field. These conditions are called the Ladyzhenskaya-Babuska-Brezzi conditions.

Ahmad and Irons (1974) [30] suggested use of an eigenvalue technique to assess a hybrid element and determine the kinematic modes.

Spilker et al (1981) [31] stated that matrix G controls the rank of the element stiffness matrix. Later on Spilker (1982) [34] investigated the 3-D hybrid elements and suggested using complete sets of each order of the stress field terms. For example, in the 3-D, 20-noded element, he suggested using the 69β element.

S.N.Atluri et al (1983,1984) [35,36], tried to solve the zero energy mode problem by using symmetric group theory. From the displacement interpolation function, they gave all the possible displacement field modes, then, using the group theory, they gave all the possible strain field modes (54 for 3-D, 20-node element). On the other hand, they gave all the equilibrated stress field modes(90 for up to 3rd-order stress modes). Thus, the displacement, strain and stress could be described by the product of their field modes and their unknown parameters respectively. By checking the integration of the products of the strain and stress modes in each subgroup,

$$\sigma:\varepsilon = \int_V \sigma_{ij}{}^k \varepsilon_{ij}{}^L dv = \begin{cases} 0, & k \neq L \\ \text{nonzero}, & k = L \end{cases} \tag{3.1.19}$$

$$\sigma_{ij} \in \Gamma_k \tag{3.1.20}$$

$$\varepsilon_{ij} \in \Gamma_L \tag{3.1.21}$$

they gave two choices for 2-D, 4-noded hybrid element(5β), 8 choices for 3-D, 8-noded elements(18β),and 384 choices for 3-D, 20-noded elements(54β), where Γ_k, Γ_L represent the subgroups.

Numerical analysis shows that for Atluri's 8 sets of stress modes for 3-D, 8-node hybrid finite element, all result in stiffness matrices with 18 nonzero eigenvalues. Hence zero energy modes do not exist in these 8 choices of stress fields. However, the first 7 choices give low eigenvalues for some high order stress modes. This means the structure is weakened for these 7 choices.

Pian and Chen (1983) [51] showed that the product $\sigma:\varepsilon$ have the physical meaning of deformation energy.

$$2U_d = \int \sigma^T \varepsilon \, dv = \boldsymbol{\beta}^T \mathbf{G} \boldsymbol{\delta} \tag{3.1.22}$$

Furthermore, they decompose the nodal displacement and matrix $\mathbf{G}$ into two parts: one represents the rigid-body modes, $\boldsymbol{\delta}_R$ and $\mathbf{G}_R$, and the other part represents the deformation modes, $\boldsymbol{\delta}_\alpha$ and $\mathbf{G}_\alpha$.

$$2U_d = \boldsymbol{\beta}^T [\mathbf{G}_\alpha, \mathbf{G}_R] \begin{Bmatrix} \boldsymbol{\delta}_\alpha \\ \boldsymbol{\delta}_R \end{Bmatrix} = \boldsymbol{\beta}^T \mathbf{G}_\alpha \boldsymbol{\delta}_\alpha \tag{3.1.23}$$

Then, Pian and Chen provided a systematic procedure for the choice of the necessary assumed stresses such that kinematic deformation modes will not appear. They indicated that an examination of the strain energy due to the applied stresses and due to each individual deformation mode or possible combined modes gives a clue to the existence of kinematic deformation modes and methods for their suppressions. It is necessary to ensure all columns of the G_α matrix in the deformation energy term are linearly independent.

Pian and Sumihara (1985) [97] investigated finite elements with shape distortion, and gave a method to select the assumed stress terms. In this case, the structure of stress mode associated with polynomial terms of coordinates may become more complicated. A selection of these separated terms may be an easy way to extract information for the choice of an assumed stress field that does not contain zero energy modes.

3.2 Modal analysis of deformable bodies with finite degrees of freedom

A finite element has finite degrees of deformation freedom. For each degree of freedom, there may exist a natural deformation mode. Stress modes that are free of zero energy problems should correspond to natural deformation modes. It is therefore necessary to find out the natural deformation modes of the finite element with a certain shape and certain constitutive properties.

In this section, the existence of natural deformation modes is assumed. Also, the energy of the element is assumed to be decomposable into these orthogonal modes. A superposition theorem of stiffness matrix is presented and proved. A postulate about invariance of eigenvalue is suggested. Based on the above assumptions and theory, an eigenvalue analysis technique is developed. It can lead to the correct stress modes in a 2-D, 4-node hybrid finite element of isotropic material with rectangular shape. The results provided by the present element show very good agreement with the elasticity solution.

In 3-D, 8-node hybrid element, a few of eigenvalues are the same. For those multi-eigenvalues, the eigenvectors have certain arbitrariness. It is difficult to find out the natural deformation modes in this ease.

Modal analysis of 3-D, 8-node hybrid element, result in uncoupled set of stress modes yet without zero energy modes. A technique of diagonalization of the compliance matrix H in stress parameter space is utilized, and the invariance of the eigenvalues in the stiffness matrix for the individual and ensemble stress modes is checked.

3.2.1 Natural Deformation Modes

In vibration, a structure has its natural modes. The energy of the structure can be seen as distributed into these separated vibration modes. Also the total number of modes is exactly the same as the vibration degrees of freedom.

In a finite element, the deformation is considered to consist of finite number of degrees of freedom. It is possible that there exists a set of natural deformation modes and the elastic energy of structure can also be distributed into these separate deformation modes. The total number of deformation modes will be the same as the number of degrees of deformation freedom.

In finite element method, for both displacement

formation and hybrid formulation, the governing equation of nodal displacements has the same form

$$\mathbf{K}\,\boldsymbol{\delta} = \mathbf{f} \tag{3.2.1}$$

where

$\mathbf{K}$ Stiffness matrix in nodal displacement space

$\boldsymbol{\delta}$ nodal displacement

$\mathbf{f}$ nodal forces

Here one element is considered as the system, thus, $\mathbf{K}$ is an nxn matrix, $\boldsymbol{\delta}$ and $\mathbf{f}$ are n-dimensional vectors, where n is the total number of generalized displacements.

The following equation,

$$(\mathbf{K}-\lambda\mathbf{I})\,\boldsymbol{\delta} = 0 \tag{3.2.2}$$

gives r zero eigenvalues for rigid body motion and m (m=n-r) nonzero eigenvalues for deformation. There are m eigenvectors corresponding to the n nonzero eigenvalues.

In the displacement formulation of the finite element method, the stiffness matrix $\mathbf{Q}$ is mapped into nodal displacements space:

$$\mathbf{K} = \int_V \mathbf{B}^T\mathbf{Q}\mathbf{B}\,dv \tag{3.2.3}$$

It can be seen that the eigenvalues and eigenvectors only depend on the geometry and elastic properties of the element.

In the hybrid finite element method, the compliance matrix could be mapped into stress parameter space as follows.

$$\mathbf{H} = \int_V \mathbf{P}^T \mathbf{S} \mathbf{P} \, dv \tag{3.2.4}$$

Its inverse, the stiffness matrix, could be further mapped into nodal displacement space.

$$\mathbf{K} = \mathbf{G}^T \mathbf{H}^{-1} \mathbf{G} \tag{3.2.5}$$

in which

$$\mathbf{G} = \int_V \mathbf{P}^T \mathbf{B} \, dv \tag{3.2.6}$$

So the eigenvalues and eigenvectors of the element stiffness matrix are sensitive to the assumed stress field modes and also depend on the geometry and property of the element.

The difficulty is how to get the natural stress modes from the natural displacement modes.

In hybrid formulation, there exists a relation between nodal displacement and stress parameter, eq. (3.1.12). For each deformation mode δ_ν (assume it is an eigenvector of the stiffness matrix in the displacement formulation), the improved stress mode σ_ν can be written as

$$\sigma_\nu = \mathbf{P} \beta_\nu \tag{3.2.7}$$

$$\beta_\nu = H^{-1}G\delta_\nu \qquad (3.2.8)$$

where P, G, H are associated with the old stress

A systematic procedure in the form of a computer program is presented based on the two points mentioned above, first is that the eigenvectors of the stiffness matrix in the displacement formulation depend only on geometry and constitutive properties of the element. These eigenvectors could be assumed to be the natural deformation modes. The other point is that the eigenvalues of the stiffness matrix in hybrid formulation is sensitive to the assumed stress field modes. There is the chance to improve the stiffness matrix to be superpositionable and uncoupled.

3.2.2 Superposition Theorem for the Stiffness Matrix and A Postulate on Energy Decomposition

Theorem: In the hybrid finite element method, if the stress field modes are assumed such that they can result in a diagonal matrix H, then, the stiffness matrix satisfies the superposition principle:

$$K = \sum_i K_i, \qquad (3.2.9)$$

where

$$K_i = G_i^T H_i^{-1} G_i \qquad (3.2.10)$$

$$H_i = \int_V P_i^T S P_i dv \qquad (3.2.11)$$

$$G_i = \int_v P_i^T B dv \tag{3.2.12}$$

$$P = [\ P_1, P_2, \ldots P_i, \ldots P_m\ ] \tag{3.2.13}$$

and

$$K = G^T H^{-1} G \tag{3.2.14}$$

$$H = \int_v P^T S P dv \tag{3.2.15}$$

$$G = \int_v P^T B dv \tag{3.2.17}$$

in which

P_i column vector of P, one mode of the stress field

G_i row vector of G,

H_i compliance matrix in 1β stress parameter space

Proof:

If we denote

$$c_i = 1/H_{ii} \tag{3.2.18}$$

for diagonal matrix H we have

$$H^{-1} = \begin{bmatrix} c_1 & 0 & \ldots & 0 \\ 0 & c_2 & \ldots & 0 \\ \vdots & & \ddots & \vdots \\ 0 & \ldots & & c_m \end{bmatrix} \tag{3.2.19}$$

and

$$H_i^{-1} = [\ c_i\ ] \tag{3.2.20}$$

Then, the stiffness matrix

$$K = [\ G_1^T, G_2^T, \ldots G_m^T] \begin{bmatrix} c_1 & 0 & \ldots & 0 \\ 0 & c_2 & & 0 \\ \vdots & & \ddots & \vdots \\ 0 & \ldots & & c_m \end{bmatrix} \begin{bmatrix} G_1 \\ G_2 \\ \vdots \\ G_m \end{bmatrix}$$

$$= \sum_i G_i{}^T c_i G_i$$

$$= \sum_i G_i{}^T H_i{}^{-1} G_i$$

$$= \sum_i K_i \qquad \text{end of proof.} \qquad (3.2.21)$$

Postulate

If and only if the elastic energy of the structure with finite degrees of freedom is decomposable, the eigenvalues obtained from separate mode equations

$$(K_i - \lambda I)\delta = 0, \quad i=1,2...m \qquad (3.2.22)$$

should be the same as the eigenvalues obtained from the total equation

$$(K - \lambda I)\delta = 0, \qquad (3.2.23)$$

where

K_i stiffness matrix for individual mode, given by equation (3.2.10)

K stiffness matrix for the ensemble of modes, given by (3.2.14)

The alternate postulate can be stated as:

If λ_i is the eigenvalue obtained from eq.(3.2.22) and α_j are the eigenvalues obtained from eq.(3.2.23) for the structure with finite degrees of freedom in a complete set of uncoupled stress modes, there is one and only one

α_i corresponding to λ_i and has the same value as λ_i.

3.3 Modal Analysis of 2-D, 4-node Hybrid Element

3.3.1 Procedure

The procedure of modal analysis for 2-dimensional 4-noded hybrid elements with isotropic elasticity and rectangular shape is as follows.

Step 1. Calculate the eigenvectors of the element stiffness matrix of the displacement finite element:

$$\delta_\nu, \qquad \nu=1,2,\ldots n-r \tag{3.3.1}$$

Step 2. Assume a complete set of the stress field modes

$$P^{(0)} = [\ \sigma_1{}^{(0)},\sigma_2{}^{(0)},\ldots\sigma_L{}^{(0)}\ ], \tag{3.3.2}$$

where

$$L \geqslant n-r \tag{3.3.3}$$

Step 3. For $i=1,2,3,\ldots k$ do step 4 - 6 until the matrix H becomes diagonal and the stress modes P are stationary.

Step 4. Calculate matrix $H^{(i)},G^{(i)}$

$$H^{(i)} = \int_V [p^{(i)}]^T S P^{(i)}\, dv \tag{3.3.4}$$

$$G^{(i)} = \int_V [p^{(i)}]^T B\, dv \tag{3.3.5}$$

Step 5. Modify the stress field modes.

$$\sigma_\nu^{(i)} = P^{(i)}[H^{(i)}]^{-1}G^{(i)}\delta_\nu, \tag{3.3.6}$$

where

$$\nu=1,2,\ldots,n-r \tag{3.3.7}$$

Step 6. Square-power normalization of the stress field modes.

$$v_\nu^{(i)} = \sigma_\nu^{(i)}/\sqrt{\sigma_\nu^{(i)}\sigma_\nu^{(i)}} \tag{3.3.8}$$

$$\sigma_\nu^{(i+1)} = v_\nu^{(i)}/\max_\nu(|v_\nu^{(i)}|) \tag{3.3.9}$$

$$P^{(i+1)}=[\sigma_1^{(i+1)},\sigma_2^{(i+1)},\ldots,\sigma_{n-r}^{(i+1)}] \tag{3.3.10}$$

Step 7. Obtain the stress modes.

$$P = P^{(k)} \tag{3.3.11}$$

Step 8. Calculate the compliance and mapping matrix.

$$H = \int_V P^T S P dv \tag{3.3.12}$$

$$G = \int_V P^T B dv \tag{3.3.13}$$

Step 9. Solve the following equation with multiple right hand terms for the unknown matrix [X].

$$H[X] = G \tag{3.3.14}$$

we have

$$[X] = H^{-1}G. \tag{3.3.15}$$

Step 10. Calculate the element stiffness matrix.

$$K = G^T[X] = G^T H^{-1} G \tag{3.3.16}$$

Step 11. Considering boundary conditions, solve the governing equation.

$$\mathbf{K}\,\boldsymbol{\delta} = \mathbf{f} \tag{3.3.17}$$

in which f is the equivalent nodal force of loading.

Step 12. Calculate the stress parameters and stresses.

$$\boldsymbol{\beta} = \mathbf{H}^{-1}\mathbf{G}\,\boldsymbol{\delta} \tag{3.3.18}$$

$$\boldsymbol{\sigma} = \mathbf{P}\,\boldsymbol{\beta} \tag{3.3.19}$$

In the above procedure, two additional considerations were given:

(1). Modification of the eigenvectors for multiple eigenvalues.

For multiple eigenvalues, there are a lot of choices for the directions of the corresponding eigenvectors. However, not every choice can result in a good stress mode which gives a diagonal matrix **H** and superpositionable element stiffness matrix **K**. This means that for multiple eigenvalues the orthogonal displacement eigenvectors may or may not result in orthogonal stress modes.

For example, from numerical results the following two eigenvectors, shown in Fig. 3.1, have the same eigenvalues.

$$\delta_{v1} = \{0.,-.5,.5,0.,0.,.5,-.5,0.\}^T \quad (3.3.20)$$

$$\delta_{v2} = \{-.5,0.,0.,-.5,.5,0.,0.,.5\}^T \quad (3.3.21)$$

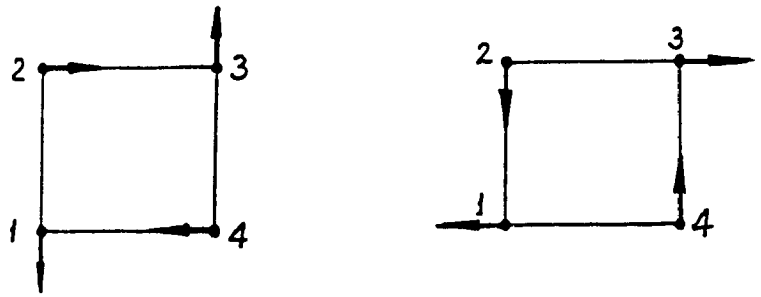

δ_{v1} δ_{v2}

Fig. 3.1 Two original eigenvectors

They can be modified as follows and shown in Fig. 3.2.

$$\hat{\delta}_{v1} = .5(\delta_{v1}+\delta_{v2}) \quad (3.3.22)$$

$$\hat{\delta}_{v2} = .5(\delta_{v1}-\delta_{v2}) \quad (3.3.23)$$

thus,

$$\hat{\delta}_{v1}=\{-.25,-.25,.25,-.25,.25,.25,-.25,.25\}^T \quad (3.3.24)$$

$$\hat{\delta}_{v2}=\{.25,-.25,.25,.25,-.25,.25,-.25,-.25\}^T \quad (3.3.25)$$

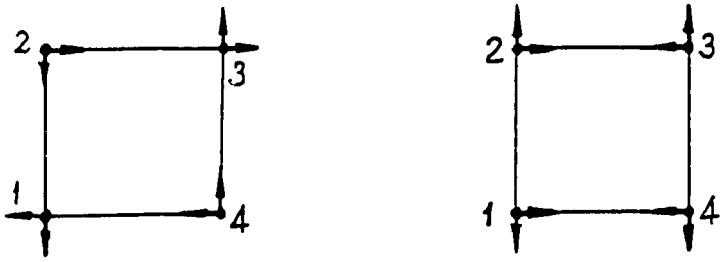

$\hat{\delta}_{v1}$ $\hat{\delta}_{v2}$

pure shear antisymmetric extension

Fig. 3.2 Modified eigenvector

Then, the following stress modes are derived from them, as

$$\sigma_{v1} = \{\ 0,\ 0,1\ \}^T \qquad (3.3.26)$$

$$\sigma_{v2} = \{\ 1,-1,0\ \}^T \qquad (3.3.27)$$

(2). The computation is always accompanied with some accumulated errors. In the 12 step iteration procedure, the stress mode is not sensitive to small errors. Therefore, small numbers which give a relatively small errors can be ignored. In addition, the nondimensionalization and normalization techniques are applied. Thus, the purification consists simply of ignoring terms of magnitude less than 10^{-20}.

3.3.2 Results

By using the displacement finite element, the computation accuracy of the hydrostatic, antisymmetric extension, and pure shear cases is perfect. Only the pure bending is poor. Denote the ratio of the numerical solution to the elasticity solution of pure bending deformation as R_b, this ratio could be taken as the index mark for the different formulations in 2-D, 4-node finite elements.

For the displacement finite element,

$$R_b = 67.4\%$$

For hybrid finite element:

Example 1.

$$p^{(0)} = \begin{bmatrix} 1 & 1 & 0 & \eta & 0 & 0 & -\xi \\ 1 & -1 & 0 & 0 & \xi & -\eta & 0 \\ 0 & 0 & 1 & 0 & 0 & \xi & \eta \end{bmatrix}, \qquad R_b^{(0)}=87.7\%$$

$$p^{(1)} = \begin{bmatrix} -\eta & .045\xi & 0 & 1 & -1 \\ .045\eta & -\xi & 0 & -1 & -1 \\ -.045\xi & -.045\eta & 1 & 0 & 0 \end{bmatrix}, \qquad R_b^{(1)}=94.7\%$$

$$p^{(2)} = \begin{bmatrix} -\eta & .002\xi & 0 & 1 & -1 \\ .002\eta & -\xi & 0 & -1 & -1 \\ -.002\xi & -.002\eta & 1 & 0 & 0 \end{bmatrix}, \qquad R_b^{(2)}=99.7\%$$

$$p^{(3)} = \begin{bmatrix} -\eta & 4E\text{-}6\xi & 0 & 1 & -1 \\ 4E\text{-}6\eta & -\xi & 0 & -1 & -1 \\ -4E\text{-}6\xi & -4E\text{-}6\eta & 1 & 0 & 0 \end{bmatrix}, \qquad R_b^{(3)}=99.999\%$$

$$p^{(4)} = \begin{bmatrix} -\eta & 2E\text{-}11\xi & 0 & 1 & -1 \\ 2E\text{-}11\eta & -\xi & 0 & -1 & -1 \\ -2E\text{-}11\xi & -2E\text{-}11\eta & 1 & 0 & 0 \end{bmatrix}, \qquad R_b^{(4)}=100.0\%$$

$$p^{(5)} = \begin{bmatrix} -\eta & 0 & 0 & 1 & -1 \\ 0 & -\xi & 0 & -1 & -1 \\ 0 & 0 & 1 & 0 & 0 \end{bmatrix}, \qquad R_b^{(5)}=100\%$$

Example 2.

$$p^{(0)} = \begin{bmatrix} 1 & 1 & 0 & \xi & 0 & 0 & \eta & 0 & 0 \\ 1 & -1 & 0 & 0 & \xi & 0 & 0 & \eta & 0 \\ 0 & 0 & 1 & 0 & 0 & \xi & 0 & 0 & \eta \end{bmatrix}, \qquad R_b^{(0)}=67.4\%$$

$$p^{(1)} = \begin{bmatrix} -\eta & .09\xi & 0 & 1 & -1 \\ .09\eta & -\xi & 0 & -1 & -1 \\ -.12\xi & -.12\eta & 1 & 0 & 0 \end{bmatrix}, \qquad R_b^{(1)}=78.8\%$$

$$p^{(2)} = \begin{bmatrix} -\eta & -.008\xi & 0 & 1 & -1 \\ -.008\eta & -\xi & 0 & -1 & -1 \\ -.015\xi & -.015\eta & 1 & 0 & 0 \end{bmatrix}, \qquad R_b^{(2)}=96.7\%$$

$$p^{(3)} = \begin{bmatrix} -\eta & -6E\text{-}5\xi & 0 & 1 & -1 \\ -6E\text{-}5\eta & -\xi & 0 & -1 & -1 \\ -2E\text{-}4\xi & -2E\text{-}4\eta & 1 & 0 & 0 \end{bmatrix}, \qquad R_b^{(3)}=99.95\%$$

$$P^{(4)} = \begin{bmatrix} -\eta & -4E\text{-}9\xi & 0 & 1 & -1 \\ -4E\text{-}9\eta & -\xi & 0 & -1 & -1 \\ -5E\text{-}8\xi & -5E\text{-}8\eta & 1 & 0 & 0 \end{bmatrix}, \quad R_b^{(4)}=100.0\%$$

$$\vdots$$

$$P^{(7)} = \begin{bmatrix} -\eta & 0 & 0 & 1 & -1 \\ 0 & -\xi & 0 & -1 & -1 \\ 0 & 0 & 1 & 0 & 0 \end{bmatrix}, \quad R_b^{(7)}=100\%$$

The comparison of displacements obtained by FEM with the elasticity solution is as follows.

Table 3.1 Comparison of 2-D, 4-node FEM

	hydrostatic pressure	pure extension	pure shear	pure bending	concentrated load beam
Atluri.1	100%	100%	100%	360%	346.5%
Atluri.2	100%	100%	100%	100%	99.3%
Present	100%	100%	100%	100%	99.3%
Displa.	100%	100%	100%	67.4%	68.2%

Note 1:

Atluri's 2-D, 4-Node element:

Choice 1.

$$P = \begin{bmatrix} 1 & 1 & 0 & 0 & -x \\ 1 & -1 & 0 & -y & 0 \\ 0 & 0 & 1 & x & y \end{bmatrix} \qquad (3.3.28)$$

Choice 2.

$$P = \begin{bmatrix} 1 & 1 & 0 & y & 0 \\ 1 & -1 & 0 & 0 & x \\ 0 & 0 & 1 & 0 & 0 \end{bmatrix} \qquad (3.3.29)$$

Pian's 2-D, 4-Node element:

$$\mathbf{P} = \begin{bmatrix} 1 & 0 & 0 & y & 0 \\ 0 & 1 & 0 & 0 & x \\ 0 & 0 & 1 & 0 & 0 \end{bmatrix} \tag{3.3.30}$$

Present 2-D, 4-Node elemer.:

$$\mathbf{P} = \begin{bmatrix} 1 & 1 & 0 & \eta & 0 \\ 1 & -1 & 0 & 0 & \xi \\ 0 & 0 & 1 & 0 & 0 \end{bmatrix} \tag{3.3.31}$$

in which

$$x = x_0 + a_1 \xi$$

$$y = y_0 + a_2 \eta \tag{3.3.32}$$

Note 2: The theoretical solution of a cantilever beam under concentrated load at the free end of the beam is taken from "Theory of Elasticity" by S.Timoshenko.

Usually, it takes time to form the element stiffness matrix in finite element method. However, for a rectangular element, it is possible to calculate the element stiffness matrix in advance, if the formulation is in nondimensional form. Especially, for 2-D, 4-node hybrid rectangular element, the nondimensional element stiffness matrix **K** and matrix **E**, **G** can be given by formula. (see [98] Froier, 1974). Using superposition theorem, the **E**, **G**, **K** matrices of 2-D, 4-node rectangular hybrid finite element with isotropic elasticity can be calculated by hand, and is shown next.

The element stiffness matrix K of present rectangular elements with isotropic elasticity is as follows.

$$K=ck\begin{bmatrix} s_1+r_1 & m_1 & s_1-r_2 & -m_2 & -s_1-t_1 & -m_1 & -s_1+t_2 & m_2 \\ m_1 & r_1+s_2 & m_2 & t_1-s_2 & -m_1 & -t_1-s_2 & -m_2 & -r_1+s_2 \\ s_1-r_2 & m_2 & s_1+r_2 & -m_2 & -s_1+t_2 & -m_2 & -s_1-t_2 & m_1 \\ -m_2 & t_1-s_2 & -m_2 & r_1+s_2 & m_2 & -r_1+s_2 & m_1 & -t_1-s_2 \\ -s_1-t_2 & -m_1 & -s_1+t_2 & m_2 & s_1+t_2 & m_2 & s_1-r_2 & -m_2 \\ -m_1 & -t_1-s_2 & -m_2 & -r_1-s_2 & m_1 & r_1+s_2 & m_2 & t_1-s_2 \\ -s_1+t_2 & -m_2 & -s_1-t_2 & m_1 & s_1-r_2 & m_2 & s_1+r_2 & -m_1 \\ m_2 & -r_1+s_2 & m_1 & -t_1-s_2 & -m_2 & t_1-s_2 & -m_1 & r_1+s_2 \end{bmatrix}$$

..... (3.3.33)

in which

$s_1=3c_1(1-\nu)$ $\quad$ $s_2=3c_2(1-\nu)$

$t_1=2c_1(2+\nu^2)$ $\quad$ $t_2=2c_2(2+\nu^2)$

$r_1=2c_1(4-\nu^2)$ $\quad$ $r_2=2c_2(4-\nu^2)$

$m_1=3(1+\nu)$ $\quad$ $m_2=3(1-3\nu)$

$ck=E/24(1-\nu^2)$

where

$c_1=a_1/a_2$ $\quad$ $c_2=a_2/a_1$

$x=x_0+a_1\xi$ $\quad$ $y=y_0+a_2\eta$

The compliance matrix in stress parameter space, **H**, is

$$\mathbf{H} = \frac{8a_1a_2}{E}\begin{bmatrix} 1-\nu & 0 & 0 & 0 & 0 \\ 0 & 1+\nu & 0 & 0 & 0 \\ 0 & 0 & 1+\nu & 0 & 0 \\ 0 & 0 & 0 & 1/6 & 0 \\ 0 & 0 & 0 & 0 & 1/6 \end{bmatrix} \tag{3.3.34}$$

and the mapping transformation matrix **G** is

$$\mathbf{G} = \begin{bmatrix} -a_2 & -a_1 & a_2 & -a_1 & a_2 & a_1 & -a_2 & a_1 \\ -a_2 & a_1 & a_2 & a_1 & a_2 & -a_1 & -a_2 & -a_1 \\ -a_1 & -a_2 & -a_1 & a_2 & a_1 & a_2 & a_1 & -a_2 \\ a_2/3 & 0 & -a_2/3 & 0 & a_2/3 & 0 & -a_2/3 & 0 \\ 0 & a_1/3 & 0 & -a_1/3 & 0 & a_1/3 & 0 & -a_1/3 \end{bmatrix} \tag{3.3.35}$$

3.4 Modal Analysis of 3-D, 8-node Hybrid Element

First, the nondimensional quantities are as follows.

$$c_1 = a_1/a_1 = 1 \tag{3.4.1}$$

$$c_2 = a_2/a_1 \tag{3.4.2}$$

$$c_3 = a_3/a_1 \tag{3.4.3}$$

$$\tilde{x} = x/a_1 \tag{3.4.4}$$

$$\tilde{x} = \tilde{x}_o + c_1\xi \tag{3.4.5}$$

$$\tilde{y} = \tilde{y}_o + c_2\eta \tag{3.4.6}$$

$$\tilde{z} = \tilde{z}_o + c_3\zeta \tag{3.4.7}$$

$$|J| = c_1c_2c_3 \tag{3.4.8}$$

$$\tilde{\delta} = \delta/a_1 \tag{3.4.9}$$

$$\tilde{\sigma} = \sigma/E \tag{3.4.10}$$

$$\tilde{B} = a_1 B \tag{3.4.11}$$

$$\tilde{G} = G/Ea_1^2 = \int_V \tilde{P}^T \tilde{B} |J| d\xi d\eta d\zeta \tag{3.4.12}$$

$$\tilde{H} = H/Ea_1^3 = \int_V \tilde{P}^T \tilde{S} \tilde{P} |J| d\xi d\eta d\zeta \tag{3.4.13}$$

$$\tilde{K} = K/Ea_1 = \tilde{G}^T \tilde{H}^{-1} \tilde{G} \tag{3.4.14}$$

in which

$$\tilde{S} = ES = \begin{bmatrix} 1 & -\nu & -\nu & 0 & 0 & 0 \\ -\nu & 1 & -\nu & 0 & 0 & 0 \\ -\nu & -\nu & 1 & 0 & 0 & 0 \\ 0 & 0 & 0 & 2(1+\nu) & 0 & 0 \\ 0 & 0 & 0 & 0 & 2(1+\nu) & 0 \\ 0 & 0 & 0 & 0 & 0 & 2(1+\nu) \end{bmatrix} \tag{3.4.15}$$

$$\tilde{B} = [\ (\partial N_1), (\partial N_2), \ldots (\partial N_n)\ ] \tag{3.4.16}$$

where

$$(\partial N_i) = \begin{bmatrix} \frac{1}{c_1}\frac{\partial N_i}{\partial \xi} & 0 & 0 \\ 0 & \frac{1}{c_2}\frac{\partial N_i}{\partial \eta} & 0 \\ 0 & 0 & \frac{1}{c_3}\frac{\partial N_i}{\partial \zeta} \\ \frac{1}{c_2}\frac{\partial N_i}{\partial \eta} & \frac{1}{c_1}\frac{\partial N_i}{\partial \xi} & 0 \\ 0 & \frac{1}{c_3}\frac{\partial N_i}{\partial \zeta} & \frac{1}{c_2}\frac{\partial N_i}{\partial \eta} \\ \frac{1}{c_3}\frac{\partial N_i}{\partial \zeta} & 0 & \frac{1}{c_1}\frac{\partial N_i}{\partial \xi} \end{bmatrix}$$

Similar to the modal analysis of 2-D, 4-noded hybrid elements, the following stress modes are obtained which satisfy the requirement of:

(1) Having a diagonal compliance matrix in stress parameter space, H:

(2) Having a stiffness matrix which is adaptable to

superposition principle in nodal displacement space, **K**:

(3) Having non-zero eigenvalues totalling n-r=18:

(4) Having the same eigenvalue for each mode in the individual case $\mathbf{K}_i$ and in the ensemble case **K**.

Hydrostatic mode

$$\sigma_1 = \begin{Bmatrix} 1 \\ 1 \\ 1 \\ 0 \\ 0 \\ 0 \end{Bmatrix} \tag{3.4.17}$$

Antisymmetric extension mode

$$\{ \sigma_2, \sigma_3 \} = \begin{Bmatrix} 1 & -1 \\ -1 & -1 \\ 0 & 2 \\ 0 & 0 \\ 0 & 0 \\ 0 & 0 \end{Bmatrix} \tag{3.4.18}$$

Pure shear mode

$$\{ \sigma_4, \sigma_5, \sigma_6 \} = \begin{Bmatrix} 0 & 0 & 0 \\ 0 & 0 & 0 \\ 0 & 0 & 0 \\ 1 & 0 & 0 \\ 0 & 1 & 0 \\ 0 & 0 & 1 \end{Bmatrix} \tag{3.4.19}$$

Symmetric bending mode

$$\{ \sigma_7, \sigma_8, \sigma_9 \} = \begin{Bmatrix} \zeta & 0 & \eta \\ \zeta & \xi & 0 \\ 0 & \xi & \eta \\ 0 & 0 & 0 \\ 0 & 0 & 0 \\ 0 & 0 & 0 \end{Bmatrix} \tag{3.4.20}$$

Anti-symmetric bending mode

$$\{\ \sigma_{10},\sigma_{11},\sigma_{12}\ \} = \begin{Bmatrix} \zeta & 0 & \eta \\ -\zeta & \xi & 0 \\ 0 & -\xi & -\eta \\ 0 & 0 & 0 \\ 0 & 0 & 0 \\ 0 & 0 & 0 \end{Bmatrix} \tag{3.4.21}$$

Symmetric torsion mode

$$\sigma_{13} = \begin{Bmatrix} 0 \\ 0 \\ 0 \\ \zeta \\ \xi \\ \eta \end{Bmatrix} \tag{3.4.22}$$

Antisymmetric torsion mode

$$\{\ \sigma_{14},\sigma_{15}\ \} = \begin{Bmatrix} 0 & 0 \\ 0 & 0 \\ 0 & 0 \\ \zeta & \zeta \\ -\xi & \xi \\ 0 & -2\eta \end{Bmatrix} \tag{3.4.23}$$

Saddle distributed mode

$$\{\ \sigma_{16},\sigma_{17},\sigma_{18}\ \} = \begin{Bmatrix} \eta\zeta & 0 & 0 \\ 0 & \xi\zeta & 0 \\ 0 & 0 & \xi\eta \\ 0 & 0 & 0 \\ 0 & 0 & 0 \\ 0 & 0 & 0 \end{Bmatrix} \tag{3.4.24}$$

The various stress cases can be formed by combining the above modes, for example, the arbitrary tensile stresses by $\sigma_1,\sigma_2,\sigma_3$: the arbitrary bending by σ_7 - σ_{12}: the arbitrary torsion by σ_{13} - σ_{15}.

The antisymmetric extensions have the same eigenvalue as the pure shears, because by rotating 45^{o} it is a pure shear exactly.

Atluri et al [35,36] gave eight choices of the stress field for the 3-D, 8-node hybrid elements according to the group theory. They assumed stress fields as follows:

Choice 1

$$P=\begin{bmatrix}
1 & 1 & 0 & 0 & 0 & 0 & 0 & 0 & 0 & 2x & 0 & 0 & 0 & 0 & 0 & 0 & 0 & 0 \\
1 & -1 & 1 & 0 & 0 & 0 & 0 & 0 & 0 & 0 & 2y & 0 & 0 & 0 & 0 & 0 & 0 & 0 \\
1 & 0 & -1 & 0 & 0 & 0 & 0 & 0 & 0 & 0 & 0 & 2z & 0 & 0 & 0 & 0 & 0 & 0 \\
0 & 0 & 0 & 1 & 0 & 0 & z & z & 0 & -y & -x & 0 & y & x & 0 & -2xz & -2yz & x^2+y^2 \\
0 & 0 & 0 & 0 & 1 & 0 & x & -x & -x & 0 & -z & -y & 0 & -z & -y & y^2+z^2 & -2xy & -2xz \\
0 & 0 & 0 & 0 & 0 & 1 & y & 0 & y & -z & 0 & -x & -z & 0 & x & -2xy & x^2+z^2 & -2yz
\end{bmatrix}$$

..... (3.4.25)

Choice 2

$$P=\begin{bmatrix}
1 & 1 & 0 & 0 & 0 & 0 & 0 & 0 & 0 & 2x & 0 & 0 & 0 & 0 & 0 & 0 & 0 & yz \\
1 & -1 & 1 & 0 & 0 & 0 & 0 & 0 & 0 & 0 & 2y & 0 & 0 & 0 & 0 & 0 & xz & 0 \\
1 & 0 & -1 & 0 & 0 & 0 & 0 & 0 & 0 & 0 & 0 & 2z & 0 & 0 & 0 & xy & 0 & 0 \\
0 & 0 & 0 & 1 & 0 & 0 & z & z & 0 & -y & -x & 0 & y & x & 0 & 0 & 0 & 0 \\
0 & 0 & 0 & 0 & 1 & 0 & x & -x & -x & 0 & -z & -y & 0 & -z & -y & 0 & 0 & 0 \\
0 & 0 & 0 & 0 & 0 & 1 & y & 0 & y & -z & 0 & -x & -z & 0 & x & 0 & 0 & 0
\end{bmatrix}$$

..... (3.4.26)

Choice 3

$$P=\begin{bmatrix}
1 & 1 & 0 & 0 & 0 & 0 & 0 & 0 & 0 & 2x & 0 & 0 & y & 0 & z & 0 & 0 & 0 \\
1 & -1 & 1 & 0 & 0 & 0 & 0 & 0 & 0 & 0 & 2y & 0 & 0 & x & -z & 0 & 0 & 0 \\
1 & 0 & -1 & 0 & 0 & 0 & 0 & 0 & 0 & 0 & 0 & 2z & -y & -x & 0 & 0 & 0 & 0 \\
0 & 0 & 0 & 1 & 0 & 0 & z & z & 0 & -y & -x & 0 & 0 & 0 & 0 & -2xz & -2yz & x^2+y^2 \\
0 & 0 & 0 & 0 & 1 & 0 & x & -x & -x & 0 & -z & -y & 0 & 0 & 0 & y^2+z^2 & -2xy & -2xz \\
0 & 0 & 0 & 0 & 0 & 1 & y & 0 & y & -z & 0 & -x & 0 & 0 & 0 & -2xy & x^2+z^2 & -2yz
\end{bmatrix}$$

..... (3.4.27)

Choice 4

$$P = \begin{bmatrix} 1 & 1 & 0 & 0 & 0 & 0 & 0 & 0 & 0 & 2x & 0 & 0 & y & 0 & z & 0 & 0 & yz \\ 1 & -1 & 1 & 0 & 0 & 0 & 0 & 0 & 0 & 0 & 2y & 0 & 0 & x & -z & 0 & xz & 0 \\ 1 & 0 & -1 & 0 & 0 & 0 & 0 & 0 & 0 & 0 & 0 & 2z & -y & -x & 0 & xy & 0 & 0 \\ 0 & 0 & 0 & 1 & 0 & 0 & z & z & 0 & -y & -x & 0 & 0 & 0 & 0 & 0 & 0 & 0 \\ 0 & 0 & 0 & 0 & 1 & 0 & x & -x & -x & 0 & -z & -y & 0 & 0 & 0 & 0 & 0 & 0 \\ 0 & 0 & 0 & 0 & 0 & 1 & y & 0 & y & -z & 0 & -x & 0 & 0 & 0 & 0 & 0 & 0 \end{bmatrix}$$

..... (3.4.28)

Choice 5

$$P = \begin{bmatrix} 1 & 1 & 0 & 0 & 0 & 0 & 0 & 0 & 0 & y & 0 & z & 0 & 0 & 0 & 0 & 0 & 0 \\ 1 & -1 & 1 & 0 & 0 & 0 & 0 & 0 & 0 & 0 & x & z & 0 & 0 & 0 & 0 & 0 & 0 \\ 1 & 0 & -1 & 0 & 0 & 0 & 0 & 0 & 0 & y & x & 0 & 0 & 0 & 0 & 0 & 0 & 0 \\ 0 & 0 & 0 & 1 & 0 & 0 & z & z & 0 & 0 & 0 & 0 & y & x & 0 & -2xz & -2yz & x^2+y^2 \\ 0 & 0 & 0 & 0 & 1 & 0 & x & -x & -x & 0 & 0 & 0 & 0 & -z & -y & y^2+z^2 & -2xy & -2xz \\ 0 & 0 & 0 & 0 & 0 & 1 & y & 0 & y & 0 & 0 & 0 & -z & 0 & x & -2xy & x^2+z^2 & -2yz \end{bmatrix}$$

..... (3.4.29)

Choice 6

$$P = \begin{bmatrix} 1 & 1 & 0 & 0 & 0 & 0 & 0 & 0 & 0 & y & 0 & z & 0 & 0 & 0 & 0 & 0 & yz \\ 1 & -1 & 1 & 0 & 0 & 0 & 0 & 0 & 0 & 0 & x & z & 0 & 0 & 0 & 0 & xz & 0 \\ 1 & 0 & -1 & 0 & 0 & 0 & 0 & 0 & 0 & y & x & 0 & 0 & 0 & 0 & xy & 0 & 0 \\ 0 & 0 & 0 & 1 & 0 & 0 & z & z & 0 & 0 & 0 & 0 & y & x & 0 & 0 & 0 & 0 \\ 0 & 0 & 0 & 0 & 1 & 0 & x & -x & -x & 0 & 0 & 0 & 0 & -z & -y & 0 & 0 & 0 \\ 0 & 0 & 0 & 0 & 0 & 1 & y & 0 & y & 0 & 0 & 0 & -z & 0 & x & 0 & 0 & 0 \end{bmatrix}$$

..... (3.4.30)

Choice 7

$$P = \begin{bmatrix} 1 & 1 & 0 & 0 & 0 & 0 & 0 & 0 & 0 & y & 0 & z & y & 0 & z & 0 & 0 & 0 \\ 1 & -1 & 1 & 0 & 0 & 0 & 0 & 0 & 0 & 0 & x & z & 0 & x & -z & 0 & 0 & 0 \\ 1 & 0 & -1 & 0 & 0 & 0 & 0 & 0 & 0 & y & x & 0 & -y & -x & 0 & 0 & 0 & 0 \\ 0 & 0 & 0 & 1 & 0 & 0 & z & z & 0 & 0 & 0 & 0 & 0 & 0 & 0 & -2xz & -2yz & x^2+y^2 \\ 0 & 0 & 0 & 0 & 1 & 0 & x & -x & -x & 0 & 0 & 0 & 0 & 0 & 0 & y^2+z^2 & -2xy & -2xz \\ 0 & 0 & 0 & 0 & 0 & 1 & y & 0 & y & 0 & 0 & 0 & 0 & 0 & 0 & -2xy & x^2+z^2 & -2yz \end{bmatrix}$$

..... (3.4.31)

Choice 8

$$P = \begin{bmatrix} 1 & 1 & 0 & 0 & 0 & 0 & 0 & 0 & 0 & y & 0 & z & y & 0 & z & 0 & 0 & yz \\ 1 & -1 & 1 & 0 & 0 & 0 & 0 & 0 & 0 & 0 & x & z & 0 & x & -z & 0 & xz & 0 \\ 1 & 0 & -1 & 0 & 0 & 0 & 0 & 0 & 0 & y & x & 0 & -y & -x & 0 & xy & 0 & 0 \\ 0 & 0 & 0 & 1 & 0 & 0 & z & z & 0 & 0 & 0 & 0 & 0 & 0 & 0 & 0 & 0 & 0 \\ 0 & 0 & 0 & 0 & 1 & 0 & x & -x & -x & 0 & 0 & 0 & 0 & 0 & 0 & 0 & 0 & 0 \\ 0 & 0 & 0 & 0 & 0 & 1 & y & 0 & y & 0 & 0 & 0 & 0 & 0 & 0 & 0 & 0 & 0 \end{bmatrix}$$

..... (3.4.32)

The assumed stress field of Pian's 3-D, 8-node element is:

$$P = \begin{bmatrix} 1 & 0 & 0 & 0 & 0 & 0 & y & z & yz & 0 & 0 & 0 & 0 & 0 & 0 & 0 & 0 & 0 \\ 0 & 1 & 0 & 0 & 0 & 0 & 0 & 0 & 0 & x & z & zx & 0 & 0 & 0 & 0 & 0 & 0 \\ 0 & 0 & 1 & 0 & 0 & 0 & 0 & 0 & 0 & 0 & 0 & 0 & y & x & xy & 0 & 0 & 0 \\ 0 & 0 & 0 & 1 & 0 & 0 & 0 & 0 & 0 & 0 & 0 & 0 & 0 & 0 & 0 & 0 & z & 0 \\ 0 & 0 & 0 & 0 & 1 & 0 & 0 & 0 & 0 & 0 & 0 & 0 & 0 & 0 & 0 & 0 & 0 & x \\ 0 & 0 & 0 & 0 & 0 & 1 & 0 & 0 & 0 & 0 & 0 & 0 & 0 & 0 & 0 & y & 0 & 0 \end{bmatrix}$$

..... (3.4.33)

The stress modes represented in this thesis is

$$P = \begin{bmatrix} 1 & 1 & -1 & 0 & 0 & 0 & \zeta & 0 & \eta & \zeta & 0 & \eta & 0 & 0 & 0 & \eta\zeta & 0 & 0 \\ 1 & -1 & -1 & 0 & 0 & 0 & \zeta & \xi & 0 & -\zeta & \xi & 0 & 0 & 0 & 0 & 0 & \xi\zeta & 0 \\ 1 & 0 & 2 & 0 & 0 & 0 & 0 & \xi & \eta & 0 & -\xi & -\eta & 0 & 0 & 0 & 0 & 0 & \xi\eta \\ 0 & 0 & 0 & 1 & 0 & 0 & 0 & 0 & 0 & 0 & 0 & 0 & \zeta & \zeta & \zeta & 0 & 0 & 0 \\ 0 & 0 & 0 & 0 & 1 & 0 & 0 & 0 & 0 & 0 & 0 & 0 & \xi & -\xi & \xi & 0 & 0 & 0 \\ 0 & 0 & 0 & 0 & 0 & 1 & 0 & 0 & 0 & 0 & 0 & 0 & \eta & 0 & -2\eta & 0 & 0 & 0 \end{bmatrix}$$

..... (3.4.34)

The advantage of present element over the others is that each stress mode corresponds to one eigenvalue of the stiffness matrix **K**. This eigenvalue is the same with the eigenvalue of the matrix K_i, which is resulted in only by the one stress mode. Each eigenvalue thus corresponds to a single stress mode without any energy coupling between these different stress modes.

The eigenvalue analysis shows that the Atluri's first 7 choices give low eigenvalues for some high order terms. These are not zero which satisfy nonzero requirement, but the structure is weakened. The eigenvalues of 8th choice agree with that of Pian and the author.

Further examination of the diagonalization of the compliance matrix H shows that only the author's method results in complete diagonalization lead to complete decomposition of the elasticity energy.

Chapter 4 Composite Finite Element for Stress Analysis of Laminate Structures

A 3-D, 8-node composite finite element is formulated based on the variational principle of combined energy with an incorporation of the modal analysis technique for a deformable body. It is suitable for stress analysis of laminate structures.

4.1 derivation procedure

The variational principle of combined energy presented in Chapter 2 can be expressed as the laminate functional taking a stationary value under the constraint conditions represented by eqs. (2.2.2, 2.2.7 and 2.2.9), i.e.

$$\Pi_L=\int_V (\frac{1}{2}q^T R q+\sigma_g{}^T e_L-\bar{F}^T u)dv-\int_{S_\sigma} \bar{T}^T u ds \tag{4.1.1}$$

$$\delta\Pi_L = 0 \tag{4.1.2}$$

in which

$$u = N\delta \tag{4.1.3}$$

$$\sigma_g = P_g\beta \tag{4.1.4}$$

$$q = \begin{Bmatrix} \varepsilon_g \\ \sigma_g \end{Bmatrix} \tag{4.1.5}$$

$$\mathbf{R} = \begin{bmatrix} \mathbf{R}_1 & \mathbf{R}_2 \\ \mathbf{R}_2^T & \mathbf{R}_3 \end{bmatrix}$$

$$= \begin{bmatrix} \mathbf{Q}_1-\mathbf{Q}_2\mathbf{Q}_3^{-1}\mathbf{Q}_2^T & \mathbf{Q}_2\mathbf{Q}_3^{-1} \\ \mathbf{Q}_3^{-1}\mathbf{Q}_2^T & -\mathbf{Q}_3^{-1} \end{bmatrix}$$

$$= \begin{bmatrix} \mathbf{S}_1^{-1} & -\mathbf{S}_1^{-1}\mathbf{S}_2 \\ -\mathbf{S}_2^T\mathbf{S}_1^{-1} & \mathbf{S}_2^T\mathbf{S}_1^{-1}\mathbf{S}_2-\mathbf{S}_3 \end{bmatrix} \qquad (4.1.6)$$

$$\mathbf{e}_L = \left\{ \frac{\partial w}{\partial z}, \frac{\partial u}{\partial z}+\frac{\partial w}{\partial x}, \frac{\partial v}{\partial z}+\frac{\partial w}{\partial y} \right\}^T = \mathbf{D}_L\ \boldsymbol{\delta} \qquad (4.1.7)$$

where,

u	displacement,
δ	nodal displacement,
N	shape function,
σ_g	globally continuous stresses,
P_g	assumed partial stress field,
β	partial stress parameter vector,
ε_g	globally continuous strains,

and

$$\sigma_g=\{\sigma_z,\tau_{xz},\tau_{yz}\}^T, \qquad (4.1.8)$$

$$\varepsilon_g= \{\varepsilon_x,\varepsilon_y,\gamma_{xy}\}^T = B_g\delta. \qquad (4.1.9)$$

From eq.(2.1.3), the locally continuous stresses and strains can be obtained as

$$\sigma_L = \begin{Bmatrix} \sigma_x \\ \sigma_y \\ \tau_{xy} \end{Bmatrix} = \mathbf{R}_1\varepsilon_g + \mathbf{R}_2\sigma_g \qquad (4.1.10)$$

$$\varepsilon_L = \begin{Bmatrix} \varepsilon_z \\ \gamma_{xz} \\ \gamma_{yz} \end{Bmatrix} = R_2^T \varepsilon_g + R_3 \sigma_g \tag{4.1.11}$$

The combined energy can be changed to the form

$$\begin{aligned} C &= \frac{1}{2} q^T R q \\ &= \frac{1}{2} \varepsilon_g^T R_1 \varepsilon_g + \frac{1}{2} \sigma_g^T R_3 \sigma_g \\ &\quad + \sigma_g^T R_2^T \varepsilon_g \end{aligned} \tag{4.1.12}$$

Thus, the laminate functional can be expressed as

$$\begin{aligned} \Pi_L &= \frac{1}{2} \delta^T \left(\int_V B_g^T R_1 B_g dv \right) \delta + \\ &\quad + \frac{1}{2} \beta^T \left(\int_V P_g^T R_3 P_g dv \right) \beta + \\ &\quad + \beta^T \left(\int_V P_g^T R_2^T B_g dv \right) \delta + \\ &\quad + \beta^T \left(\int_V P_g^T D_L dv \right) \delta - \\ &\quad - \delta^T \left(\int_V N^T \bar{F} dv + \int_{S_\sigma} N^T \bar{T} ds \right) \end{aligned} \tag{4.1.13}$$

It can be seen from eq.(4.1.6) that

$$R_1 = S_1^{-1}, \tag{4.1.14}$$

$$R_2 = -S_1^{-1} S_2, \tag{4.1.15}$$

$$R_3 = -Q_3^{-1}. \tag{4.1.16}$$

If we define

$$K_d = \int_V B_g^T S_1^{-1} B_g dv \tag{4.1.17}$$

$$H = -\int_V P_g^T Q_3^{-1} P_g dv \tag{4.1.18}$$

$$G = \int_V P_g^T (D_L - S_2^T S_1^{-1} B_g) dv \tag{4.1.19}$$

$$f = \int_V N^T \bar{F} dv + \int_{S_\sigma} N^T \bar{T} ds \tag{4.1.20}$$

then

$$\Pi_L = \frac{1}{2}\delta^T K_d \delta - \frac{1}{2}\beta^T H \beta + \beta^T G \delta - \delta^T f \tag{4.1.21}$$

Taking the partial stationary condition

$$\frac{\partial \Pi_L}{\partial \beta} = 0, \tag{4.1.22}$$

we have

$$H\beta = G\delta \tag{4.1.23}$$

Therefore, the stress parameter can be expressed by nodal displacement.

$$\beta = H^{-1} G \delta \tag{4.1.24}$$

Using symmetry of stiffness matrix, i.e.,

$$Q_3{}^T = Q_3 \tag{4.1.25}$$

and eq.(4.1.18), it can be shown that

$$H^T = H \tag{4.1.26}$$

Substituting stress parameter β into the laminate functional Π_L, we get

$$\begin{aligned} \Pi_L &= \frac{1}{2}\delta^T K_d \delta - \frac{1}{2}\delta^T G^T H^{-1} G \delta + \\ &\quad + \delta^T G^T H^{-1} G \delta - \delta^T f \\ &= \frac{1}{2}\delta^T K_d \delta + \frac{1}{2}\delta^T (G^T H^{-1} G) \delta - \delta^T f \end{aligned} \tag{4.1.27}$$

Denoting

$$K_h = G^T H^{-1} G \tag{4.1.28}$$

and

$$K = K_d + K_h \tag{4.1.29}$$

then the laminate functional is transformed into the following final form,

$$\Pi_L = \frac{1}{2}\delta^T K \delta - \delta^T f \tag{4.1.30}$$

Carrying out the other partial stationary condition of the functional Π_L

$$\frac{\partial \Pi_L}{\partial \delta} = 0 \tag{4.1.31}$$

the governing equation in nodal displacement space is finally obtained as follows.

$$K\delta = f \tag{4.1.32}$$

It can be seen that the stiffness matrix of the present finite element consists of two semi-stiffness matrices, K_d and K_h. Therefore the present finite element can be referred to as the composite finite element.

The first semi-stiffness matrix, K_d, in displacement formulation, is based on the globally continuous strains, i.e., the in-plane strains $\varepsilon_x, \varepsilon_y, \gamma_{xy}$. It can be called semi-displacement stiffness matrix. Another semi-stiffness matrix, K_h, in hybrid formulation, is based on the globally continuous stresses, i.e., the transverse stresses $\sigma_z, \tau_{xz}, \tau_{yz}$. It can be named the semi-hybrid stiffness

matrix.

4.2 Composite finite element method

In the composite FEM, the governing equation for the unknown nodal displacement δ is

$$\mathbf{K}\delta = \mathbf{f} \tag{4.2.1}$$

where $\mathbf{K}$ is the stiffness matrix in nodal displacement space, and $\mathbf{f}$ is the equivalent nodal force. They are assembled from elements.

The element stiffness matrix is

$$\mathbf{K}^e = \int_{V^e} \mathbf{B}_g^T \mathbf{S}_1^{-1} \mathbf{B}_g dv + \mathbf{G}^T \mathbf{H}^{-1} \mathbf{G} \tag{4.2.3}$$

and the element equivalent force is

$$\mathbf{f}^e = \int_{V^e} \mathbf{N}^T \bar{\mathbf{F}} dv + \int_{S_\sigma{}^e} \mathbf{N}^T \bar{\mathbf{T}} ds \tag{4.2.4}$$

The matrices $\mathbf{H}$ and $\mathbf{G}$ are

$$\mathbf{H} = \int_{V^e} \mathbf{P}_g^T \mathbf{Q}_3^{-1} \mathbf{P}_g dv \tag{4.2.5}$$

$$\mathbf{G} = \int_{V^e} \mathbf{P}_g^T (\mathbf{D}_L - \mathbf{S}_2^T \mathbf{S}_1^{-1} \mathbf{B}_g) dv \tag{4.2.6}$$

where,

$\mathbf{P}_g$ assumed partial stress field,

$\mathbf{B}_g$ partial strain-nodal displacement relation,

$\mathbf{D}_L$ compatibility relation,

$\mathbf{S}_1, \mathbf{S}_2, \mathbf{Q}_3$ submatrices of constitutive relations.

We have

$$\begin{Bmatrix} \sigma_z \\ \tau_{xz} \\ \tau_{yz} \end{Bmatrix} = P_g \beta \tag{4.2.7}$$

$$\begin{Bmatrix} \varepsilon_x \\ \varepsilon_y \\ \gamma_{xy} \end{Bmatrix} = \begin{bmatrix} \frac{\partial}{\partial x} & 0 & 0 \\ 0 & \frac{\partial}{\partial y} & 0 \\ \frac{\partial}{\partial y} & \frac{\partial}{\partial x} & 0 \end{bmatrix} u^e = B_g \delta^e \tag{4.2.8}$$

$$\begin{Bmatrix} \frac{\partial w}{\partial z} \\ \frac{\partial u}{\partial z}+\frac{\partial w}{\partial x} \\ \frac{\partial v}{\partial z}+\frac{\partial w}{\partial y} \end{Bmatrix} = \begin{bmatrix} 0 & 0 & \frac{\partial}{\partial z} \\ \frac{\partial}{\partial z} & 0 & \frac{\partial}{\partial x} \\ 0 & \frac{\partial}{\partial z} & \frac{\partial}{\partial y} \end{bmatrix} u^e = D_L \delta^e \tag{4.2.9}$$

$$\begin{Bmatrix} \varepsilon_x \\ \varepsilon_y \\ \gamma_{xy} \\ \varepsilon_z \\ \gamma_{xz} \\ \gamma_{yz} \end{Bmatrix} = \begin{bmatrix} S_1 & S_2 \\ S_2{}^T & S_3 \end{bmatrix} \begin{Bmatrix} \sigma_x \\ \sigma_y \\ \tau_{xy} \\ \sigma_z \\ \tau_{xz} \\ \tau_{yz} \end{Bmatrix} \tag{4.2.10}$$

$$\begin{Bmatrix} \sigma_x \\ \sigma_y \\ \tau_{xy} \\ \sigma_z \\ \tau_{xz} \\ \tau_{yz} \end{Bmatrix} = \begin{bmatrix} Q_1 & Q_2 \\ Q_2{}^T & Q_3 \end{bmatrix} \begin{Bmatrix} \varepsilon_x \\ \varepsilon_y \\ \gamma_{xy} \\ \varepsilon_z \\ \gamma_{xz} \\ \gamma_{yz} \end{Bmatrix} \tag{4.2.11}$$

$$B_g = \begin{bmatrix} \frac{1}{a_1}\frac{\partial N_1}{\partial \xi} & 0 & 0 \\ 0 & \frac{1}{a_2}\frac{\partial N_1}{\partial \eta} & 0 \\ \frac{1}{a_2}\frac{\partial N_1}{\partial \eta} & \frac{1}{a_1}\frac{\partial N_1}{\partial \xi} & 0 \end{bmatrix} , \ldots\ldots \tag{4.2.12}$$

$$D_L=\begin{bmatrix} 0 & 0 & \frac{1}{a_3}\frac{\partial N_1}{\partial \zeta} \\ \frac{1}{a_3}\frac{\partial N_1}{\partial \zeta} & 0 & \frac{1}{a_1}\frac{\partial N_1}{\partial \xi},..... \\ 0 & \frac{1}{a_3}\frac{\partial N_1}{\partial \zeta} & \frac{1}{a_2}\frac{\partial N_1}{\partial \eta} \end{bmatrix} \qquad (4.2.13)$$

where β is the stress parameter.

The displacement u, stress σ and strain ε can be given by following relations, in terms of nodal displacement δ.

$$u = N\delta^e \qquad (4.2.14)$$

$$\beta = H^{-1}G\delta^e \qquad (4.2.15)$$

$$\sigma_g = P_g\,\beta = P_gH^{-1}G\delta^e \qquad (4.2.16)$$

$$\sigma_L = R_1\varepsilon_g + R_2\sigma_g = [S_1^{-1}B_g - S_1^{-1}S_2P_gH^{-1}G]\,\delta^e \qquad (4.2.17)$$

$$\varepsilon_g = B_g\,\delta^e$$

$$\varepsilon_L = R_2^T\varepsilon_g + R_3\sigma_g = [-S_2^TS_1^{-1}B_g - Q_3^{-1}P_gH^{-1}G]\,\delta^e \qquad (4.2.18)$$

or say

$$\sigma = \Gamma^e\delta^e = \begin{bmatrix} S_1^{-1}B_g - S_1^{-1}S_2P_gH^{-1}G \\ P_gH^{-1}G \end{bmatrix}\delta^e \qquad (4.2.19)$$

$$\varepsilon = \Phi^e\,\delta^e = \begin{bmatrix} B_g \\ -S_2^TS_1^{-1}B_g - Q_3^{-1}P_gH^{-1}G \end{bmatrix}\delta^e \qquad (4.2.20)$$

where,

$$\sigma = \{ \sigma_x, \sigma_y, \tau_{xy}, \sigma_z, \tau_{xz}, \tau_{yz} \}^T \qquad (4.2.21)$$

$$\varepsilon = \{ \varepsilon_x, \varepsilon_y, \gamma_{xy}, \varepsilon_z, \gamma_{xz}, \gamma_{yz} \}^T \qquad (4.2.22)$$

From the above equations, the stiffness matrix K^e, stress mapping matrix Γ^e and strain mapping matrix Φ^e can be calculated by assuming the partial stress field P_g. Then, the procedure is similar to the displacement FEM.

4.3 Nondimensional formulation

In order to generate the element stiffness matrix and to calculate stress and strain, in the composite FEM and the hybrid FEM the computer takes more time than it does using the displacement FEM. Stiffness matrix , stress mapping matrix and strain mapping matrix can be made to be nondimensional, provided the above mentioned elements have the same ratios in three dimensions, elastic property and orientation. The nondimensionization makes it possible to calculate stiffness matrices and stress - nodal displacement, strain - nodal displacement matrices in advance. Thus, when the FEM program is running, it reads them from storage, and adjusts them to real dimensions and real elastic modulus.

The nondimensionization procedure is as follows. Take a_1, the first lamé coefficient, as a characteristic length, and E_L, the largest elastic modulus, as a characteristic modulus, i.e. $a=a_1$, $E=E_L$, and denote

$$c_1 = a_1/a = 1 \tag{4.3.1}$$

$$c_2 = a_2/a \tag{4.3.2}$$

$$c_3 = a_3/a \tag{4.3.3}$$

$$|J| = c_1c_2c_3 \tag{4.3.4}$$

$$\tilde{x} = x/a \tag{4.3.5}$$

or

$$\tilde{x} = \tilde{x}_o+c_1\xi \tag{4.3.6}$$

$$\tilde{y} = \tilde{y}_o+c_2\eta \tag{4.3.6}$$

$$\tilde{z} = \tilde{z}_o+c_3\zeta$$

and

$$\tilde{\sigma} = \sigma/E \tag{4.3.7}$$

$$\tilde{P}_g = P_g/E \tag{4.3.8}$$

$$\tilde{S} = ES \tag{4.3.9}$$

$$\tilde{Q} = Q/E \tag{4.3.10}$$

$$\tilde{B}_g = aB_g \tag{4.3.11}$$

$$\tilde{D}_L = aD_L \tag{4.3.12}$$

$$\tilde{G} = G/Ea^2 \tag{4.3.13}$$

$$\tilde{H} = H/Ea^3 \tag{4.3.14}$$

$$\tilde{K} = K/Ea \tag{4.3.15}$$

$$\tilde{\Gamma} = a\Gamma/E \tag{4.3.16}$$

$$\tilde{\Phi} = a\Phi \tag{4.3.17}$$

then we have

$$\tilde{B}_g = \begin{bmatrix} \frac{1}{c_1}\frac{\partial N_1}{\partial \xi} & 0 & 0 \\ 0 & \frac{1}{c_2}\frac{\partial N_1}{\partial \eta} & 0 \\ \frac{1}{c_2}\frac{\partial N_1}{\partial \eta} & \frac{1}{c_1}\frac{\partial N_1}{\partial \xi} & 0 \end{bmatrix} , \ldots\ldots \tag{4.3.18}$$

$$\tilde{D}_L = \begin{bmatrix} 0 & 0 & \frac{1}{c_3}\frac{\partial N_1}{\partial \zeta} \\ \frac{1}{c_3}\frac{\partial N_1}{\partial \zeta} & 0 & \frac{1}{c_1}\frac{\partial N_1}{\partial \xi}, \\ 0 & \frac{1}{c_3}\frac{\partial N_1}{\partial \zeta} & \frac{1}{c_2}\frac{\partial N_1}{\partial \eta} \end{bmatrix} \ldots\ldots \tag{4.3.19}$$

$$\tilde{G} = \int_{-1}^{1}\int_{-1}^{1}\int_{-1}^{1} \tilde{P}_g^T(\tilde{D}_L - \tilde{S}_2^T\tilde{S}_1^{-1}\tilde{B}_g)|J|d\xi d\eta d\zeta \tag{4.3.20}$$

$$\tilde{H} = \int_{-1}^{1}\int_{-1}^{1}\int_{-1}^{1} \tilde{P}_g^T\tilde{Q}_3^{-1}\tilde{P}_g|J|d\xi d\eta d\zeta \tag{4.3.21}$$

$$\tilde{K}_d = \int_{-1}^{1}\int_{-1}^{1}\int_{-1}^{1} \tilde{B}_g^T\tilde{S}_1^{-1}\tilde{B}_g|J|d\xi d\eta d\zeta \tag{4.3.22}$$

$$\tilde{K}_h = \tilde{G}^T\tilde{H}^{-1}\tilde{G} \tag{4.3.23}$$

$$\tilde{K} = \tilde{K}_d + \tilde{K}_h \tag{4.3.24}$$

$$\tilde{\Gamma} = \begin{bmatrix} \tilde{S}_1^{-1}\tilde{B}_g - \tilde{S}_1^{-1}\tilde{S}_2\tilde{P}_g\tilde{H}^{-1}\tilde{G} \\ \tilde{P}_g\tilde{H}^{-1}\tilde{G} \end{bmatrix} \tag{4.3.25}$$

$$\tilde{\Phi} = \begin{bmatrix} \tilde{B}_g \\ -\tilde{S}_2^T \tilde{S}_1^{-1} \tilde{B}_g - \tilde{Q}_3^{-1} \tilde{P}_g \tilde{H}^{-1} \tilde{G} \end{bmatrix} \tag{4.3.26}$$

The nondimensional matrices $\tilde{K}$, $\tilde{\Gamma}$, $\tilde{\Phi}$ can be stored into some files. The real element stiffness matrix, real stress and strain matrices will be adjusted as follows.

$$K = Ea\tilde{K} \tag{4.3.27}$$

$$\Gamma = E\tilde{\Gamma}/a \tag{4.3.28}$$

$$\Phi = \tilde{\Phi}/a \tag{4.3.29}$$

The real stress and strain will be

$$\sigma = \Gamma\delta \tag{4.3.30}$$

$$\varepsilon = \Phi\delta \tag{4.3.31}$$

4.4 3-D, 8-node composite element for isotropic materials

Chapter 3 investigates the deformation modes and their stress field modes of 3-D, 8-node hybrid FEM. It could be useful to have the corresponding stress field modes in the 3-D, 8-node composite finite element for isotropic materials.

4.4.1 Nondimensional constitutive relation for isotropic materials

Isotropic materials have two elastic constants, for example, E and ν. The nondimensional constitutive relations are as follows.

$$\tilde{S} = \begin{bmatrix} 1 & -\nu & 0 & -\nu & 0 & 0 \\ -\nu & 1 & 0 & -\nu & 0 & 0 \\ 0 & 0 & 2(1+\nu) & 0 & 0 & 0 \\ -\nu & -\nu & 0 & 1 & 0 & 0 \\ 0 & 0 & 0 & 0 & 2(1+\nu) & 0 \\ 0 & 0 & 0 & 0 & 0 & 2(1+\nu) \end{bmatrix} \tag{4.4.1}$$

$$\tilde{Q} = \frac{1}{(1+\nu)(1-2\nu)} \begin{bmatrix} 1-\nu & \nu & 0 & \nu & 0 & 0 \\ \nu & 1-\nu & 0 & \nu & 0 & 0 \\ 0 & 0 & (1-2\nu)/2 & 0 & 0 & 0 \\ \nu & \nu & 0 & 1-\nu & 0 & 0 \\ 0 & 0 & 0 & 0 & (1-2\nu)/2 & 0 \\ 0 & 0 & 0 & 0 & 0 & (1-2\nu)/2 \end{bmatrix} \tag{5.4.2}$$

$$\tilde{S}_1^{-1} = \frac{1}{1-\nu^2} \begin{bmatrix} 1 & \nu & 0 \\ \nu & 1 & 0 \\ 0 & 0 & (1-\nu)/2 \end{bmatrix} \tag{4.4.3}$$

$$\tilde{Q}_3^{-1} = \frac{1+\nu}{1-\nu} \begin{bmatrix} 1-2\nu & 0 & 0 \\ 0 & 2(1-\nu) & 0 \\ 0 & 0 & 2(1-\nu) \end{bmatrix} \tag{4.4.4}$$

$$\tilde{S}_2^T \tilde{S}_1^{-1} = \frac{-\nu}{1-\nu} \begin{bmatrix} 1 & 1 & 0 \\ 0 & 0 & 0 \\ 0 & 0 & 0 \end{bmatrix} \tag{4.4.5}$$

4.4.2 Number of modes of the assumed stress field

There are a total of 24 degrees of freedom for 3-D, 8-node element, 6 of which are the rigid body motion. So the total number of degrees of deformation freedom for the 3-D, 8-node element is 18, or

$$m = n-r$$
$$= 24-6 = 18 \qquad (4.4.6)$$

According to the numerical test, the displacement semi-stiffness matrix of 3-D, 8-node element, $\mathbf{K}_d$, have 10 nonzero eigenvalues.

$$m_d = 10 \qquad (4.4.7)$$

To avoid the zero-energy kinematic modes, the hybrid semi-stiffness matrix must have the orthogonal stress field modes of at least

$$m_h = m-m_d$$
$$= 18-10 = 8$$

On the other hand, when as many stress field modes as possible are incorporated intc the assumed stress field $\mathbf{P}_g$, the maximum number of nonzero eigenvalues of the semi-hybrid stiffness matrix $\mathbf{K}_h$ must be 8. So the semi-hybrid stiffness matrix can have at most 8 orthogonal stress field modes.

In summary, according to numerical tests, the correct number of modes of the assumed stress field is 8 for the 3-D, 8-node composite finite element.

If the number of nonzero eigenvalues of the hybrid semi-stiffness matrix in stress parameter space, H^{-1}, is equal to 8, and those of the semi-stiffness matrix in nodal displacement space, K_h, is equal to 8, then, the composite finite element will be free from zero-energy kinematic modes.

4.4.3 Assumed stress field of the 3-D, 8-node composite element for isotropic materials

The following assumed stress field satisfes the requirments in the above section.

$$P_g = \{ \sigma_1, \sigma_2, \ldots, \sigma_8 \}$$

$$= \begin{bmatrix} 1 & 0 & 0 & \xi & \eta & 0 & 0 & \xi\eta \\ 0 & 1 & 0 & 0 & 0 & \eta & \eta & 0 \\ 0 & 0 & 1 & 0 & 0 & \xi & -\xi & 0 \end{bmatrix} \qquad (4.4.8)$$

in which

$$\sigma_i = \{ \sigma_{zi}, \tau_{xzi}, \tau_{yzi} \}^T \qquad (4.4.9)$$

Based on this stress field, the semi-hybrid stiffness matrix in stress parameter space, H^{-1}, is diagonal and has 8 nonzero eigenvalues.

It is easy to formulate 3-D, 8-node composite finite elements for isotropic materials by means of the formulae stated in section 4.3 and based on the partial stress field P_g as described in eq.(4.4.8)

Numerical tests show that composite FEM gives perfect agreement with hybrid finite element solution in constant stress cases and in two transverse bending modes for laminate plate shown in Fig.4.1 and Fig.4.2. These two bending cases are of importance for plate and shell elements.

Once the valid shape function of displacement field and mode function of stress field for anisotropic laminates is found, it will be possible to use only one composite element to span the whole thickness of laminate, satisfying the continuity of in-plane strains and transverse stresses as well allowing the possible discontinuity of in-plane stress and transverse strains at interlaminar surfaces. This will be the advantage of composite FEM over traditional displacement FEM and hybrid FEM.

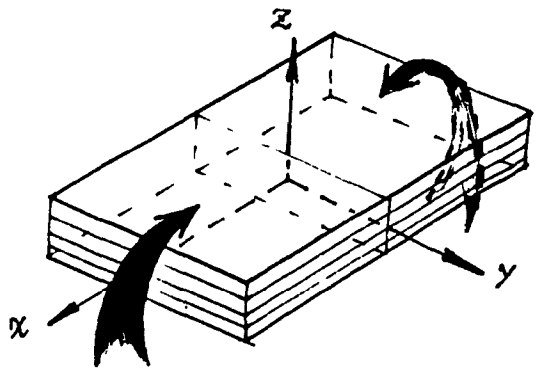

Fig. 4.1 Bending mode A solved by composite FEM

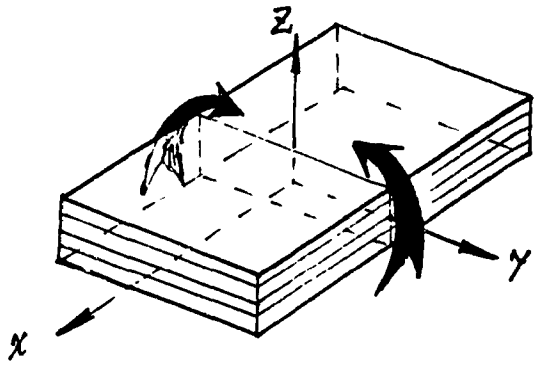

Fig. 4.2 Bending mode B solved by composite FEM

Chapter 5 Numerical Results for A Symmetric Angle-ply Subjected to Uniaxial Tension

By using the present composite finite element, and the traditional displacement element and hybrid element, a calculation is made for a symmetric angle-ply laminate under uni-axial extension. For this simple loading, the results from these three elements agree very closely. However they are quite different from those given by classical laminate theory.

The classical laminate theory is based on the assumption of constant strains across the whole thickness. When a symmetric angle-ply laminate is subjected to a uni-axial tension, the shear coupling deformations are cancelled by adjacent layers with opposite orientation.

The numerical results show that this is not true. In most part of the lamina, the shear coupling deformation exists and has almost the same value as in the case of free extension of unbound layers. Only within a thin region near the interlaminar surface, the coupling shearing is constrained and in-plane stiffness has a higher value. This causes a strong stress concentration.

5.1 example

The geometry of the sample is shown in Fig.5.1. Its elastic constants are:

$$E_L = 145 \text{ GPa}$$
$$E_T = 10.7 \text{ GPa}$$
$$G_{LT} = 4.5 \text{ GPa} \qquad (5.1.1)$$
$$G_{TT} = 3.6 \text{ GPa}$$
$$\nu_{LT} = 0.31$$
$$\nu_{TT} = 0.49$$

where the subscript L denotes the value along the fiber direction, T denotes the property in the transverse direction.

The loading and boundary conditions are given by fixing the amount of displacement in X-direction at two ends of the strip given a strain of ε_X=0.01. The reaction force is in the X-direction only.

For constraining the rigid body motion in the transverse Y-Z plane, another three displacements in Y-Z plane have to be restricted also.

When the strip is very long along X-direction, the stresses and strains should be independent of the X coordinate. The displacement along X-direction in identical

Y-Z planes should be the same. If the same displacement is assumed in any of the two Y-Z boundary planes, then the length of sample in the X-direction does not matter for the stress analysis.

The real size of the sample is

$$L = 1.0 \quad mm$$
$$2b = 12.125 \quad mm \qquad (5.1.2)$$
$$4h_o = 10.25 \quad mm$$

The constitutive relation is anisotropic and is as follows.

$$\begin{Bmatrix} \varepsilon_1 \\ \varepsilon_2 \\ \gamma_{12} \\ \varepsilon_3 \\ \gamma_{13} \\ \gamma_{23} \end{Bmatrix} = \begin{bmatrix} 1/E_L & -\nu_{TL}/E_T & 0 & -\nu_{TL}/E_T & 0 & 0 \\ -\nu_{LT}/E_L & 1/E_T & 0 & -\nu_{TT}/E_T & 0 & 0 \\ 0 & 0 & 1/G_{LT} & 0 & 0 & 0 \\ -\nu_{LT}/E_T & -\nu_{TT}/E_T & 0 & 1/E_T & 0 & 0 \\ 0 & 0 & 0 & 0 & 1/G_{LT} & 0 \\ 0 & 0 & 0 & 0 & 0 & 1/G_{TT} \end{bmatrix} \begin{Bmatrix} \sigma_1 \\ \sigma_2 \\ \tau_{12} \\ \sigma_3 \\ \tau_{13} \\ \tau_{23} \end{Bmatrix} \qquad (5.1.3)$$

where subscript 1 indicates the direction along the fiber, 2 and 3 are transverse to it, and more specifically 3 is in the thickness direction.

The compliance matrix can be mapped into x,y,z space by transformation matrix T

$$S_{(x,y,z)} = T^T S_{(1,2,3)} T \qquad (5.1.4)$$

in which

$$T = \begin{bmatrix} m^2 & n^2 & 2mn & 0 & 0 & 0 \\ n^2 & m^2 & -2mn & 0 & 0 & 0 \\ -mn & mn & m^2-n^2 & 0 & 0 & 0 \\ 0 & 0 & 0 & 1 & 0 & 0 \\ 0 & 0 & 0 & 0 & m & n \\ 0 & 0 & 0 & 0 & -n & m \end{bmatrix} \qquad (5.1.5)$$

where,

$$m = \cos\theta$$
$$n = \sin\theta \qquad (5.1.6)$$

5.2 Numerical Results

The numerical results for uniaxial tension on the symmetric angle-ply laminate are shown in Fig.5.2 - Fig.5.36.

5.2.1 Main tensile stress σ_x

The classical laminate theory gives a uniformly distributed tensile stress σ_x, which is indicated by "LTH" or "Laminate theory" in Fig.5.2 - Fig.5.10.

If the layers of the laminate are not bound together, they also should have a uniformly distributed

tensile stress, which is indicated by "free extension" in the figures. Also the average stress calculated by dividing reaction force with the cross section area is shown, this is indicated as "average". The reaction force was calculated using finite element method.

The stress values calculated by composite FEM are denoted by "at mid-line" or "near free edge". Mid-line means:

$$x = 0$$

$$y = 0$$

$$0 < z < 2h_o \qquad (5.2.1)$$

Near free edge means:

$$x = 0$$

$$y = 0.9997b$$

$$0 < z < 2h_o \qquad (5.2.2)$$

From Fig.5.2 - Fig.5.10, it can be seen that

a) Tensile stress is not uniform across the thickness.

b) In most part of laminate, i.e. when,

$$z < 0.8h_o$$

or

$$z > 1.2h_o \qquad (5.2.3)$$

the numerical results of tensile stress σ_x is almost the same as with the free extension either at mid-line or near the free edge.

c) There is a tensile stress concentration near the

interlaminar surfaces within 1/5 of the ply-thickness, i.e.

$$h_o-0.2h_o < z < h_o+0.2h_o \qquad (5.2.4)$$

d) At mid-line, the peak value of tensile stress at the interface may be higher than the solution of laminate theory for locations within 1/20 of the ply-thickness, i.e.

$$h_o-0.05h_o < z < h_o+0.05h_o \qquad (5.2.5)$$

e) The peak value of tensile stress σ_x at mid-line is higher than laminate theory, if the orientation is within the following range.

$$0^o < \theta < \sim 68^o \qquad (5.2.6)$$

In the rest of the orientation range, it is lower.

The error is more than 10%, if the orientation is between

$$20^o < \theta < 60^o \qquad (5.2.7)$$

The Maximum error is 86% at about $\theta = 42^o$.

f) The tensile stress σ_x near the free edge is close to the laminate theory for all orientations.

g) The average tensile stress σ_x (total reaction force divided by section area) is close to the free extension for all orientations.

h) In comparison with laminate theory, the average tensile stress σ_x is lower. The error is more than 10% when

$$5^o < \theta < 50^o \qquad (5.2.8)$$

The maximum error is 60% at about $\theta = 24^o$.

i) In comparison with the average tensile stress, the peak value at mid-line is higher when the orientation is in the range of eq.(5.2.6). The stress concentration coefficient is larger than 1.1 when,

$$5^{o} < \theta < 60^{o} \qquad (5.2.9)$$

The maximum concentration coefficient is 3.3 at about $\theta = 30^{o}$.

5.2.2 In-plane stress due to Poisson's effect

In classical laminate theory, Poisson's effect is uniform across the thickness of the whole laminate. So σ_y remains zero.

However, in the numerical test, the in-plane shear coupling deformation is restricted just near interlaminar surfaces. The in-plane contraction in the transverse direction is somewhat restricted. The non-uniformity of Poisson contraction in the Y-direction causes a concentration in σ_y. For equilibrium, the average σ_y must be zero.

From Fig.5.11 - Fig.5.18, it is shown that

a) There is a concentration of σ_y near the interlaminar surface within 4/25 of the ply-thickness, i.e.

$$h_o-.16h_o < z < h_o+.16h_o \qquad (5.2.10)$$

Outside this range, σ_y has value of opposite sign to the peak value.

b) The peak value of σ_y is positive if the fiber orientation is

$$0^o < \theta < \sim 68^o, \qquad (5.2.11)$$

negative when

$$68^o < \theta < 90^o \qquad (5.2.12)$$

c) In comparison with the average tensile stress σ_x, the peak value of σ_y is larger than 10%, when

$$15^o < \theta < \sim 65^o$$

and at about

$$\theta = 45^o \qquad (5.2.13)$$

The maximum concentration coefficient of σ_y to average tensile stress σ_x is

$$c = \sigma_{y.max}/\sigma_{x.average} = 1.26 \qquad (5.2.14)$$

5.2.3 The in-plane shear stress τ_{xy}

Restriction of the shear coupling deformation in classical laminate theory results in the in-plane shear stress τ_{xy} uniform within each layer, and it changes its sign at the interface.

However in the numerical results generated by the composite FEM, the in-plane shear stress τ_{xy} appears just within a thin portion near the interlaminar surface, and it remains zero in the rest of the laminate.

From Fig.5.19 - Fig.5.27, it can be seen that

a) The in-plane shear stress τ_{xy} is not uniform within each lamina.

b) In the majority of lamina, i.e.

$$z < 0.8h_o$$

and

$$z > 1.2h_o \qquad (5.2.15)$$

the shear stress τ_{xy} remains at zero.

c) There is a concentration of shear stress τ_{xy} near the interlaminar surface within 1/5 of the ply-thickness, i.e.

$$h_o-0.2h_o < z < h_o+0.2h_o \qquad (5.2.16)$$

d) There is a finite discontinuity for the in-plane shear stress τ_{xy} at the interface.

e) The peak value of shear stress τ_{xy} is positive when the fiber orientation is

$$0^o < \theta < \sim 68^o \qquad (5.2.17)$$

and negative when

$$\sim 68^o < \theta < 90^o \qquad (5.2.18)$$

f) In comparison with laminate theory, the peak value of the shear stress τ_{xy} is higher for all fiber orientations.

The error is larger than 10% when

$$20^{o} < \theta < 80^{o} \qquad (5.2.19)$$

The maximum error is +255% at about $\theta=57^{o}$.

g) The concentration coefficient of shear stress τ_{xy} to average tensile stress σ_x is more than 1.1 when

$$5^{o} < \theta < \sim 63^{o} \qquad (5.2.20)$$

The maximum concentration coefficient of the shear stress to average tensile stress is 1.76 at about $\theta= 37^{o}$.

5.2.4 The transverse stress σ_z, τ_{xz}, τ_{yz}

Classical lamination theory neglects these transverse stresses. These stresses are assumed non-existent away from free edges and traction boundaries. This is confirmed by numerical results which show that their magnitudes remain quite small in the central region.

It can be seen from Fig.5.28 - Fig.5.34 that

a) Near free edge, there is a steep concentration for σ_z within 1/5 of the ply-thickness, i.e.

$$h_o-0.2h_o < z < h_o+0.2h_o \qquad (5.2.21)$$

b) There is a smaller slope of concentration of τ_{xz} within 1/2 of the ply-thickness near free edge.

c) The peak value of σ_z is negative when

$$0^{o} < \theta < \sim 68^{o} \qquad (5.2.22)$$

It is positive when

$$68^{o} < \theta < 90^{o} \qquad (5.2.23)$$

The maximum peak value appears at about

$$\theta = \sim 30^{o} \qquad (5.2.24)$$

d) The maximum peak value of τ_{xz} appears at about

$$\theta = 12^{o} \qquad (5.2.25)$$

5.2.5 The effect of a free edge

This computer test gives its main attention to the central part of laminate far from the free edge in the arrangement of the element mesh.

However the results also show some effect from the the free edge. It can be seen from Fig.5.35 and 5.36 that:

a) The main tensile stress σ_x looses its high peak value at interlaminar surface near free edge.

There is still some concentration of tensile stress σ_x at interface. Near the free edge, for the most part,tensile stress is close to that of free extension and near the interlaminar surface, there is a peak value, which is close to the uniform solution of laminate theory.

b) The first coupling stress is the in-plane shear stress. It looses its high peak value near the free edge. It should be zero at the free edge. But in the FEM calculation, at those stress sampling stations very close to the free edge, it still has a quite high value which is close to the uniform solution of laminate theory so as to restrict the coupling shear deformation at interface.

c) The second coupling stress σ_y is caused by the differences of shear coupling deformation. It vanishes near the free edge.

The numerical results of σ_y show some instability near the free edge.

d) The decreasing of τ_{xy} and vanishing of σ_y causes a disorder in the transverse stresses σ_z and τ_{xz}. These stresses increase abruptly near the free edge.

e) If the algorithm is changed so as to show the vanishing of τ_{xy}, then σ_z and τ_{xz} must increase much more than in these numerical results.

5.3 Conclusion

1. The stress analysis of anisotropic laminated structures is necessary both for the free edge and central region.

2. In the central region, the shear coupling deformation is restricted only within a thin piece $0.2h^{o}$. This causes a strong concentration of tensile stress σ_x, in-plane shear stress τ_{xy} and Poisson effect stress σ_y:

a) of σ_x when $5^{o} < \theta < 60^{o}$,

at $\theta=30^{o}$, $\sigma_x/\sigma_{x.average} = 3.3$

b) of σ_y when $15^{o} < \theta < 65^{o}$,

at $\theta=42^{o}$, $\sigma_y/\sigma_{x.average} = 1.26$

c) of τ_{xy} when $5^{o} < \theta < 63^{o}$,

at $\theta=37^{o}$, $\tau_{xy}/\sigma_{x.average} = 1.76$.

The laminate theory has a significant error:

a) of σ_x when $20^{o} < \theta < 60^{o}$,

at $\theta=42^{o}$ the maximum error is 86%,

b) of τ_{xy} when $20^{o} < \theta < 80^{o}$,

at $\theta=57^{o}$ the maximum error is 255%.

3. If we use one composite or hybrid element to span the whole thickness of the laminate, i.e. use of plate or shell element, the stress mode and shape function must be

modified by considering the discontinuity of τ_{xy} and the concentration of σ_x, σ_y, τ_{xy} at the interlaminar surfaces.

4. For stress analysis of laminated structures, it is better to use a 3-D composite element. Because the continuity conditions of in-plane strains and transverse stresses will be satisfied surely and the possible discontinuity of in-plane stress and transverse strains will be allowed.

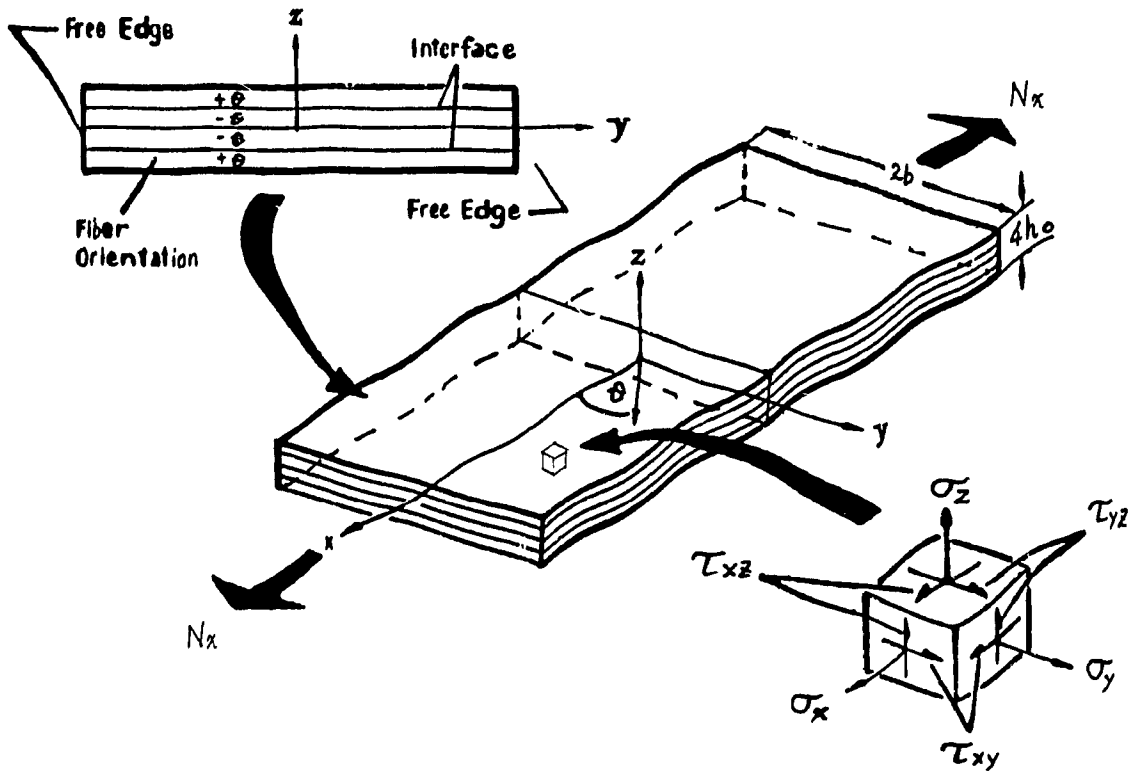

Fig.5.1 Laminate geometry

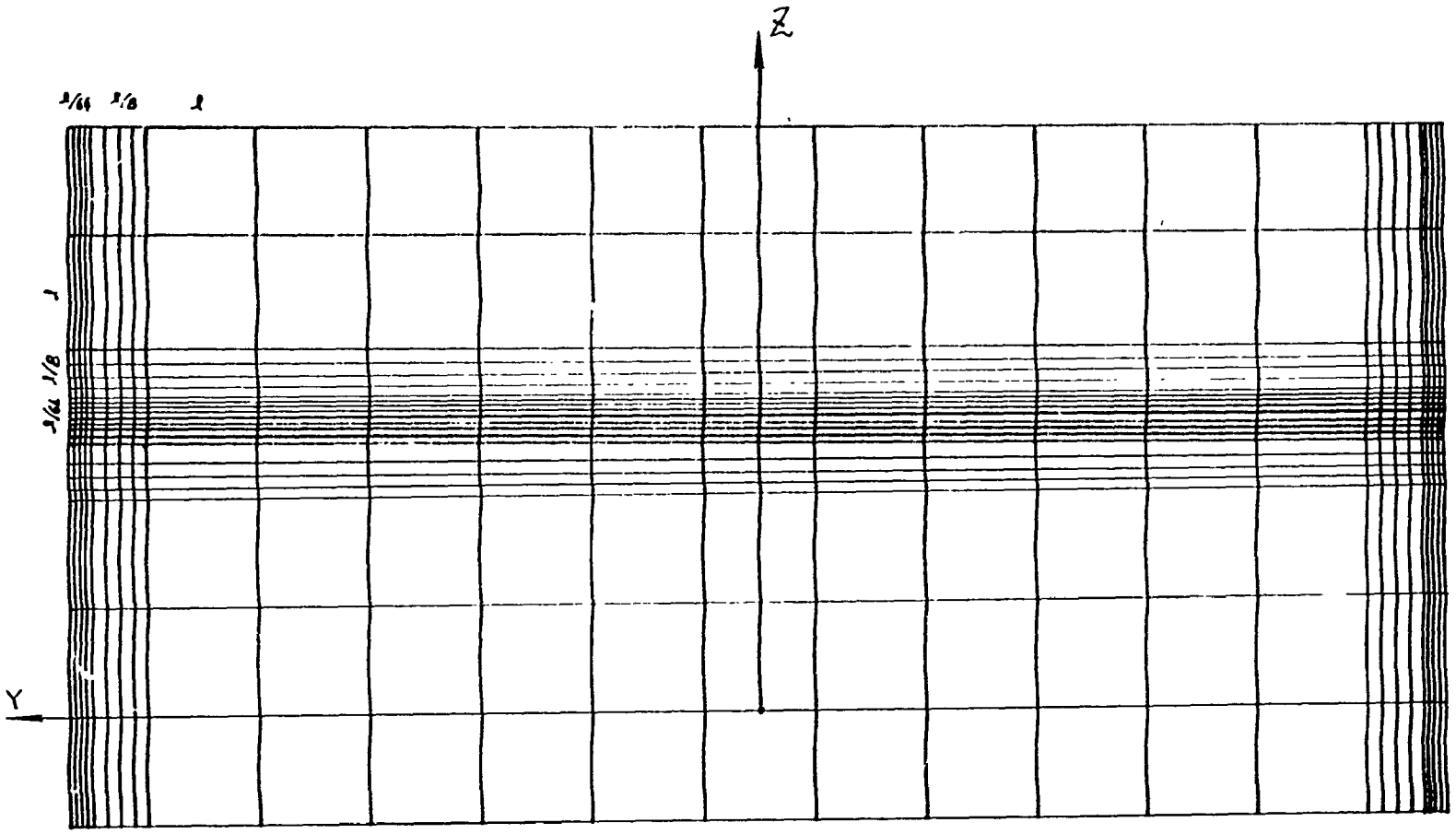

Fig.5.37 Mesh Configuration of
Symmetric Angle-ply Laminate

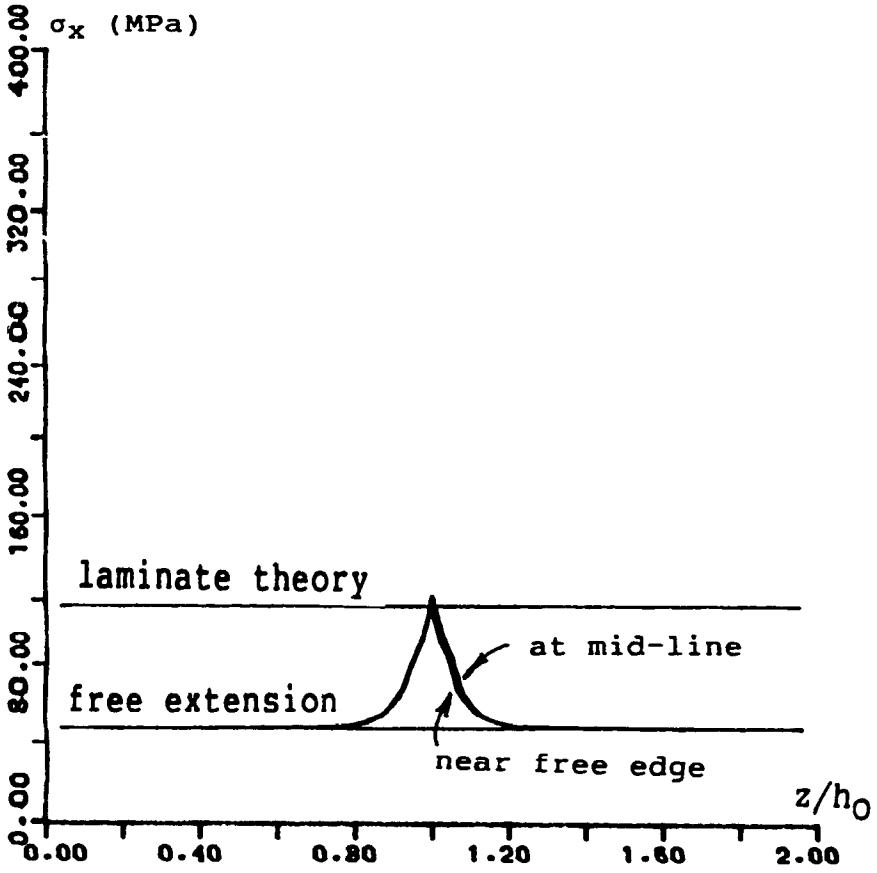

Fig.5.2 Stress distribution along thickness

σ_x versus z/h_o for [15/-15]s

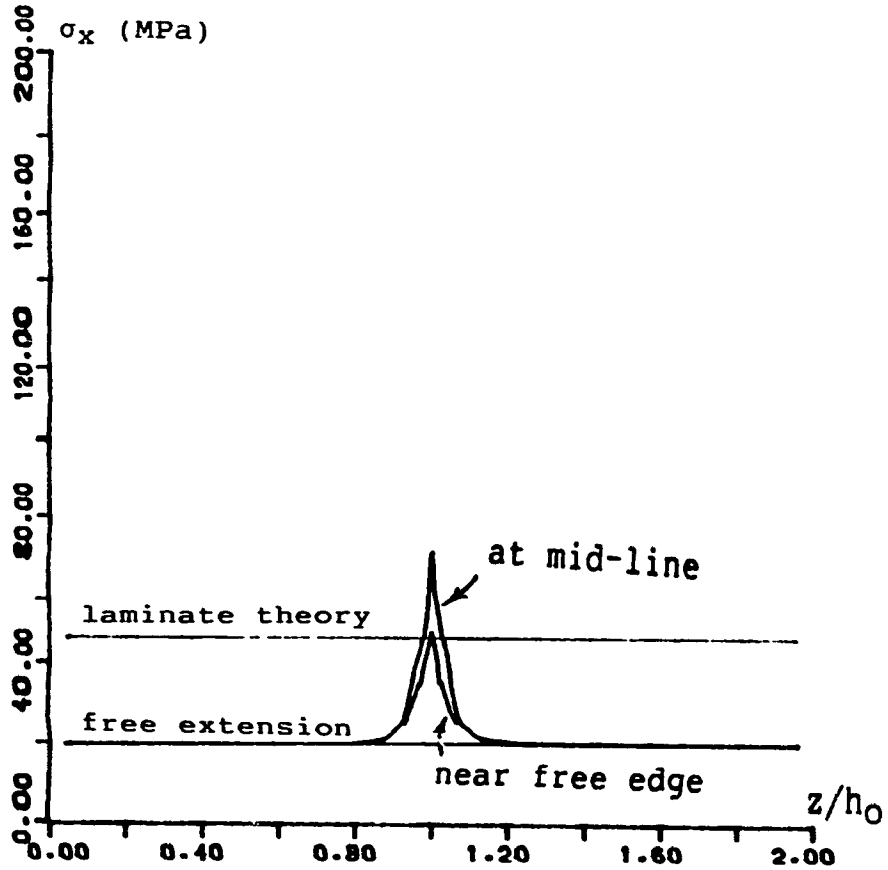

Fig.5.3 Stress distribution along thickness

σ_x versus z/h_o for [30/-30]s

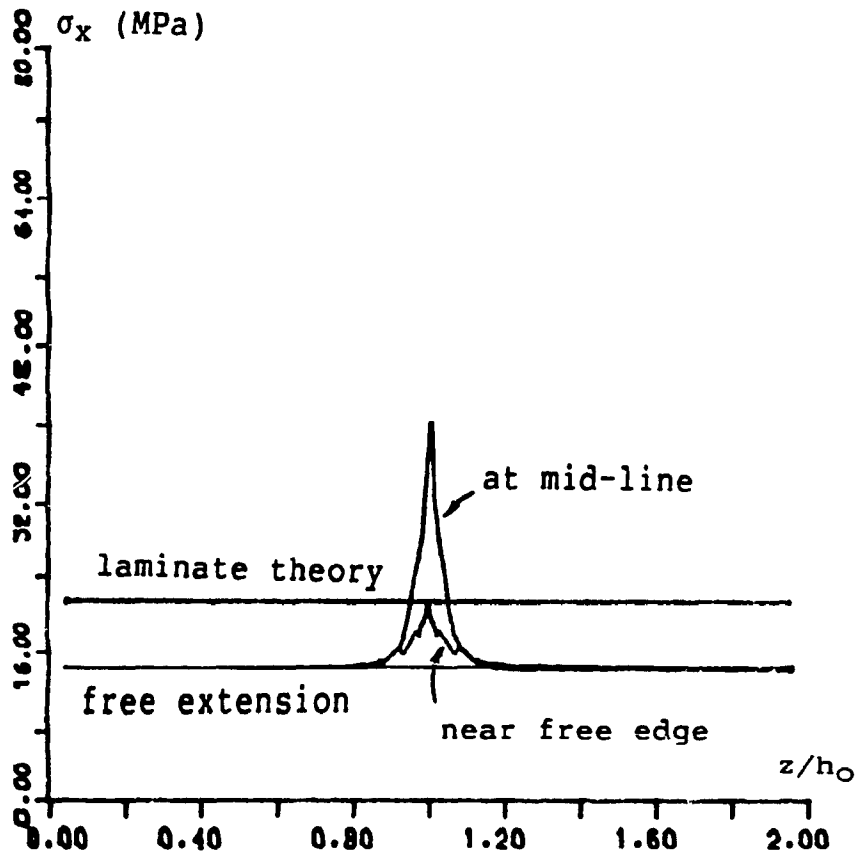

Fig.5.4 Stress distribution along thickness σ_x versus z/h_o for [40/-40]s

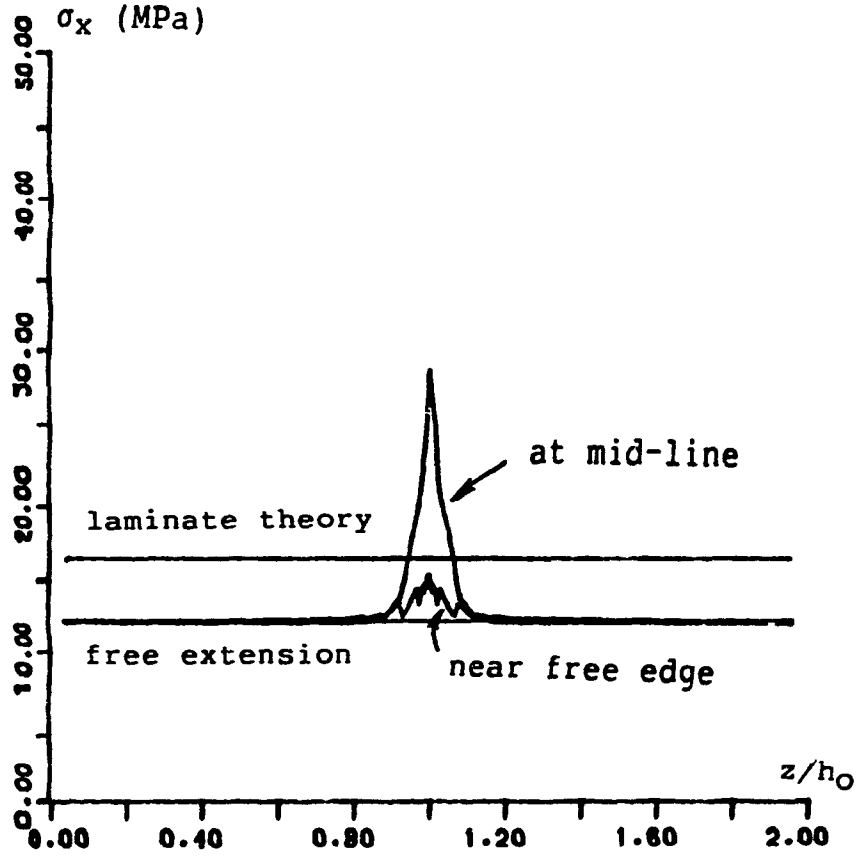

Fig.5.5 Stress distribution along thickness σ_x versus z/h_o for [45/-45]s

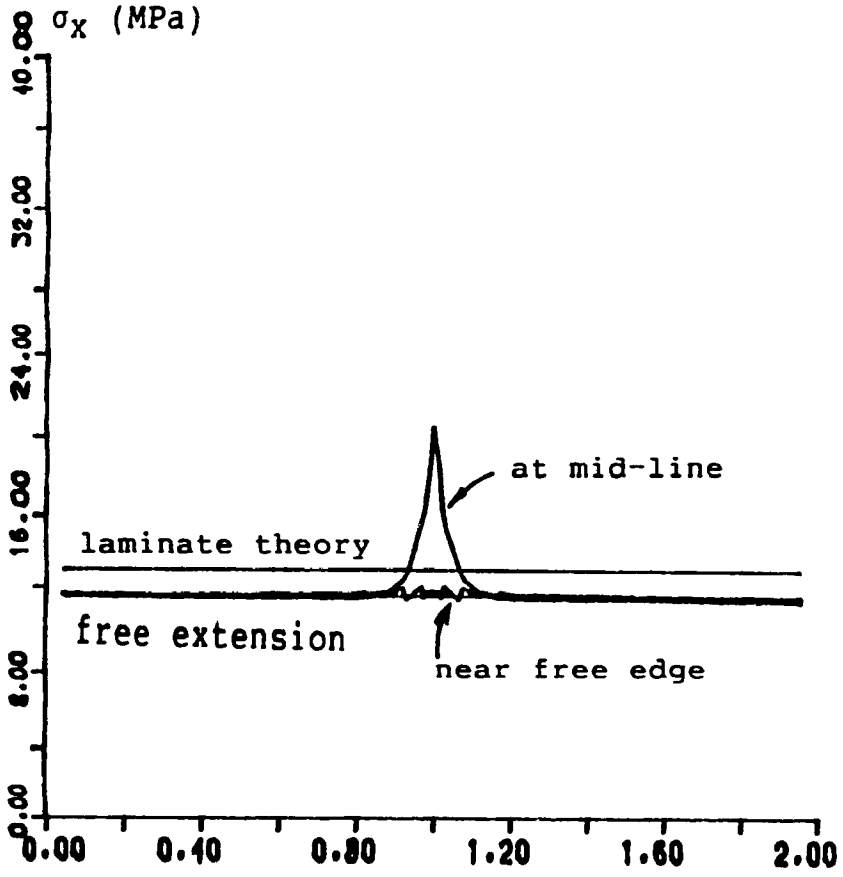

Fig.5.6 Stress distribution along thickness
σ_x versus z/h_o for [50/-50]s

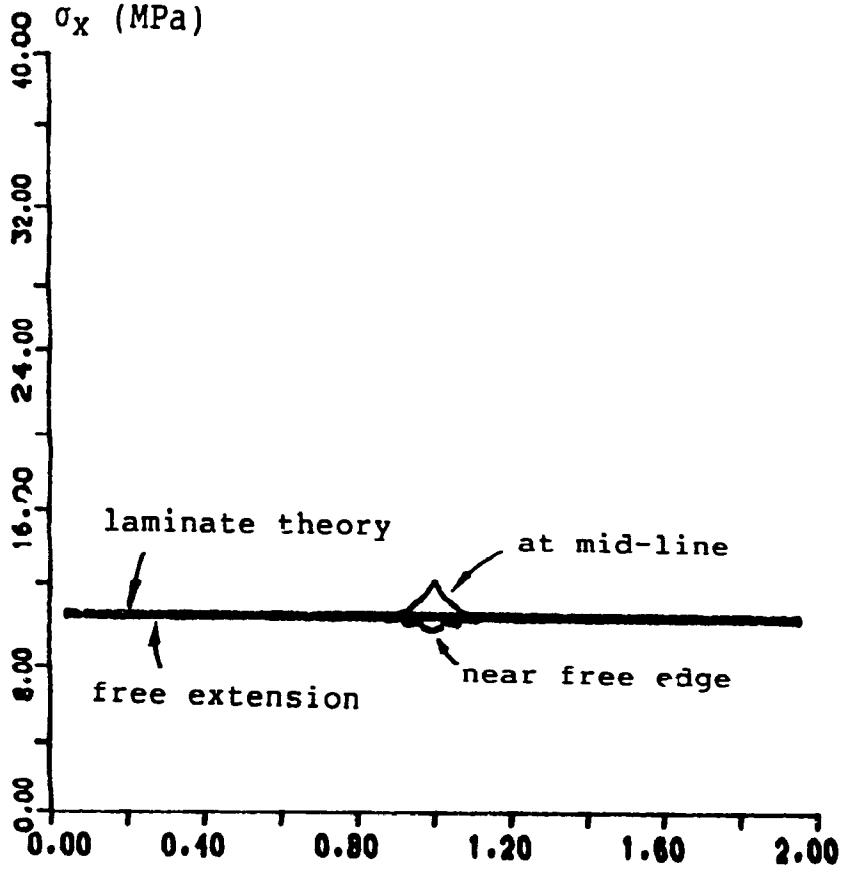

Fig.5.7 Stress distribution along thickness
σ_x versus z/h_o for [60/-60]s

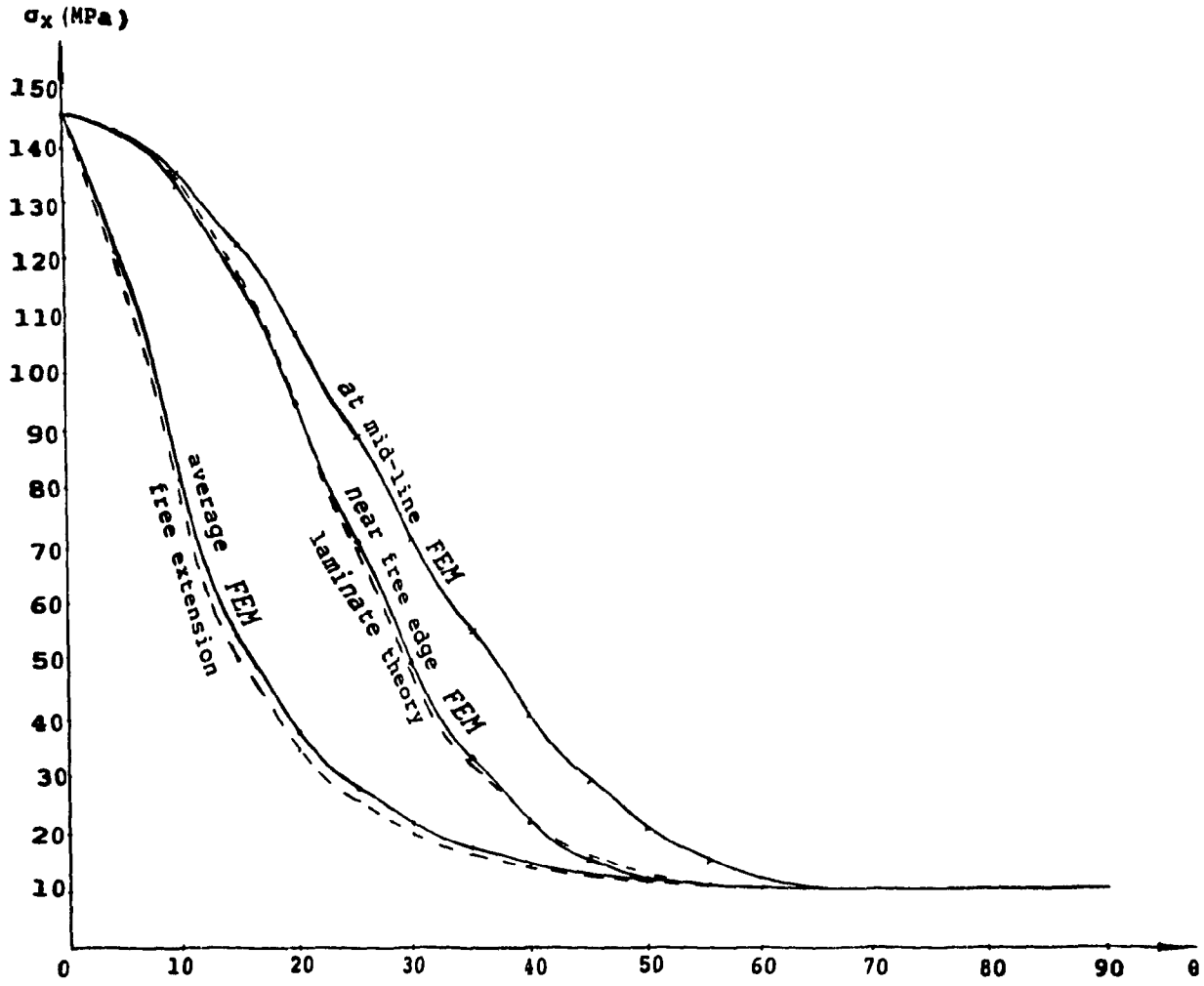

Fig.5.8 Stress - fiber orientation relation

σ_x versus θ for symmetric angle-ply laminate

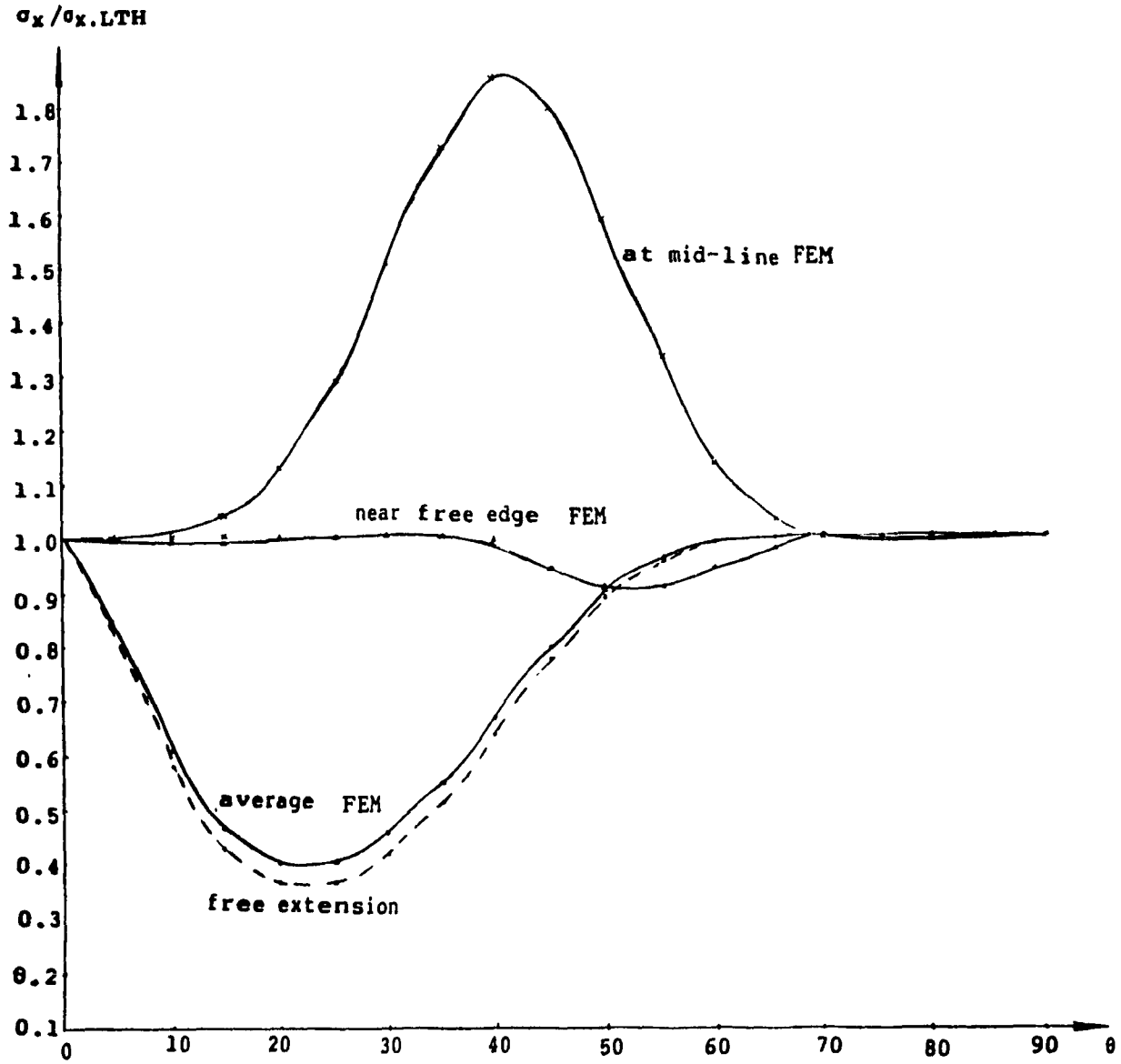

Fig.5.9 Stress - fiber orientation relation

$\sigma_x/\sigma_{x.LTH}$ versus θ

for symmetric angle-ply laminate

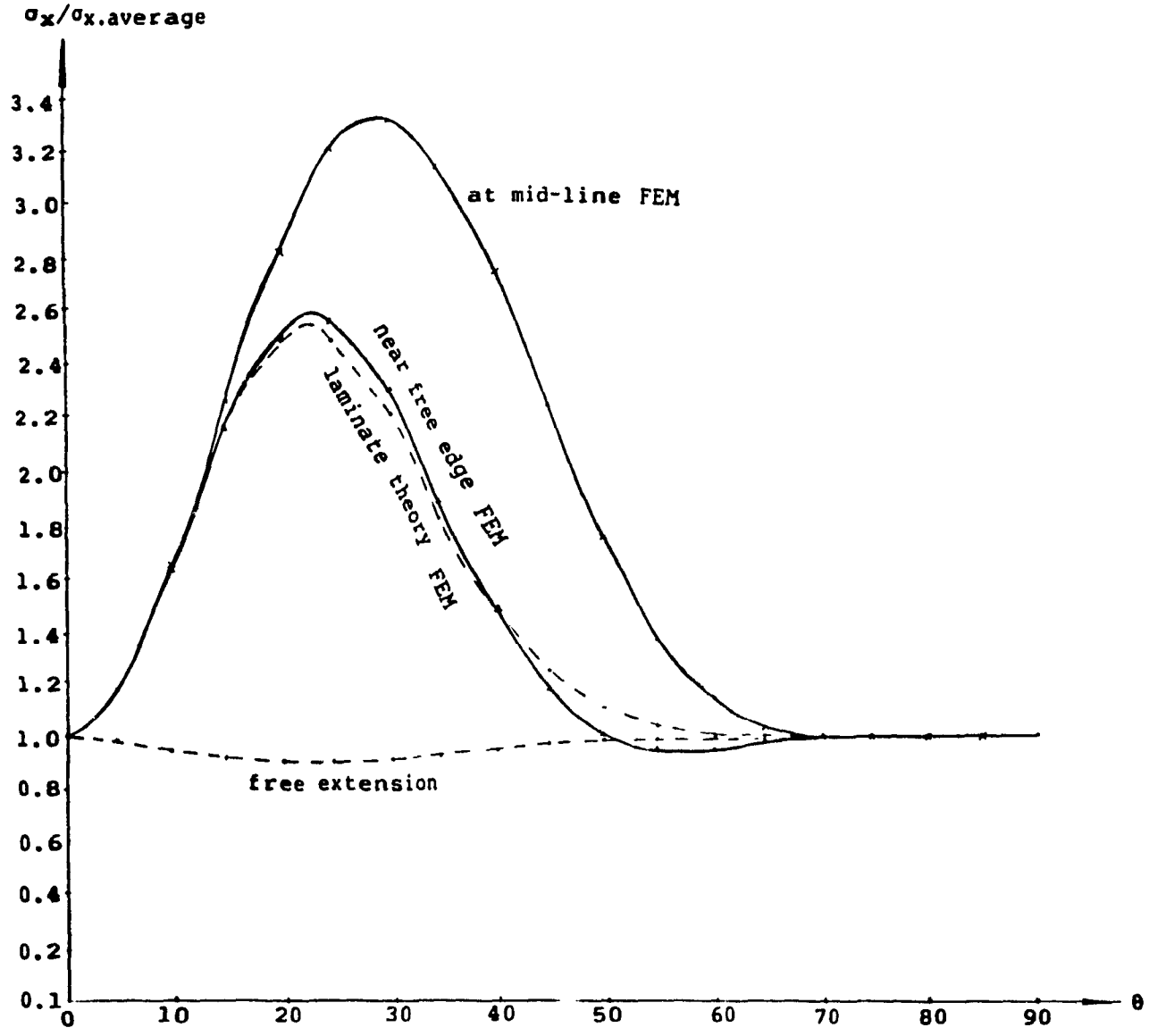

Fig.5.10 Stress - fiber orientation relation

$\sigma_{x.max}/\sigma_{x.average}$ versus θ

for symmetric angle-ply laminate

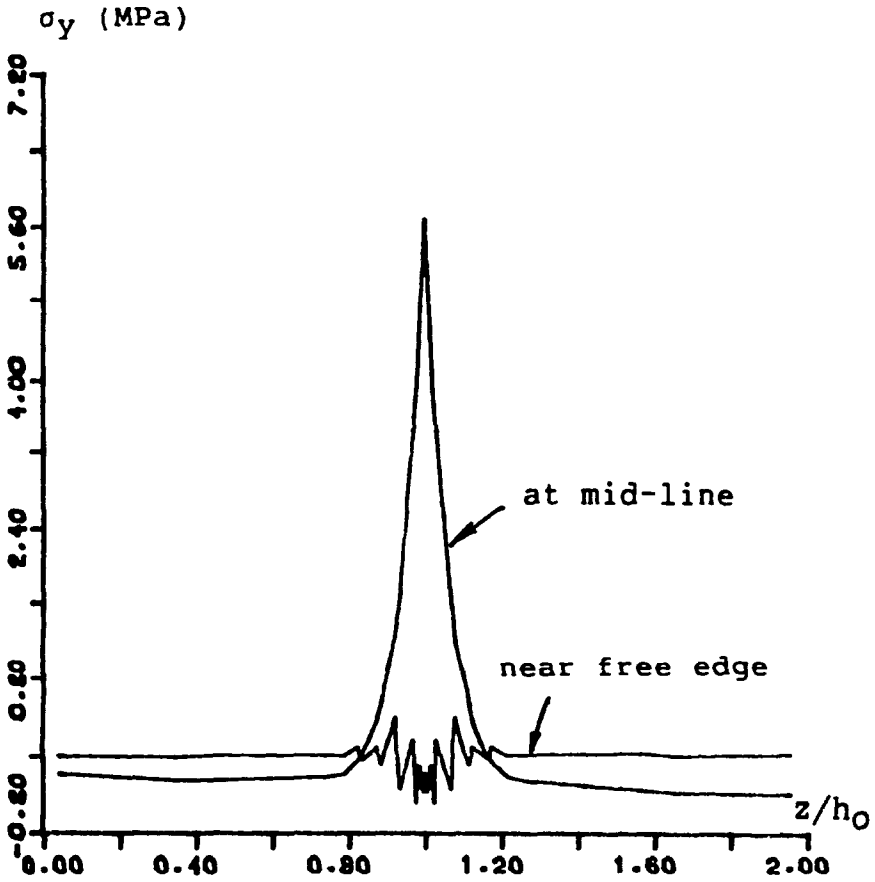

Fig.5.11 Stress distribution along thickness σ_y versus z/h_o for [15/-15]s

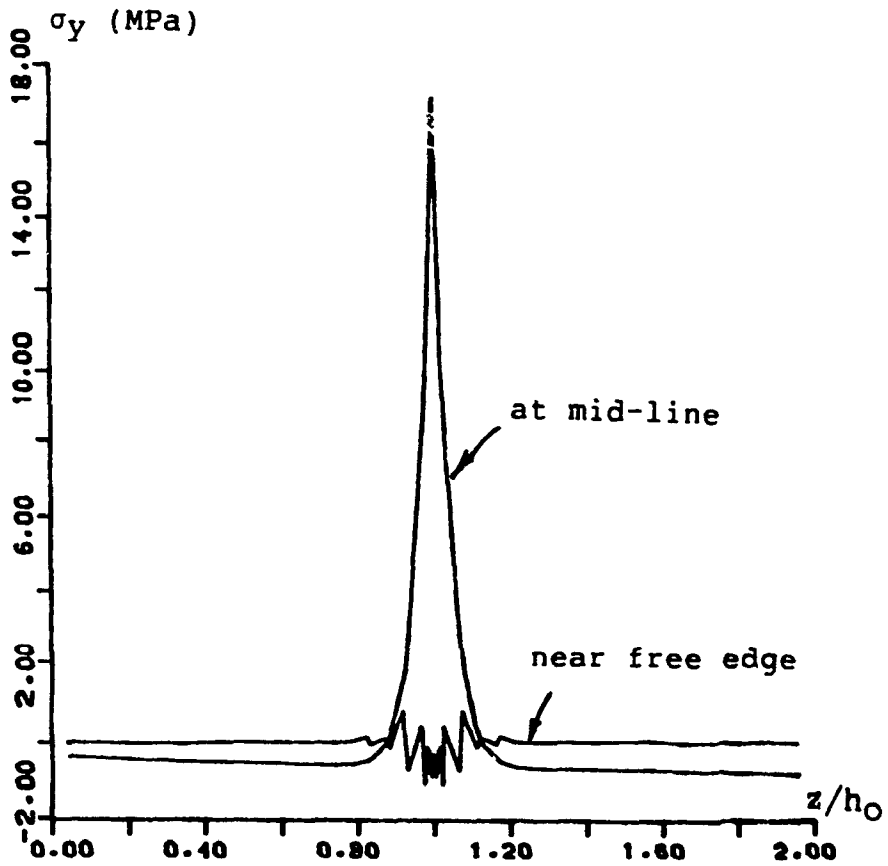

Fig.5.12 Stress distribution along thickness σ_y versus z/h_o for [30/-30]s

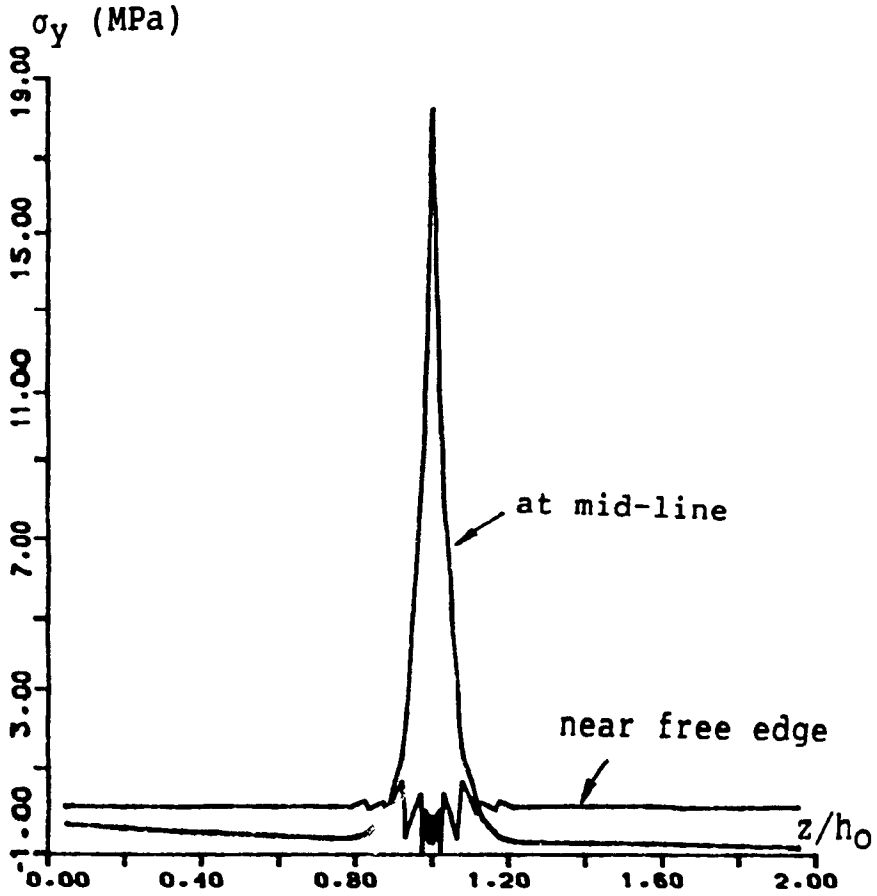

Fig.5.13 Stress distribution along thickness σ_x versus z/h_o for [40/-40]s

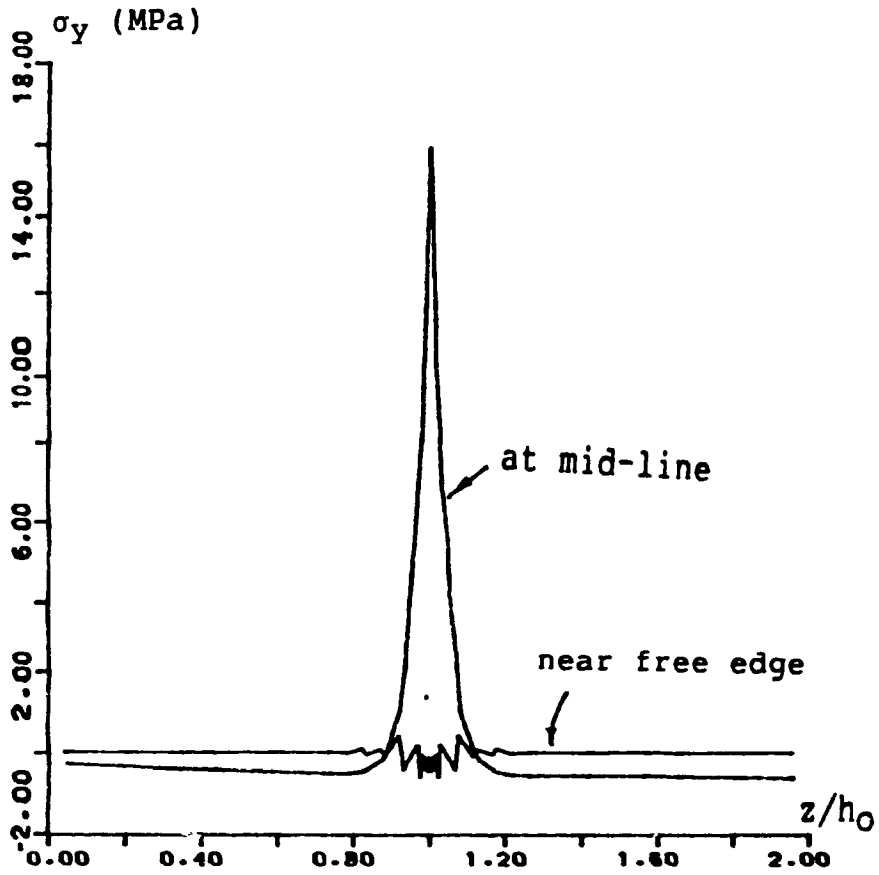

Fig.5.14 Stress distribution along thickness σ_y versus z/h_o for [45/-45]s

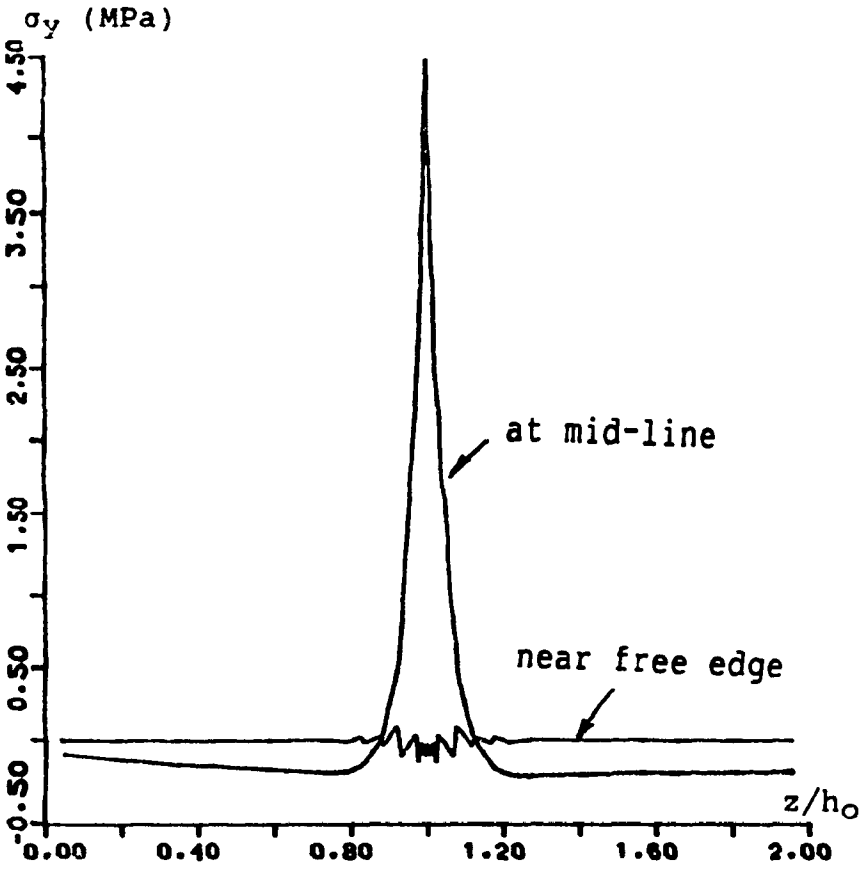

Fig.5.15 Stress distribution along thickness
σ_y versus z/h_o for [60/-60]s

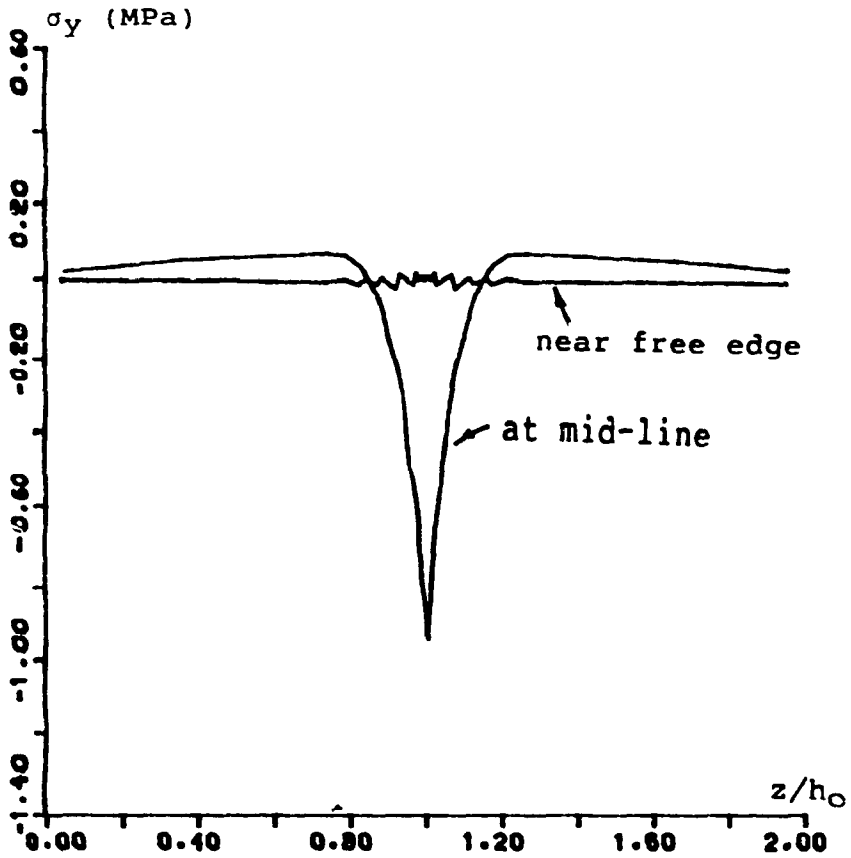

Fig.5.16 Stress distribution along thickness
σ_y versus z/h_o for [75/-75]s

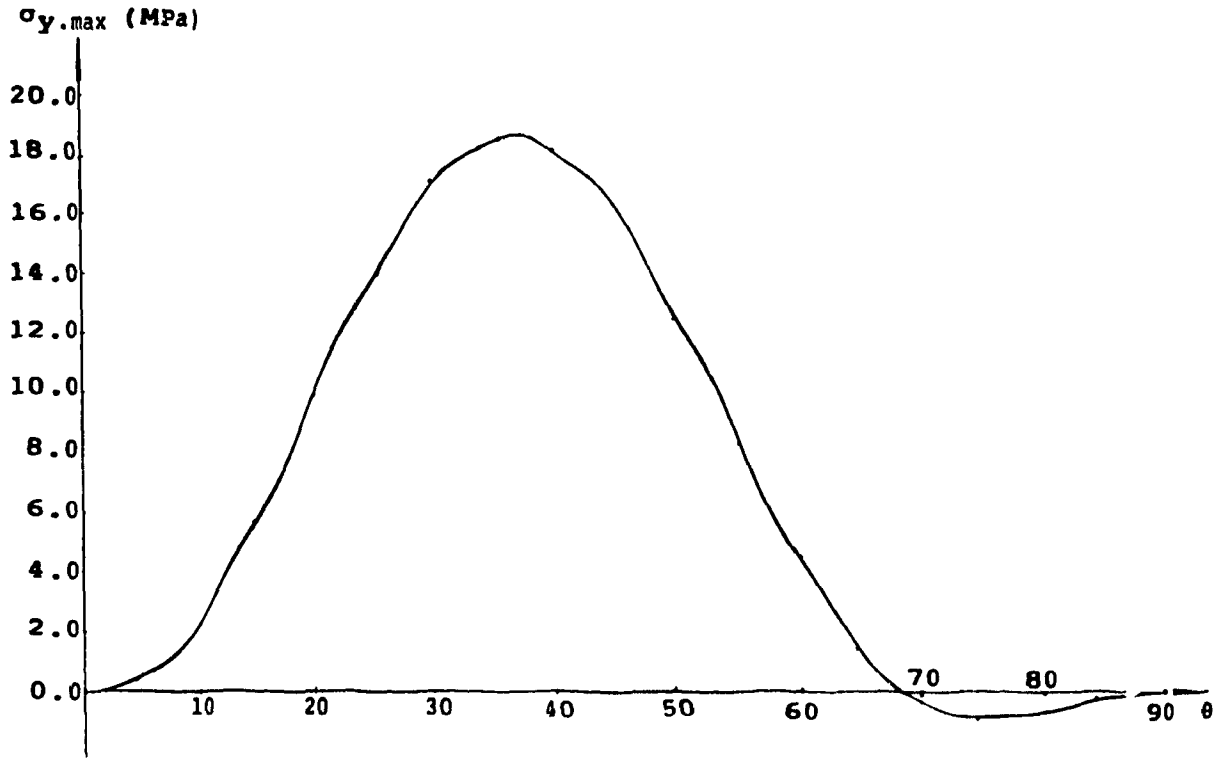

Fig.5.17 Stress - fiber orientation relation

$\sigma_{y.max}$ versus θ for symmetric angle-ply

for symmetric angle-ply laminate

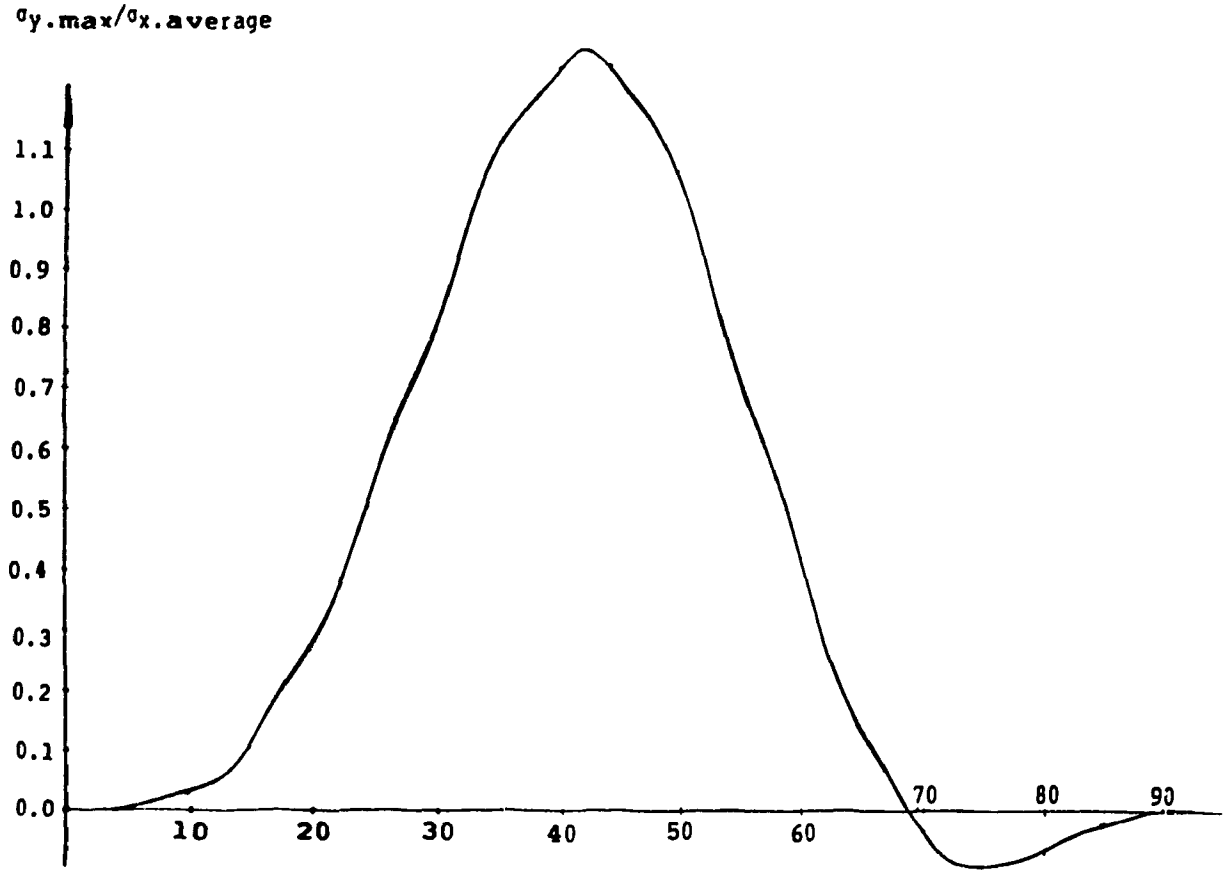

Fig.5.18 Stress - fiber orientation relation

$\sigma_{y.max}/\sigma_{x.average}$ versus θ

for symmetric angle-ply laminate

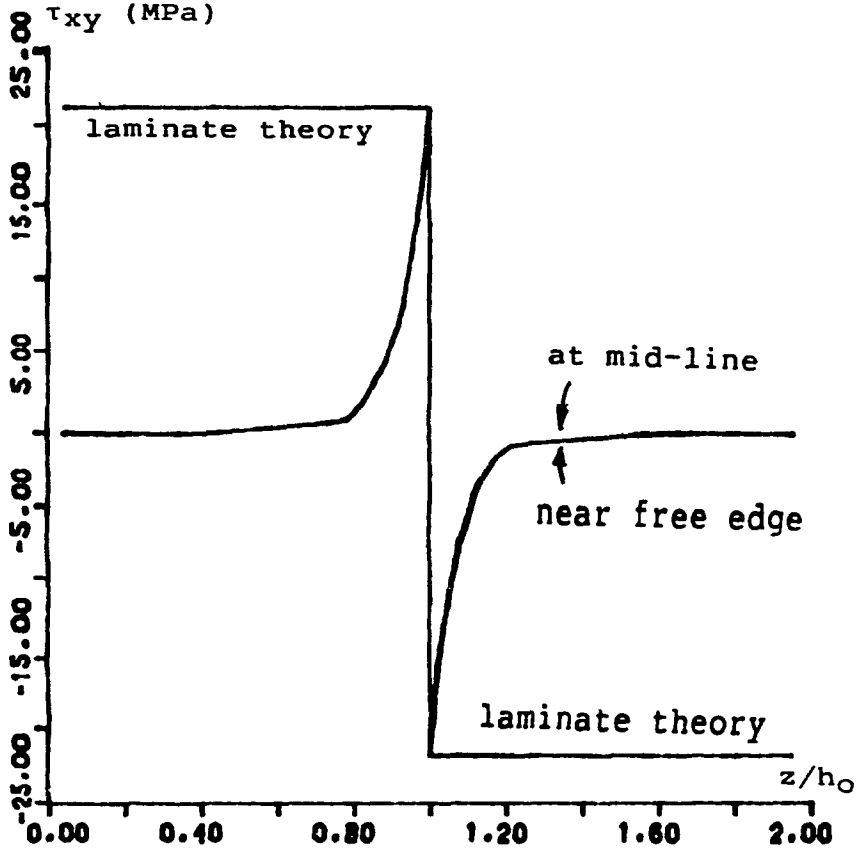

Fig.5.19 Stress distribution along thickness
τ_{xy} versus z/h_o for [10/-10]s

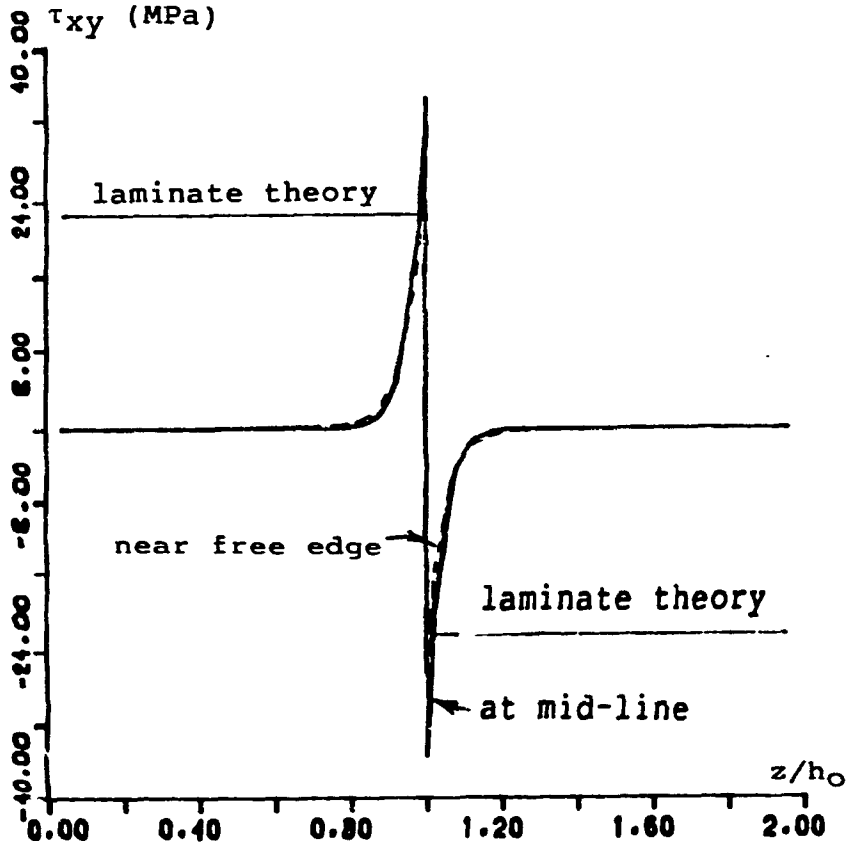

Fig.5.20 Stress distribution along thickness
τ_{xy} versus z/h_o for [30/-30]s

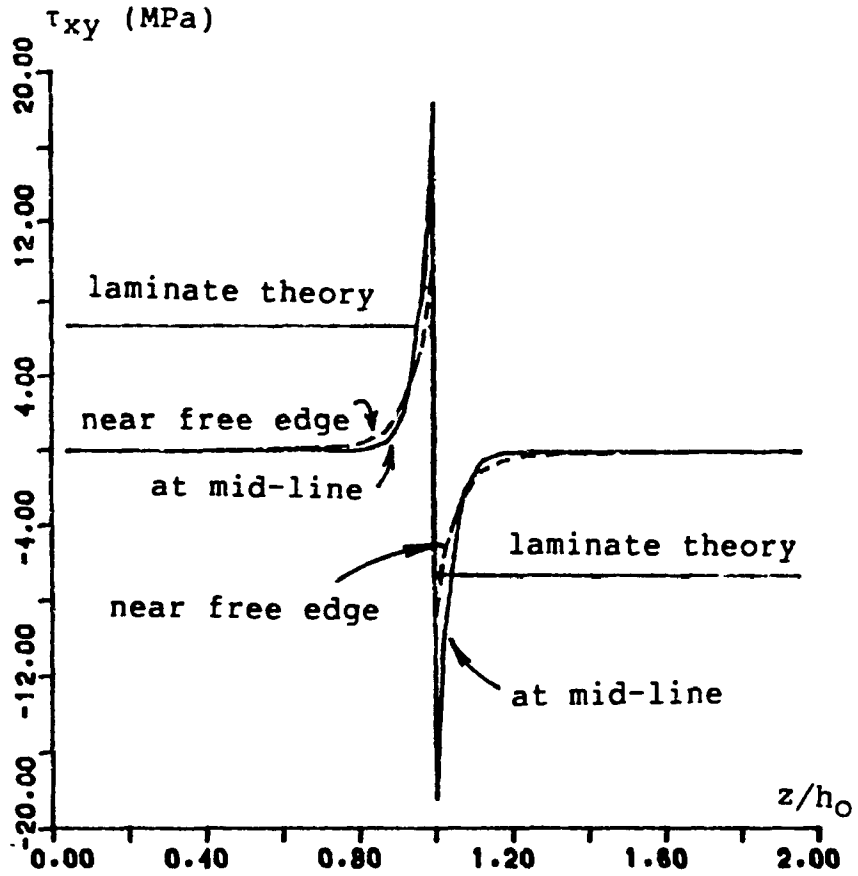

Fig.5.21 Stress distribution along thickness τ_{xy} versus z/h_o for [45/-45]s

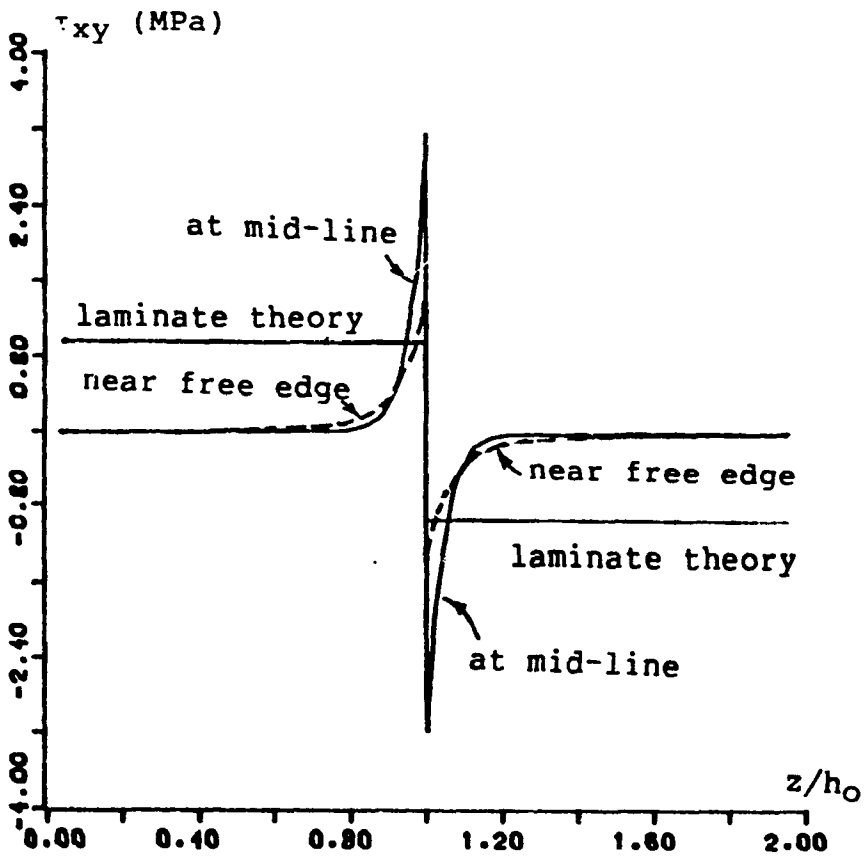

Fig.5.22 Stress distribution along thickness τ_{xy} versus z/h_o for [60/-60]s

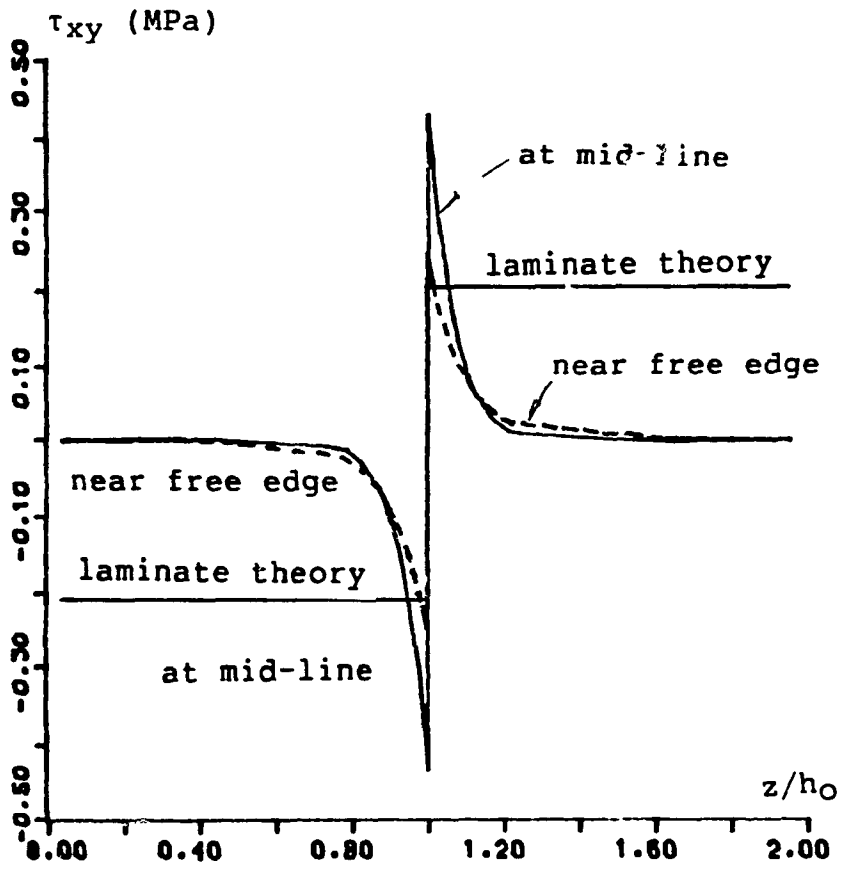

Fig.5.23 Stress distribution along thickness τ_{xy} versus z/h_o for [75/-75]s

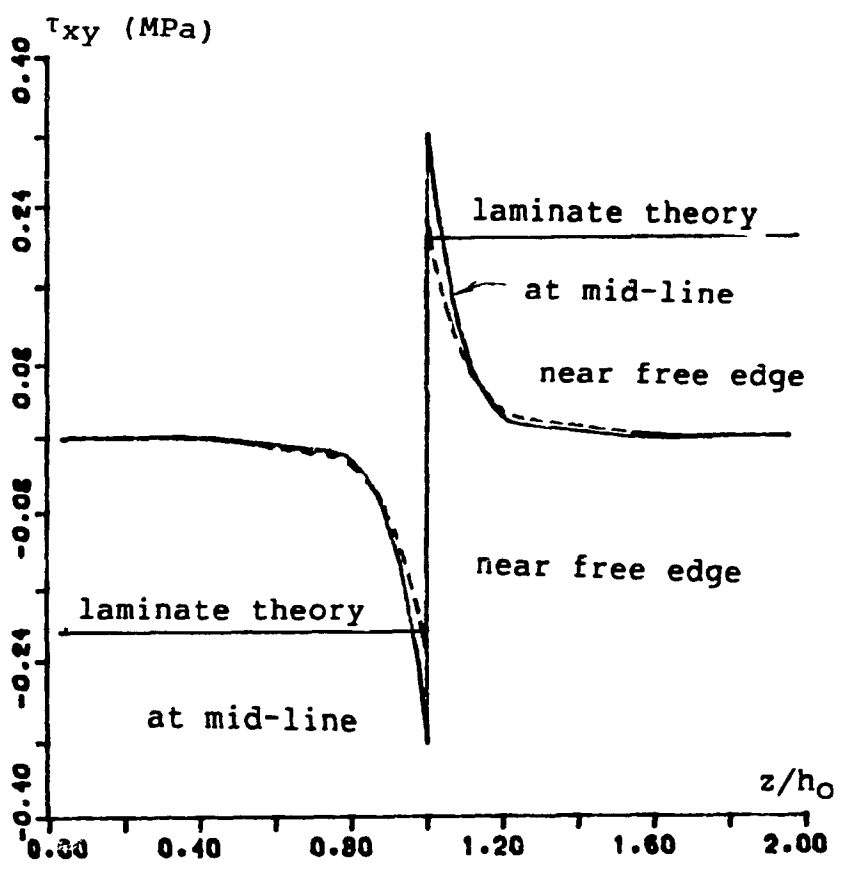

Fig.5.24 Stress distribution along thickness τ_{xy} versus z/h_o for [80/-80]s

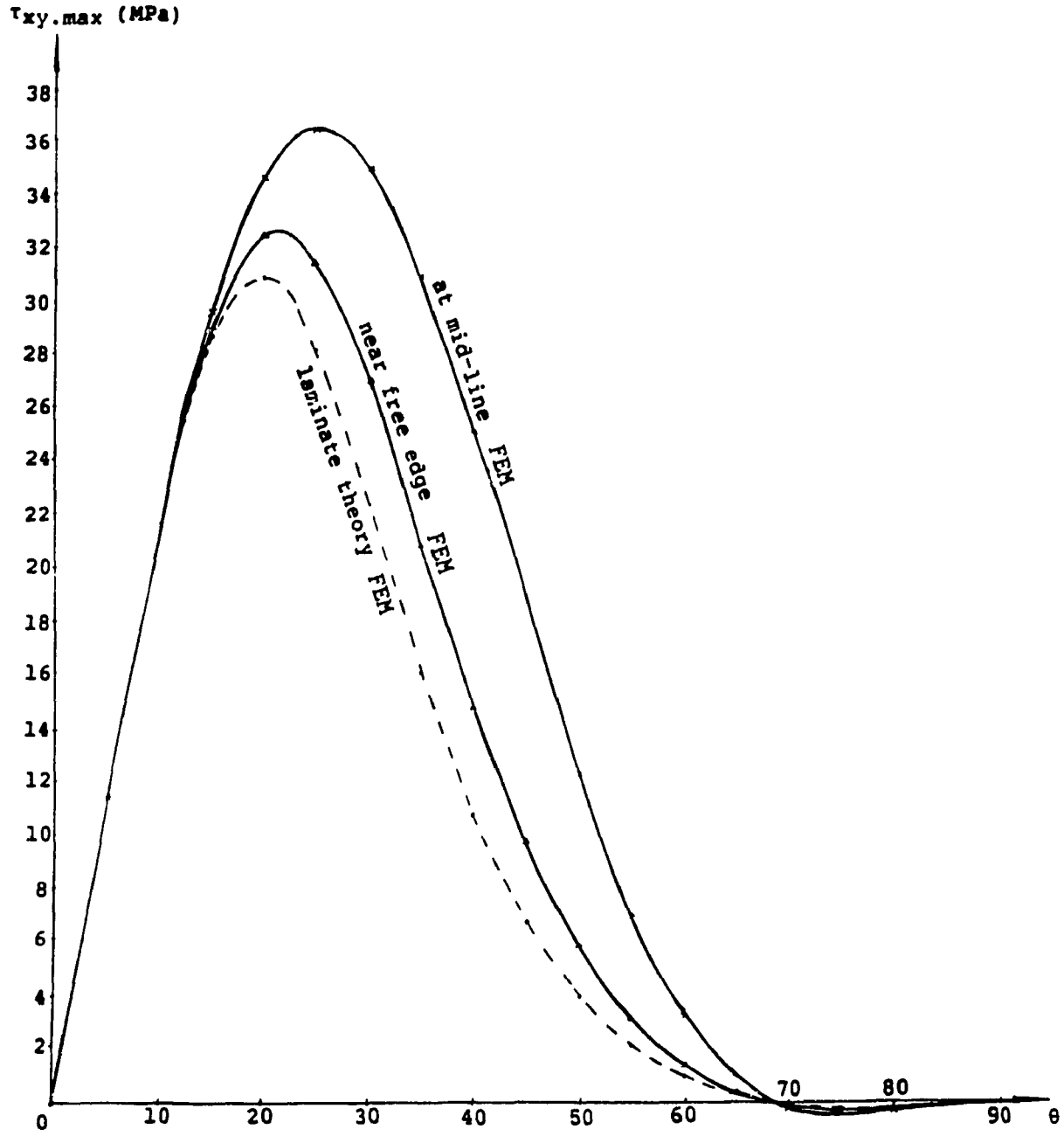

Fig.5.25 Stress - fiber orientation relation

τ_{xy} versus θ for symmetric angle-ply laminate

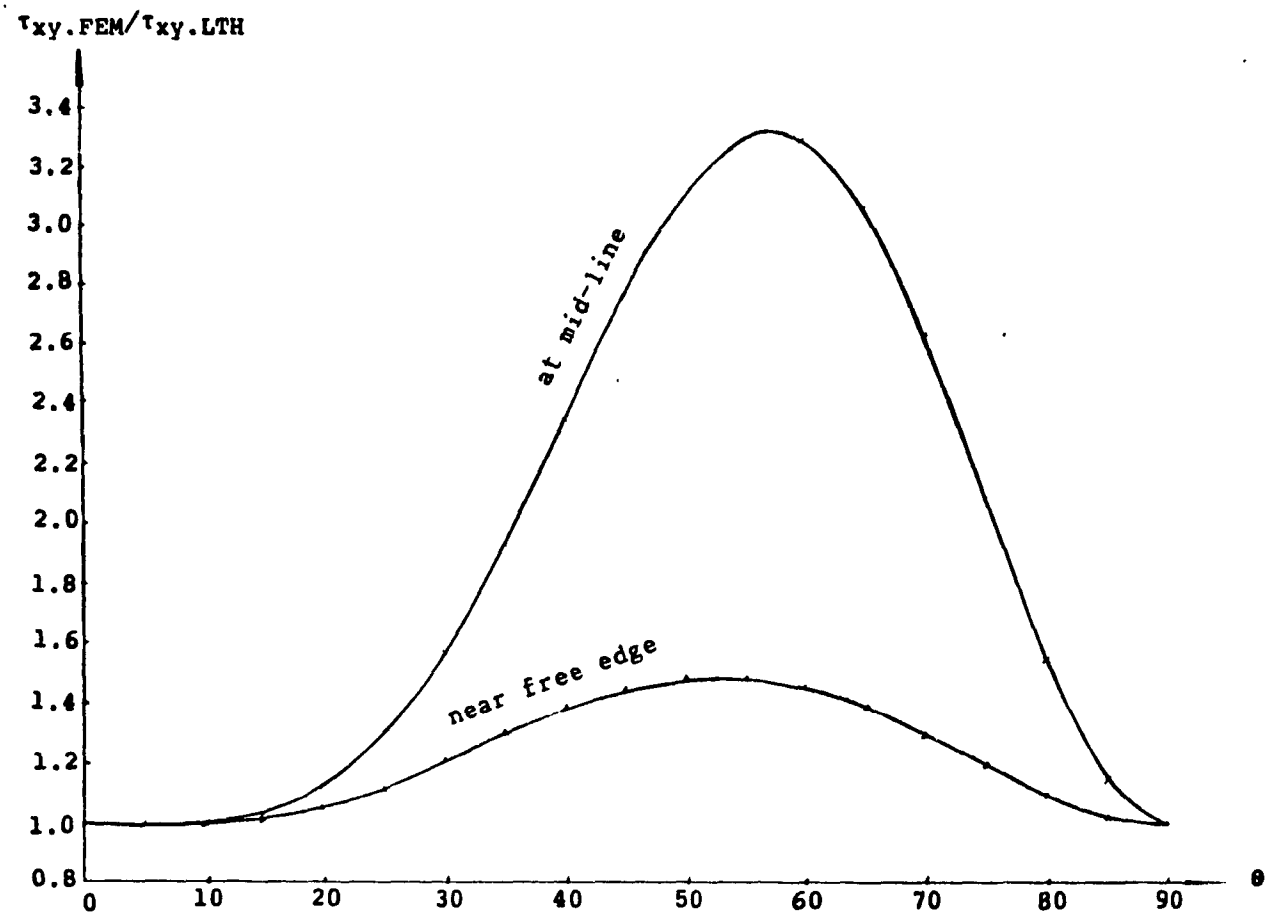

Fig.5.26 Stress - fiber orientation relation

$\tau_{xy.FEM}/\tau_{xy.LTH}$ versus θ

for symmetric angle-ply laminate

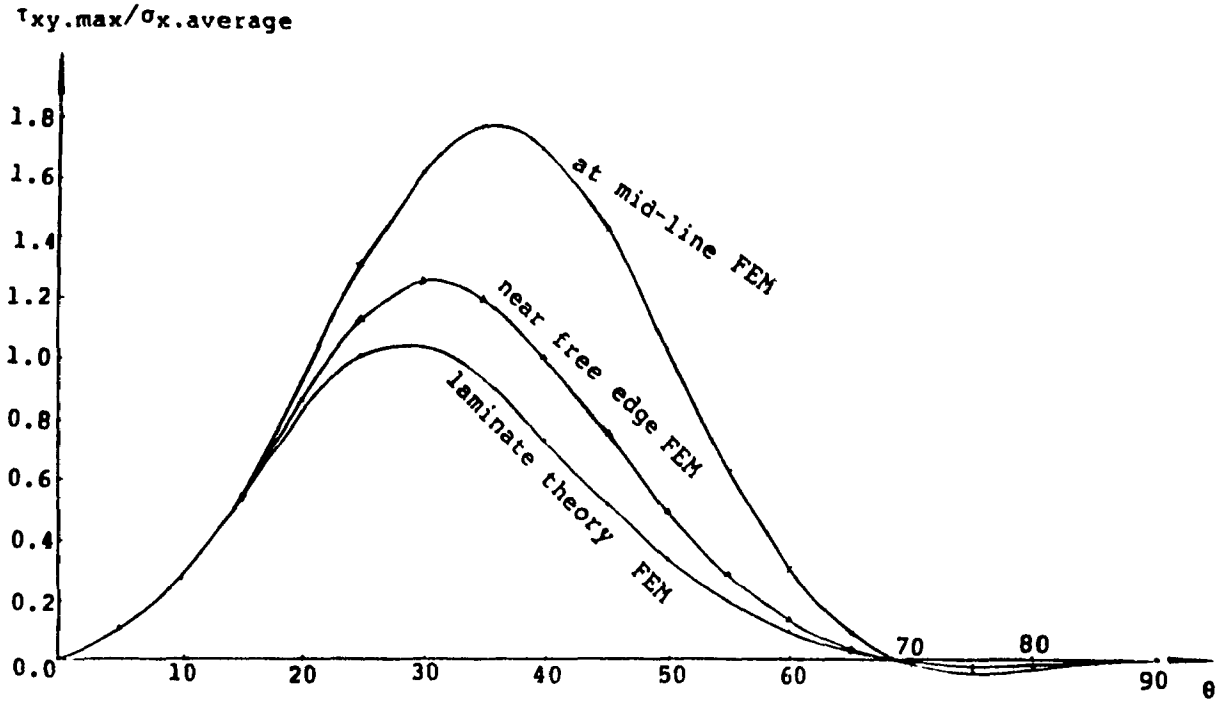

Fig.5.27 Stress - fiber orientation relation

$\tau_{xy.max}/\sigma_{x.average}$ versus θ

for symmetric angle-ply laminate

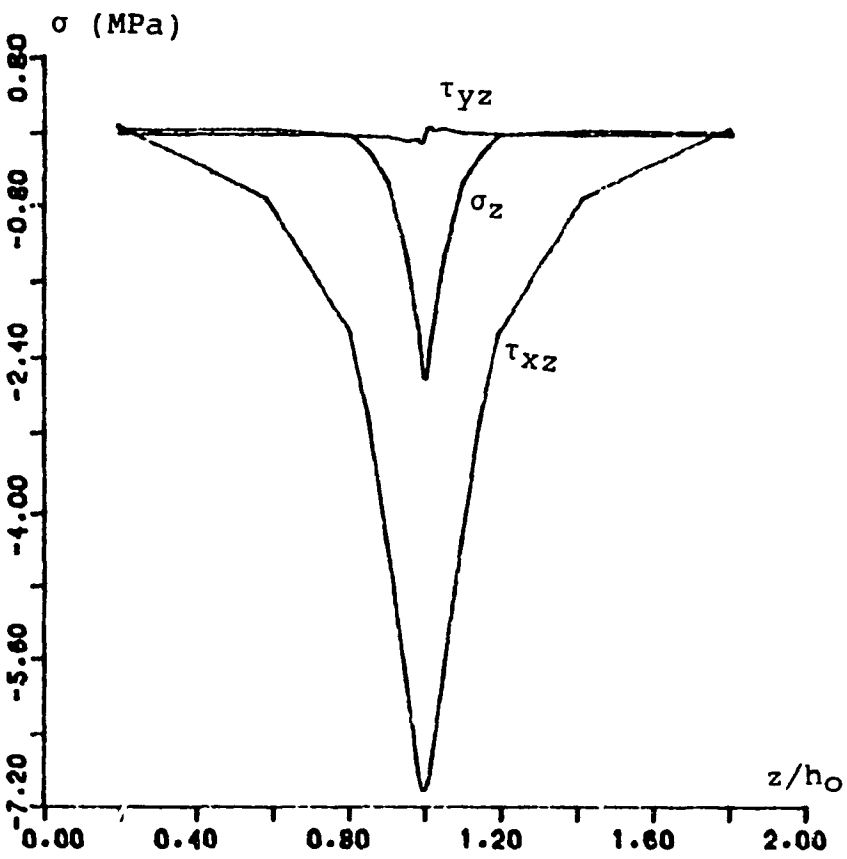

Fig.5.28 Stress distribution along thickness $\sigma_z, \tau_{xz}, \tau_{yz}$ versus z/h_o for [10/-10]s

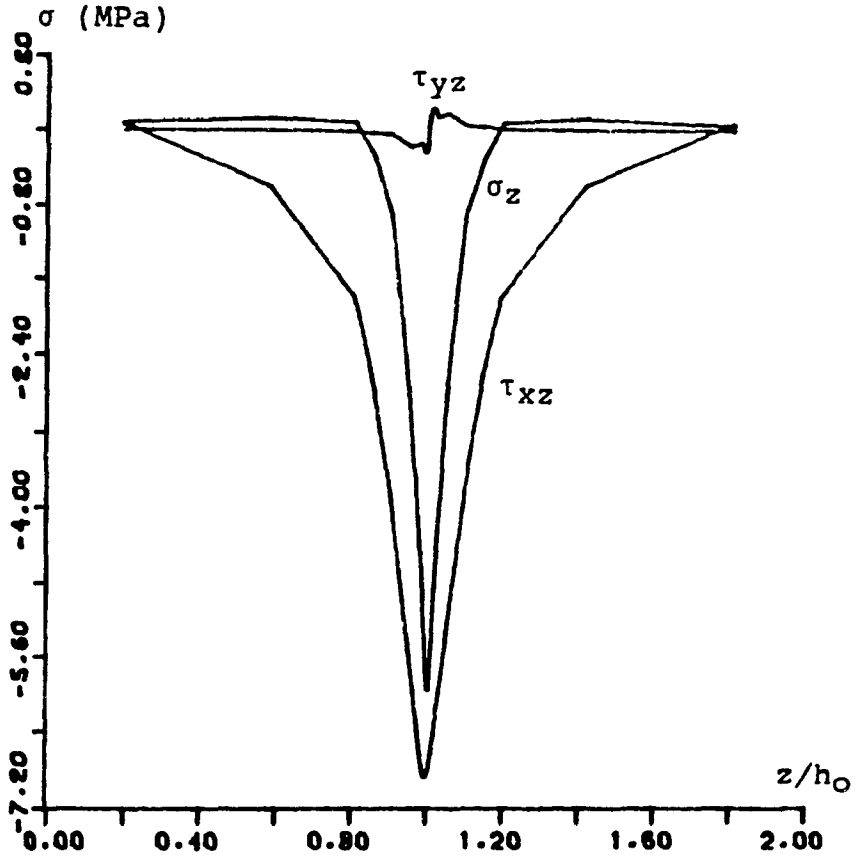

Fig.5.29 Stress distribution along thickness $\sigma_z, \tau_{xz}, \tau_{yz}$ versus z/h_o for [15/-15]s

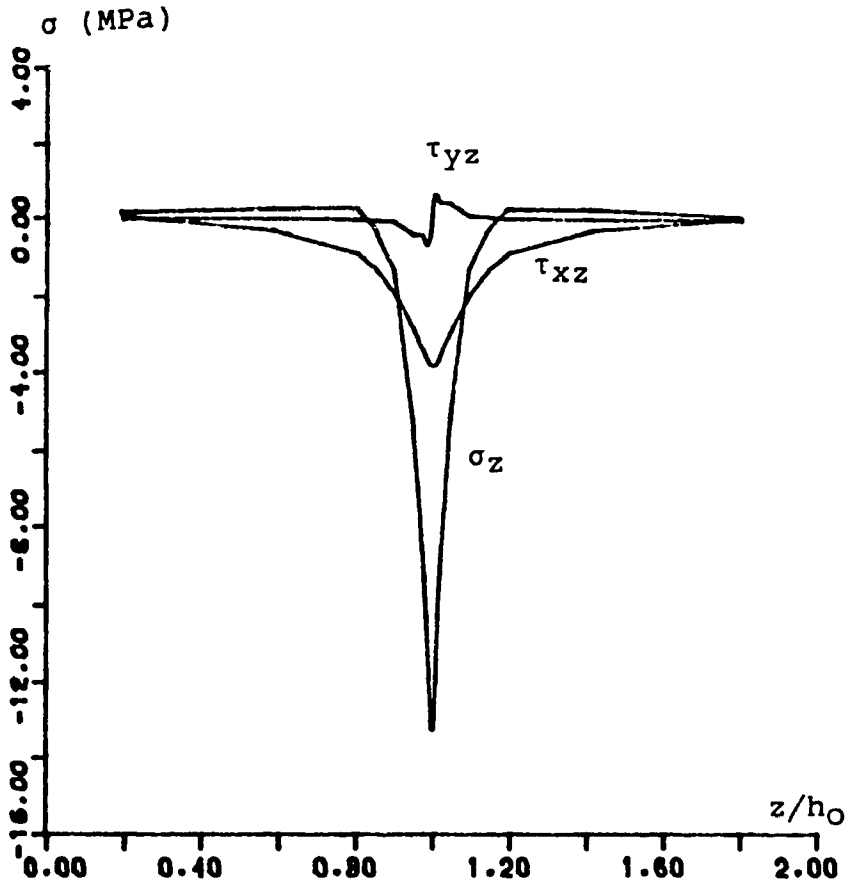

Fig.5.30 Stress distribution along thickness $\sigma_z, \tau_{xz}, \tau_{yz}$ versus z/h_o for [30/-30]s

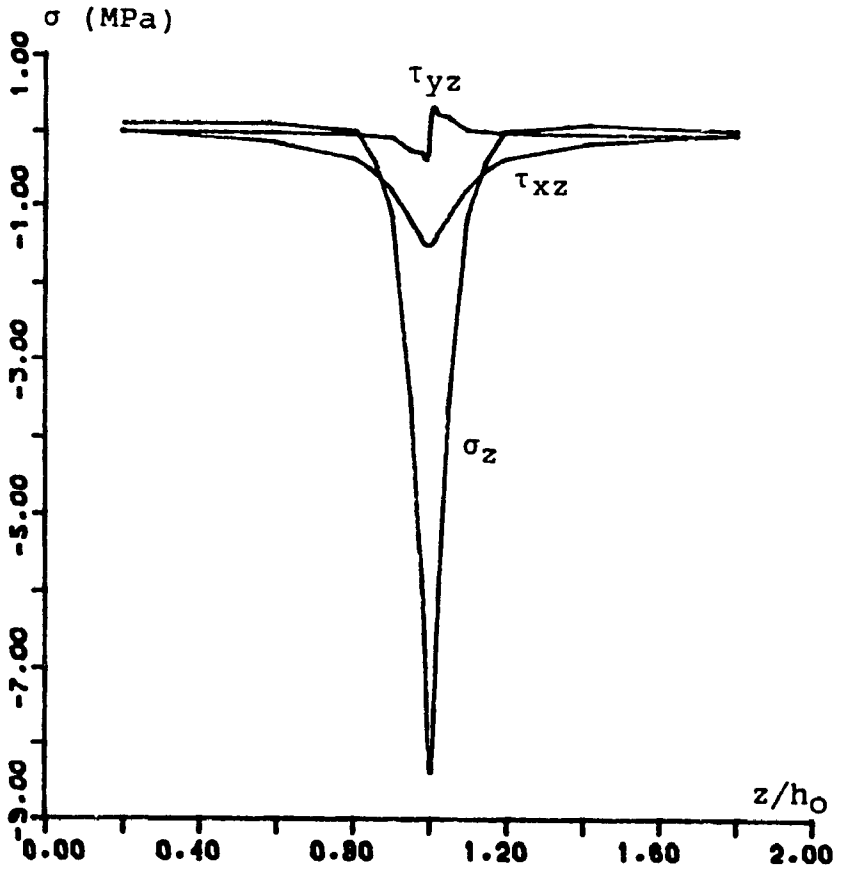

Fig.5.31 Stress distribution along thickness $\sigma_z, \tau_{xz}, \tau_{yz}$ versus z/h_o for [45/-45]s

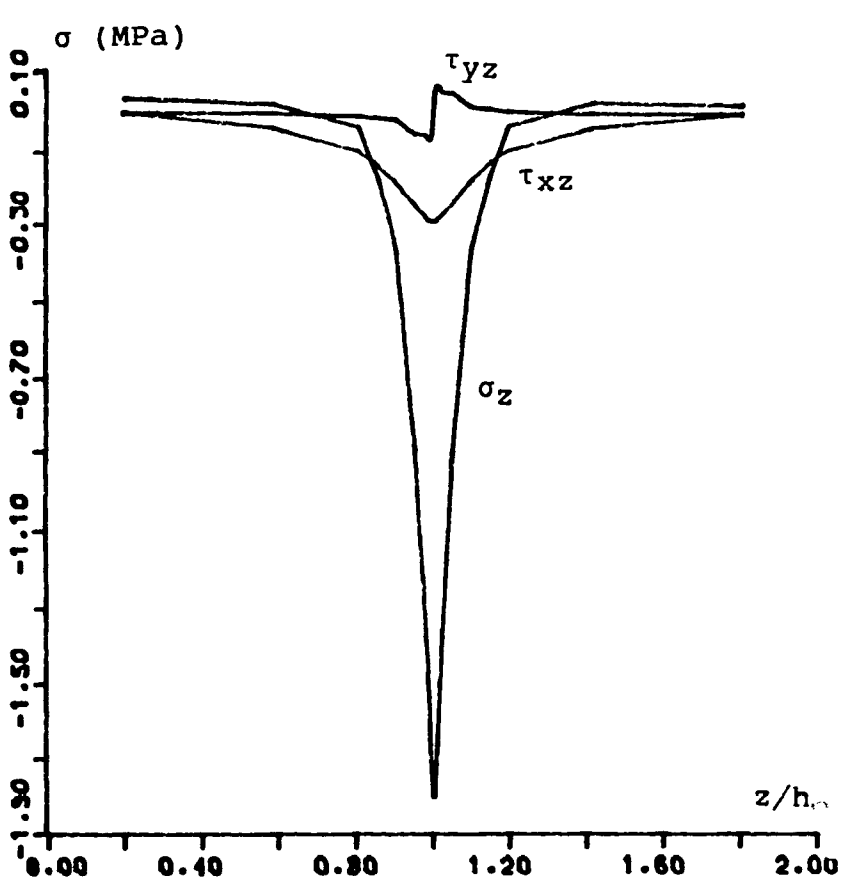

Fig.5.32 Stress distribution along thickness $\sigma_z, \tau_{xz}, \tau_{yz}$ versus z/h_o for [60/-60]s

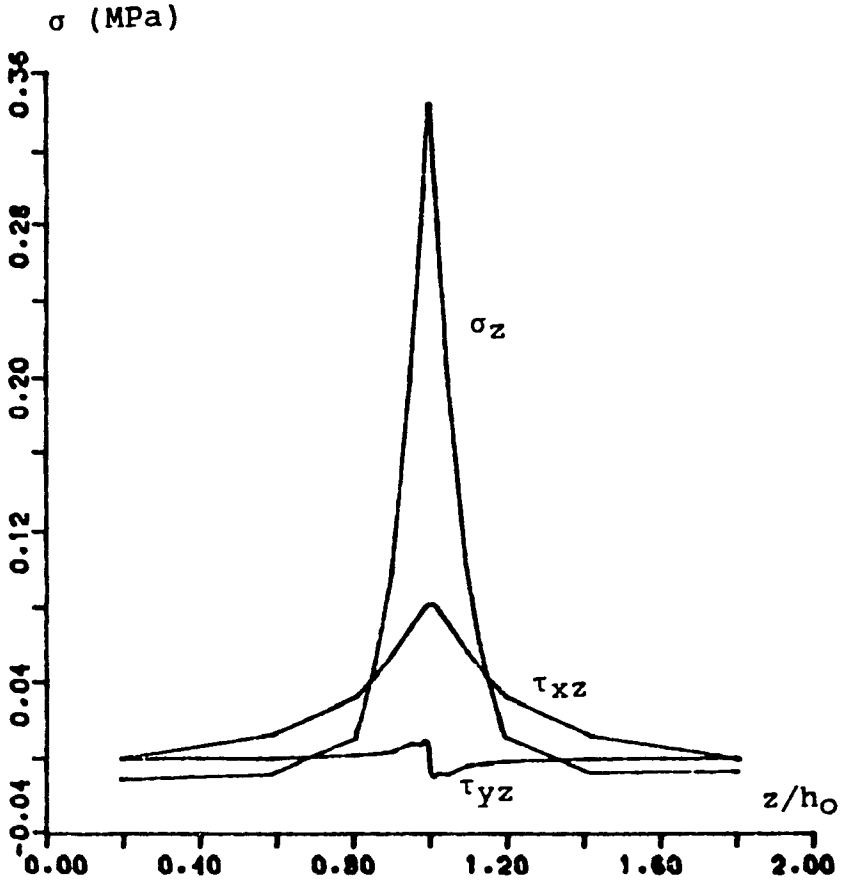

Fig.5.33 Stress distribution along thickness $\sigma_z, \tau_{xz}, \tau_{yz}$ versus z/h_o for [75/-75]s

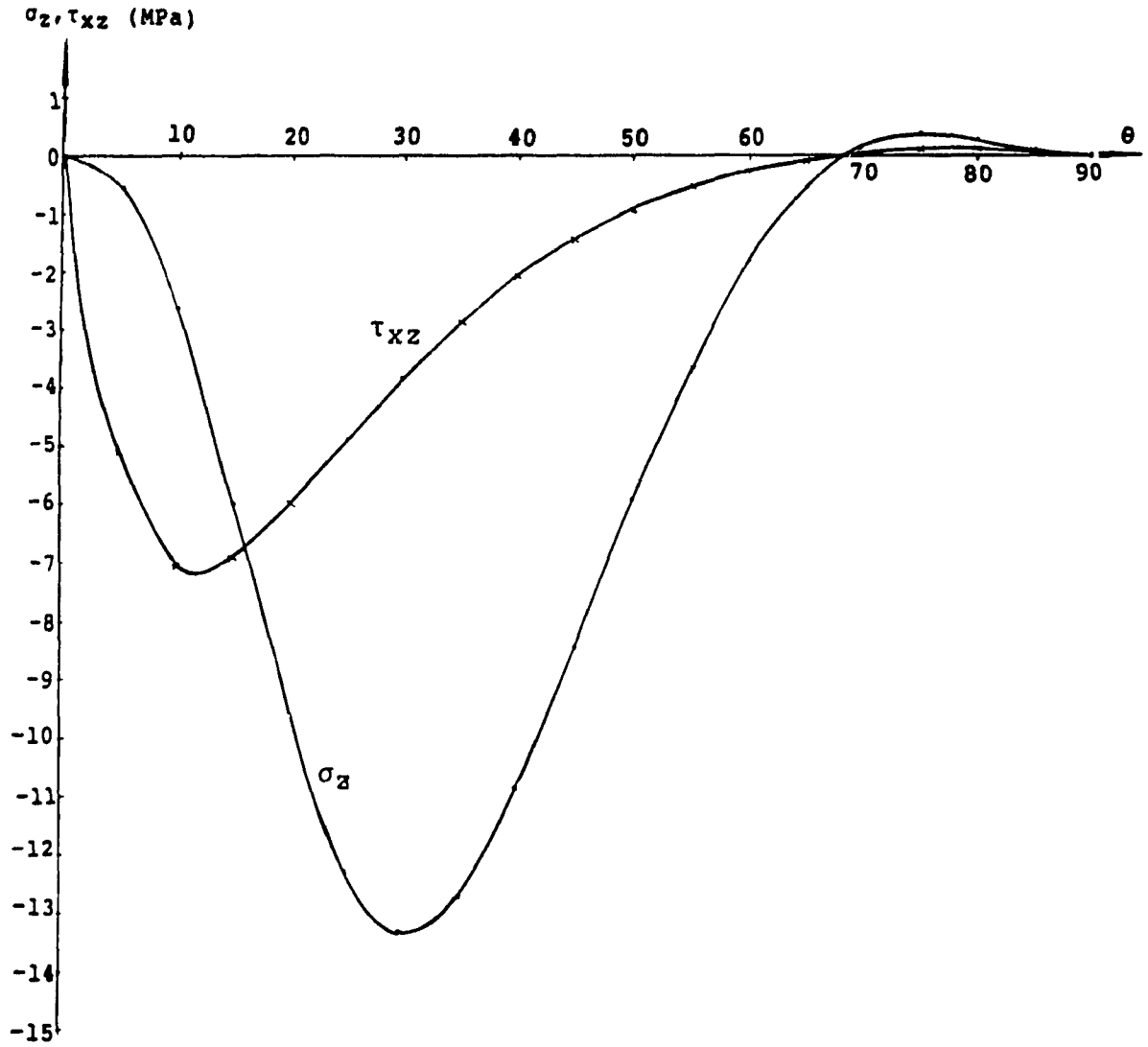

Fig.5.34 Stress - fiber orientation relation

σ_z, τ_{xz} versus θ

for symmetric angle-ply laminate

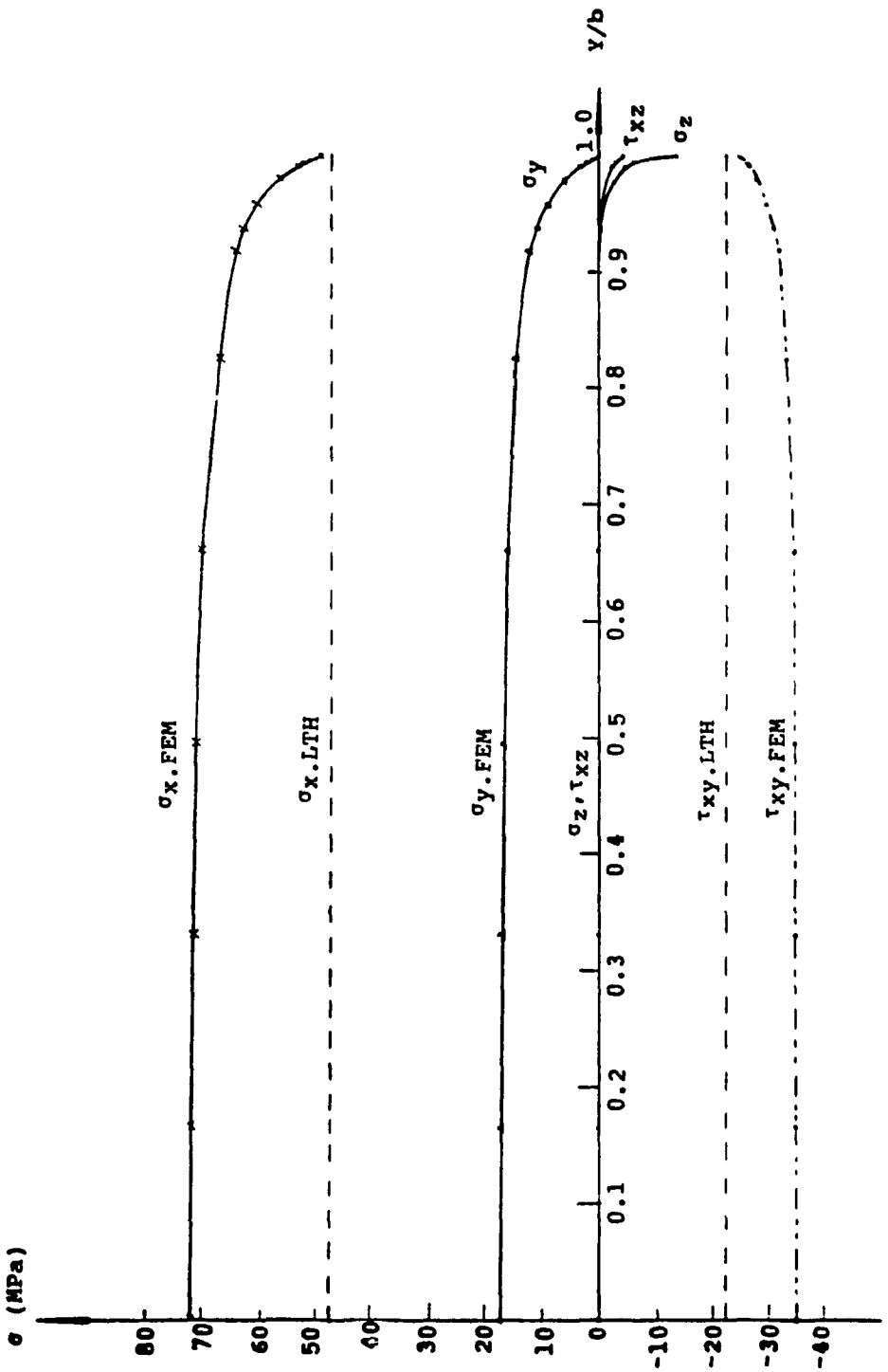

Fig.5.35 Stress distribution along interface

σ versus y/b for [30/-30]s

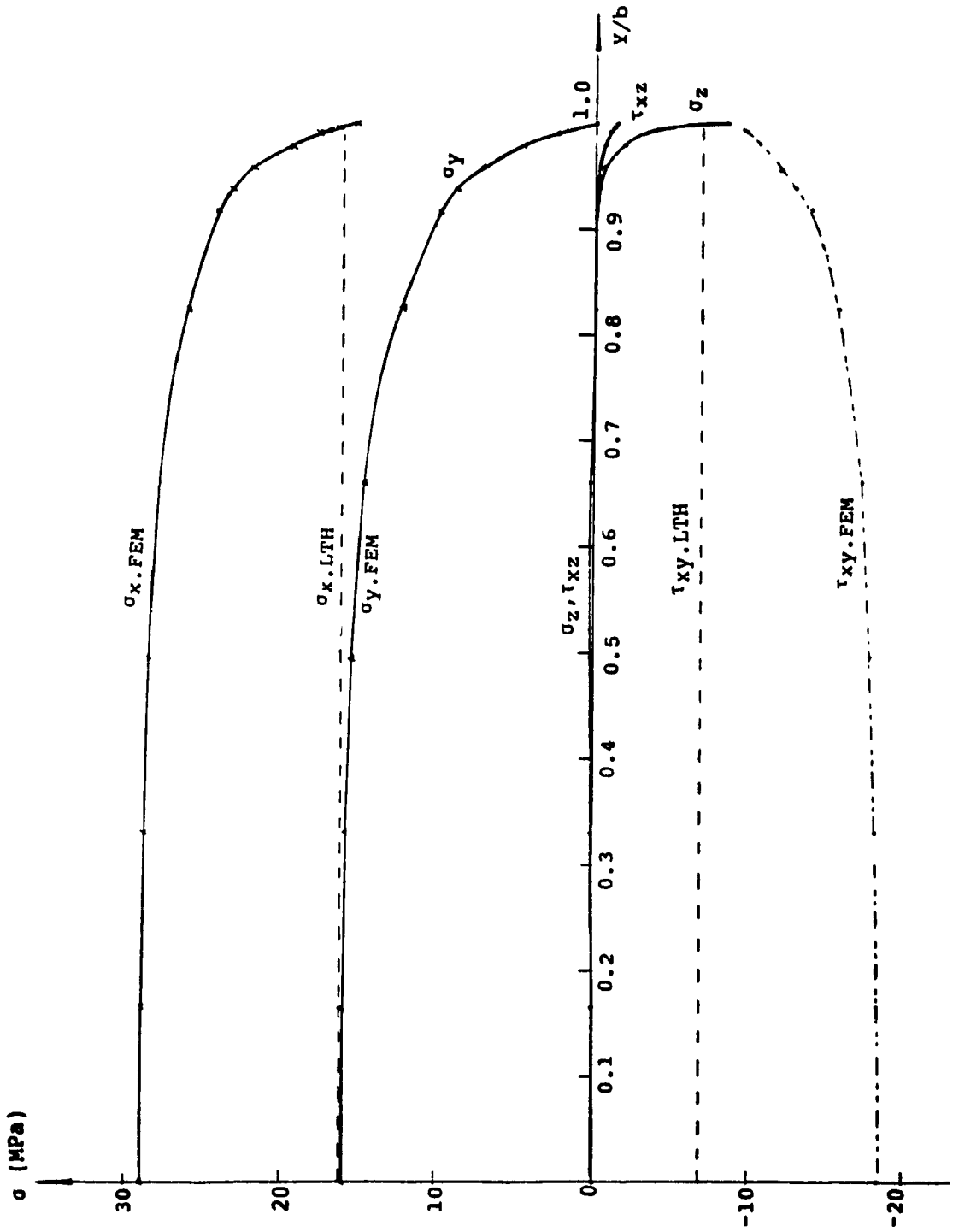

Fig.5.36 Stress distribution along interface

σ versus y/b for [45/-45]s

Chapter 6 Contribution And Suggestion For Future Work

The contributions made in this thesis are:

1) Introduction of the concept of combined energy, formulation of the laminate functional and verification of the variational principle of combined energy.

2) Introduction of the concept of modal analysis of deformable bodies with finite degrees of freedom, a superposition theorem of stiffness matrix and a postulate of energy decomposition in hybrid finite element. Development of a procedure to find out natural stress modes from natural deformation modes. Modal analysis for 2-D, 4-node and 3-D, 8-node hybrid finite elements.

3) Formulation of three dimensional composite finite element which consists of two semi-stiffness matrix, one is semi-displacement stiffness matrix, another is semi-hybrid stifness matrix.

4) Calculation of the in-plane stress concentration near interlaminar surfaces for laminate structures.

The following future works are suggested:

1) Development of the modal analysis technique for 3-D.

20-node hybrid finite element and other plate and shell elements.

2) Modal analysis for anisotropic materials.

3) Development of the distribution of the displacements and stresses in various laminate structures using many elements per each layer.

4) Determination of the rational shape function N for displacement field and mode function P for stress field for laminate structures.

5) Modal analysis for laminates.

6) Stress analysis by means of composite FEM with one element to span the whole thickness for laminate structures.

References

[1] Lekhnitskii,S.G., Theory of Elasticity of An Anisotropic Body, Gostekhizdat, Moscow, 1950 (in Russian). Transl., Holden-Day, San Francisco, 1963. Second edition, Nauka, Moscow, 1977 (in Russian). Transl., Mir Publishers, Moscow, 1981.

[2] Pipes,R.B. and Pagano,N.J., "Interlaminar stresses in composite laminates under uniform axial extension", J.Compos.Mater.v.4 Oct 1970 p.538-548

[3] Altus,E., Rotem,A. and Shmueli,M., "Free edge effect in angle-ply laminates - a new three dimensional finite difference solution", J.Compos.Mater.v.14 1980 p.21-30

[4] Engblom,J.J. and Ochoa,O.O., "Through-the-thickness stress predictions for laminated plate of advanced composite materials", Int.J.Numer.Methods Eng.v.21 N.10 Oct.1985 p.1759-1776

[5] Heppler,G.R. and Hansen,J.S., "High precision singular finite element for fracture analysis of composite structures", Adv.in Compos.Mater.v.1 Agu.1980 p.666-692

[6] Yeh,J.R. and Tabjbakhsh,I.G., "Stress singularity in composite laminates by finite element method", J.Compos. Mater.v.20 N.4 Jul.1986 p.347-364

[7] Natarajan,R., Hoa,S.V. and Sankar,T.S., "Stress analysis of filament wound tanks using three-dimensional finite elements", Int. Numer. Methods

Eng v 23 N 4 Apr 1986 p 623-633

[8] Lucking,W.M., Hoa,S.V. and Sankar,T.S., "Effect of geometry on interlaminar stresses of (0/90)//s composite laminates with circular holes", J.Compos. Mater. v.18 N.2 Mar.1984 p.188-198

[9] Rybicki,E.F., "Approximate three-dimensional solution for symmetric laminates under inplane loading", J.Compos.Mater.v. 5 1971 p.354-360

[10] Khalil,S.A., Sun,C.T. and Hwang,W.C., "Application of a Hybrid finite element method to determine stress intensity factors in unidirectional composites", Int. J. Fract. v.31 N.1 May 1986 p.37-51

[11] Reissner,E., "Note on the effect of transverse shear deformation in laminated anisotropic plates", Compu.Meth.in Appl.Mech.and Eng., v. 20, 203-209, 1986

[12] Spilker,R.L. and Jakobs,D.M., "Hybrid stress reduced-mindlin elements for thin multilayer plates", Int. Numer. Methods Eng. v. 23 N. 4 Apr. 1986 p.555-578

[13] Wang,S.S. and Yuan,F.G., "A Hybrid finite element approach to composite laminate elasticity problems with singularities", J. Appl. Mech. v. 50 1983 p. 835-844

[14] Hsu,P.W. and Herakovich,C.T., "Edge effects in angle-ply composite laminates", J. Compos. Mater. v. 11 1977 p.422-427

[15] Tang,S. and Levy,A., "Interlaminar stresses of uniformly loaded rectangular composite plates", J. Compos.Mater.v.10 N.1 Jan.1976 p.69-78

[16] Bar-Yoseph,P. and Pian,T.H.H., "Calculation of interlaminar stress concentration in composite laminates", J. Compos. Mater. v. 15 N. 3 May 1981 p. 225-239

[17] Bar-Yoseph,P., "On the accuracy of interlaminar stress calculation in laminated plates", Comput. Methods Appl. Mech. Eng. v. 36 N. 3 Mar. 1983 p. 309-329

[18] Pagano,N.J., "Free-edge stress fields in composite laminates", Int. J. Solids Structures v. 14 1978 p. 385-400

[19] Wang,J.T.S. and Dickson,J.N., "Interlaminar stresses in symmetric composite laminates", J. Compos. Mater. v. 12 1978 p. 390-401

[20] Oery,H., Reimerdes,H. and Dieker,S., "Calculation of Interlaminar stresses in multi-layer composite materials using a transfer matrix method", Z Flugwiss Weltraumforsch v. 8 N. 6 Nov-Dec 1984 p. 392-404

[21] Whitney,J.M. and Browning,C.E., "Free-edge delamination of tensile coupons", J. Compos. Mater. v. 6 1972 p. 300-303

[22] Berghaus,D.G. and Aderholdt,R.W., "Photoelastic analysis of interlaminar matrix stresses in fibrous composite models", Exp. Mech. v. 15 N. 4 Jul. 1975 p. 173-176

[23] Spilker,R.L.and Chou,S.C., "Edge effects in symmetric composite laminates: importance of satisfying the traction-free-edge condition", J. Compos. Mater. v. 14 1980 p. 2-20

[24] Chien, W.Z., On the Generalized Variational Principles, Knowledge Press, 1985 (in Chinese),

Shanghai

[25] Tsai, S.W. and Hahn, H.T., Introduction to Composite Materials, Technomic Publishing Co. Inc., 1980

[26] Christensen, R.M., Mechanics of Composite Materials, John Wiley & Sons Inc., 1979

[27] Hull, D., An Introduction to Composite Materials, Cambridge University Press, 1981

[28] Pian,T.H.H. and Tong,P., "Basis of finite element method for solid continua", Int.J. Num.Meth.Eng.1, 3-28, 1969

[29] Fraeijs de Veubeke,B.M., "Bending and stretching of plates, special models for upper and lower bounds", in Proc. Conf. on Matrix Methods in Struct. Mech. AFFDL-TR-66-80, 1966

[30] Ahamd,S. and Irons,B.M., "An Assumed stress approach to refined isoparametric finite elements in three dimensions", Finite element method in eng. Proc. Conf. on Fin.Ele.Met.Eng.1974

[31] Spilker,R.L., Maskeri,S.M. and Kania,E., "Plane isoparametric hybrid-stress elements: invariance and optimal sampling", Int. J. Num. Meth. Eng. 17, 1469-1496,1981

[32] Brezzi,F., "On the existence, uniqueness and approximation of saddle-point problems arising from Lagrangeg multipliers", RAIRO 8(R2), 129-151, 1974

[33] Babuska,I., Oden,J.T. and Lee,J.K., "Mixed-hybrid finite element approximations of second-order elliptic

boundary-value problems", Part I, Comput Meth Appl Mech Eng , 11, 175-206, 1977: Part II — weak hybrid methods, Comp. Meth. Appl. Mech. Eng., 14, 1-22, 1978

[34] Spilker,R.L., "Three-dimensional hybrid-stress isoparametric quadratic displacement element", Int J Num Meth Eng, 18, 445-465, 1982

[35] Rubinstein,R., Punch,E.F. and Atluri,S.N., "An analysis of, and remedies for, kinematic modes in hybrid finite elements: selection of stable, invariant stress fields", Computer Methods Appl. Mech. Eng., 38, 63-92, 1983

[36] Punch,E.F. and Atluri,S.N., "Application of isoparametric three-dimensional hybrid-stress finite elements with least-order stress fields", Comput. and Struct., 19, 3, p409-430, 1984

[37] Pian,T.H.H., "Derivation of element stiffness matrices by assumed stress distributions", AIAA J.2, No. 7, 1333-1336, 1964

[38] Peterson,K., "Derivation of the stiffness matrix for hexahedron element by the assumed stress hybrid method", S.M.Thesis MIT,1972

[39] Lee,S.W., "An assumed stress hybrid finite element for three dimentional elastic structural analysis", MIT, ASRL TR170-3, 1974

[40] Pian,T.H.H., Chen,D.P. and Kang,D., "A new formulation of hybrid/mixed finite element", Comput. Struct.16, 81-87, 1983

[41] Irons,B.M., "An assumed stress version of the Wilson 8-node element", Univ. of Wales, CNME/CR/56, 1972

[42] Spilker,R.L. and Singh,S.P., "Three-dimentional hybrid-stress isoparametric quadratic displacement element", Int.J. Num.Meth.Eng. 18, 445-465, 1982

[43] Atluri,S.N., Kathiresan,K. and Kobayashi,A.S., "Three-dimensional linear fracture mechanics analysis by a displacement-hybrid finite element model", Int. Conf. on Struct.Mech.in Reat Technol, 1975

[44] Atluri,S.N., Kathiresan,K., Kobayashi,A.S. and Nakagaki,M., "Inner surface cracks in an internally pressurized cylinder analyzed by a three dimentional displacement-hybrid finite element method", Int.Conf. on Pressure Vessel Technol 3rd PT.2

[45] Atluri,S.N. and Kathiresan,K., "3D analyses of surface flaws in thick-walled reactor pressure vessels using displacement-hybrid finite element method", Nuclear Eng. and Design 51, 2, 163-176, 1979

[46] Atluri,S.N., Nakagaki,M. and Kathiresan,K., "Hybrid-finite-element analysis of some nonlinear and 3-dimentional problems of engineering fracture mechanics", Comput.and Struct., 12, 4, 1980

[47] Nishioka,T. and Atluri,S.N., "Analysis of cracks in adhesively bonded metallic laminates by a 3-dimensional assumed stress hybrid FEM", AIAA (cp811) pap. 81-0497, pp66-70,1981

[48] Reissner,E., "On a certain mixed variational

theorem and a proposed application", Int. J. Numer. Meth. Eng., v. 20, 1366-1368, 1984

[49] Reissner,E., "On a mixed variational theorem and on shear deformable plate theory", Int. J. Numer. Meth. Eng., v. 23, 193-198, 1986

[50] Moriya,K., "Laminated plate and shell elements for finite element analysis of advanced fiber reinforced composite structures", Nippon Kikai Gakkai Ronbunshu a Hen v. 52 N. 478 Jun. 1986 p. 1600-1607

[51] Pian,T.H.H. and Chen,D.P., "On the suppression of zero energy deformation modes", Int. J. Numer. Meth. in Eng., vol. 19, 1741-1752, 1983

[52] Reissner,E., "Reflection on the theory of elastic plates", Appl. Mech. Rev. vol. 38, No. 11, Nov. 1985

[53] Karamanlidis,D. and Atluri,S.N., "Mixed finite element model for plate bending analysis", Compu. Struct., vol. 19, No. 3, 431-445, 1984

[54] Mau,S.T., Tong,P. and Pian T.H.H., "Finite Element Solutions for laminated thick plates", J. Compos. Mater., vol. 6, 304-311, 1972

[55] Huang,Q., "Variational principle of hybrid energy and the fundamentals of 3-D laminate theory - a new approach for the analysis of interlaminar stresses in composite materials", read at International Conference on Computational Engineering Mechanics, June 1987, Beijing, China

[56] Pipes,R.B., "Solution of certain problems in the

theory of elasticity for laminated anisotropic systems", Ph.D. dissertation, Univ. of Texas, Arlington, 1972

[57] Pipes,R.B. and Pagano,N.J., "Interlaminar stresses in composite laminates - an approximate elasticity solution", J. Appl. Mech. Trans. ASME, vol. 41, ser. E, No. 3, Sep. 1974, 668-672

[58] Chatterjee,S.N. and Ramnath,V., "Modeling laminated composite structures as assemblage of sublaminates", Int. J. of Solid and struct. v. 24 n.5 1988 p. 439-458

[59] Hwang,W.C. and Sun,C.T., "Analysis of interlaminar stresses near curved free-edges of laminated composites using iterative finite element method", Comput. and struct. v. 28 n. 4 1988 p. 461-467

[60] Sun,C.T. and Liou,W.J., "Three-dimensional hybrid-stress finite element formulation for free vibrations of laminated composite plates", J. of Sound and Vibr. v. 119 n.1 Nov. 1987 p. 1-14

[61] Kwon,Y.W. and Akin,J.E., "Analysis of layered composite plates using a high-order deformation theory", Comput. and Struct. v. 27 n.5 1987 p. 619-623

[62] Whitney,J.M., "Stress analysis of thick laminated composite and sandwich plates", J. of Compos. Mater. v. 6 1972 p. 426-440

[63] Liou,W.J. and Sun,C.T., "Three-dimensional hybrid stress isoparametric element for the analysis of laminated composite plates", Comput. and Struct. v. 25 n. 2

1987 p.241-249

[64] Murthy,P.L.N. and Chamis,C.C., "Composite interlaminar fracture toughness: three-dimensional finite element modeling for mixed mode I, II, and III fracture", NASA Tech.Memo.88872 1986 26p

[65] Chaudhuri,R. and Seide,P., "Approximate semi-analytical method for perdiction of interlaminar shear stresses in an arbitrarily laminated thick plate", Comput.and Struct.v.25 n.4 1987 p.627-636

[66] Toledano,A. and Murakami,H., "High-order laminated plate theory with improved in-plane responses", Int. J. of Solid and Struct.v.23 n.1 1987 p.111-131

[67] Toledano,A. and Murakami,H., "Composite plate theory for arbitrary laminate configurations", J. of Appl.Mech.ASME v.54 n.1 Mar.1987 p.181-189

[68] Murakami,H. and Hegemier,G.A., "Mixed model for unidirectionally fiber-reinforced composites", J. Appl. Mech.ASME v.53 n.4 Dec.1986 p.765-773

[69] Spilker,R.L., "Finite element models in composite materials", Advances in Bioengineering, 1985 publ. by ASME, New York, p.37-38

[70] Bar-Yoseph,P. and Avrashi,J., "New variational-asymptotic formulations for interlaminar stress analysis in laminated plates", ZAMP v.37 n.3 May 1986 p.305-321

[71] Vong,T.S., "New variational approach to the delamination problem", Compos. Struct. v.5 n.4 1986 p.

245-250

[72] Wang,S.S., "Three-dimensional Hybrid-stress finite element analysis of composite laminates with cracks and cutouts", Proceedings of the 5th Engineering Mechanics Division Specialty Conference, v.1, publ.by ASCE, New York, p.116-119, 1984

[73] Nishioka,T. and Atluri,S.N., "Assumed stress finite element analysis of through-cracks in angle-ply laminates", AIAA Journal v.18 n.9 Sep.1980 p.1125-1132

[74] Pandya,B.N. and Kant,T., "Finite element analysis of laminated composite plates using a high-order displacement model", Compos.Sci.and Tech.v.32 n.2 1988 p.137-155

[75] Zhang,Fufan, "Interlaminar stresses of a laminated composite lap joint", Scientia sinica, series A v.31 n.1 Jan.1988 p.69-78

[76] Moriya,K. and Ichikawa,T., "Study on edge protection against delamination for composite laminates(the effects of edge shapes on stress singularities for cross-ply laminates)", JSME international Journal, series 1, v.31 n2 Apr.1988 p.209-214

[77] Krishna Murty,A.V., "Theoretical modelling of laminated composite plates", Sadhana v.11 pt 3-4 Dec.1987 p.357-365

[78] Garg,A.C., "Delamination - a damage mode in composite structures", Eng.Fract.Mech.v.29 n.5 1988 p.

557-584

[79] Ye,Lin and Yang,B.X., "Boundary layer approach to interlaminar stresses in composite laminates with curved edges", J.of Reinforced Plastics and Composites v.7 n.2 Mar.1988 p.179-198

[80] Krishna Murty,A.V. and Vellaichamy,S., "On higher order shear deformation theory of laminate panels", Composite structures v.8 n.4 1987 p.247-270

[81] Hong,C.S., "Suppression of interlaminar stresses of thick composite laminates using sublaminate approach", International SAMPE Symposium and Exhibition v. 32 publ. by SAMPE, Covina, CA, USA p.558-565, 1987

[82] Kassapoglou,C. and Lagace,P.A., "Closed form solutions for the interlaminar stress field in angle-ply and cross-ply laminates", J. of Compos. Mater. v. 21 n.4 Apr.1987 p.292-308

[83] Kassapoglou,C.and Lagace,P.A., "Effecient method for the calculation of interlaminar stresses in composite materials", J. of Appl.Mech., ASME, v. 53 n. 4 Dec.1986 p.744-750

[84] Whitcomb,J.D. and Raju,I.S., "Analysis of interlaminar stresses in thick composite laminates with and without edge delamination", ASTM Special Publication 876, Publ.by ASTM, Philadelphia, PA, USA p. 69-94, 1985

[85] Conti,P. and De Paulis,A., "Simple model to simulate the interlaminar stresses generated near the

free edge of a composite laminate", ASTM Special Technical Publication 876, Publ.by ASTM, Philadelphia, PA, USA p.35-51, 1985

[86] Herakovich,C.T., Post,D., Buczek,M.B. and Czarnek,R., "Free edge strain concentrations in real composite laminates, experimental - theoretical correlation", ASME (Paper) Publ. by ASME, New York, 85-WA/APH-10, 7p, 1985

[87] Ueng,C.E. and Zhang,K.D., "Simplified approach for interlaminar stresses in orthotropic laminated strips", J.of Reinforced Plastics and Composites v. 4 n. 3 Jul. 1985 p.273-286

[88] Valisetty,R.R. and Rehfield,L.W., "Theory for stress analysis of composite laminates", AIAA Journal v. 23 n.7 Jul.1985 p.1111-1117

[89] Rehfield,L.W., Armanios,E.A. and Valisetty,R.R., "Simplified sublaminate analysis of composites and applications", Computers and Struct.v.20 n.1-3 1985 p. 401-411

[90] Whitcomb,J.D. and Raju,I.S., "Superposition method for analysis of free-edge stresses", J.of Compos.Mater. v.17 n.6 Nov.1983 p.492-507

[91] Lo,K.H., Christensen,R.M.and Wu,E.M., "A high-order theory of plate deformation - part 2, laminated plates", ASME J.of Appl.Mech.v.44 1977 p.669

[92] Reddy,J.N., "A simple high-order theory for laminated composite plates", ASME J.of Appl.Mech. v.51

1984 p.745

[93] Pagano,N.J., "Exact solutions for composite laminates in cylindrical bending", J.Compos.Mater. v.3 1969 p.398

[94] Murakami,H., "Laminated composite plate theory with improved in-plane responses", ASME J.of Appl.Mech.v.53 1986 p.661-666

[95] Kim,R.Y. and Soni,S.R., "Suppression of free-edge delamination by hybridization", Fifth International Coference on Composite Materials, San Diego, CA, USA, July 1985, Publ.by Metallurgical Soc.Inc., Warrendale, PA, USA, p.1557-1572, 1985

[96] Pian,T.H.H. and Tong,P., "Finite element method in continuum mechanics", Advances in Applied Mechanics, Edited by C.S. Yih, Academic Press, New York, 1972

[97] Pian,T.H.H. and Sumihara,K., "Rational approach for assumed stress finite elements", Int. J. for Numer. Meth. in Eng. v.20, 1685-1695, 1984

[98] Froier,M., Nilsson,L. and Samuelsson,A., "The rectangular plane stress element by Turner, Pian and Wilson", Int. J. for Num. Meth. in Eng. v.8, 433-437, 1974

Appendix

SIMILARITIES AND DIFFERENCES BETWEEN REISSNER'S THEOREMS AND HUANG'S ONE

	REISSNER 1	REISSNER 2	HUANG
ENERGY FUNCTION	POTENTIAL A(ε)	COMPLEMENTARY B(σ)	COMBINED C(q)
ENERGY PRINCIPLE	MODIFIED POTENTIAL	GENERALIZED POTENTIAL	COMBINED
CONSTRAINS	PARTIAL STRAIN-DISP. COMPLETE CONSTITUTIVE	COMPLETE STRAIN-DISP. PARTIAL CONSTITUTIVE	PARTIAL STRAIN-DISP. DISP. BOUNDARY (CONTINUITY AT BOUNDARY)
EULER EQS. AND NATURAL CONDITIONS	EQUILIBRIUM PARTIAL COMPATIBILITY	EQUILIBRIUM PARTIAL CONSTITUTIVE	EQUILIBRIUM PARTIAL COMPATIBILITY COMBINED CONSTITUTIVE FORCE BOUNDARY
HOW TO RELIEVE C^1 AT Z-DIRECTION	LAGRANGE MULTIPLIER	LEGENDRE TRANSFORMATION	SINCE BEGINNING